CZECH TECHNICAL UNIVERSITY IN PRAGUE

FACULTY OF MECHANICAL ENGINEERING

DEPARTMENT OF ENERGY ENGINEERING

Desulphurization during oxyfuel combustion in a fluidized bed

(DISSERTATION)

Ing. Pavel SKOPEC

Doctoral Study Programme: Mechanical Engineering

Study Field: Power Engineering

Supervisor: Doc. Ing. Jan Hrdlička, Ph.D.

Prague February, 2019

DECLARATION OF AUTHORSHIP

I declare that this dissertation entitled "Desulphurization during oxyfuel combustion in a fluidized bed" is my own work performed under the supervision of doc. Ing. Jan Hrdlička, Ph.D. with the use of available literature.

Further, I certify that this work is free of plagiarism and all materials appearing in this thesis have been properly quoted and attributed.

I do not have any compelling reason against the use of this thesis in accordance with §60 of the Law 121/2000 Coll. on authorship copyright, on rights related to the authorship copyright and on amending laws.

In Prague _____

ANOTACE

Tato dizertační práce se zabývá technologií „oxyfuel“ spalování, což je jedna z možností snižování emisí oxidu uhličitého ze spalovacích procesů. Proces „oxyfuel“ spalování spočívá v nahrazení vzduchu, jakožto okysličovadla, čistým kyslíkem. Výsledkem jsou spaliny obsahující z převážné většiny oxid uhličitý a vodní páru. Důležitou otázkou CCS technologií je čistota CO_2, která hraje důležitou roli v ekonomické bilanci celého procesu. Jednou ze složek snižujících čistotu oxidu uhličitého je oxid siřičitý, který vzniká oxidací síry přítomné v palivu. Práce se zaměřuje na „oxyfuel“ spalování v bublinkové fluidní vrstvě a jejím cílem je ověřit a optimalizovat proces suché aditivní metody odsiřování vedoucí ke snížení koncentrace této látky ve spalinách.

V práci je nejdříve podrobně rozebrán proces „oxyfuel“ spalování, je vytvořen matematický bilanční model „oxyfuel“ spalování, který je validován s výsledky měření. Tato část práce je nezbytnou pro pochopení samotného procesu fungování „oxyfuel“ spalování a definuje specifika „oxyfuel“ spalování ve fluidních kotlích.

Suchá aditivní metoda odsíření spočívá v přídavku vhodného aditiva, v tomto případě vápence, do spalovací komory. K záchytu SO_2 tedy dochází ještě v ohništi a produkty odsíření (síran vápenatý) odcházejí v tuhé formě spolu s popelovinami. V práci je uveden současný stav poznání z hlediska snižování emisí SO_2 v bublinkující fluidní vrstvě a to ve vzduchovém i „oxyfuel“ režimu.

Samotné experimenty byly provedeny na dvou zařízeních o různých výkonech (30 kW a 500 kW), které byly navrženy tak aby byly schopné pracovat jak v režimu vzduchového, tak i v režimu „oxyfuel“ spalování. Byly provedeny experimenty zabývající se hlavními aspekty ovlivňujícími proces odsíření. Mezi zkoumané aspekty patří vliv přebytku vápence, vliv teploty fluidní vrstvy a přebytek okysličovadla.

ABSTRACT

Presented dissertation deals with oxyfuel combustion, which is one of the possible methods for decreasing emissions of carbon dioxide from combustion process. Oxyfuel combustion is based on substitution of air as an oxidant by pure oxygen. Resulting flue gas contains mainly carbon dioxide and water vapour. Important requirement in the CCS technologies is the purity of CO_2, which plays an significant role in the economical balance of the whole process. One of the substances lowering the purity of CO_2 is sulphur dioxide formed by oxidation of sulphur in a fuel. This thesis focuses on the oxyfuel combustion in bubbling fluidized bed and the main focus is to verify and optimize the process of dry additive desulphurization method leading to lowering the final SO_2 concentration in flue gas.

The oxyfuel combustion process is analysed in detail and a balance oxyfuel combustion model is created and is validated with the measurement results. This part of the work is necessary to understand the process of oxyfuel combustion itself and defines the specifics of oxyfuel combustion in fluidized bed boilers.

The dry additive desulphurization method is based on addition of a suitable sorbent, in this case limestone, to the combustion chamber. Sulphur dioxide is captured directly in combustion chamber and the product of desulphurisation reaction mechanism (calcium sulphate) leaves the combustion process together with ash. The current state of the art of SO_2 emission reduction in fluidized bed boilers under air and oxyfuel mode is presented in this thesis.

The experiments were carried out in two facilities with different power outputs – 30 kW and 500 kW, which were designed to be able to operate in both air and oxyfuel combustion modes. Experiments were focused on the main aspects influencing the desulphurization process. The examined aspects include the effect of limestone excess, effect of fluidized bed temperature and the excess of oxidant.

ACKNOWLEDGMENT

My sincere acknowledgement goes to my supervisor, doc. Ing. Jan Hrdlička, Ph.D. for his continuous support of my Ph.D. study, invaluable advice, patience throughout this work and much help with experimental part of this thesis. Many thanks belongs also to doc. Ing. Tomáš Dlouhý, CSc. and prof. Ing. František Hrdlička, CSc. for their encouragement, insightful comments, and difficult questions. I could not imagine having better advisors and mentors not just for my Ph.D. study but exceeding to my personal life.

Many great thanks belong to my colleagues Ing. Matěj Vodička and Ing. Jan Opatřil, Ph.D. for assisting during designing the experimental facilities and spending innumerable hours preparing and commissioning the measurements. Special thanks belong to the technical assistance of Petr Stříž for solving each technical issue with the experimental facilities. All my colleagues at the Department of Energy Engineering are greatly acknowledged for creating a beautiful and relaxed working atmosphere.

Both the financial support by the Grant Agency of the Czech Technical University in Prague, grant No. SGS13/181/OHK2/3T/12 "Investigation of fluidized bed behaviour for combustion of nonconventional fuels" and the grant of the Technology Agency of the Czech Republic, grant No. TA03020312 "Research of oxyfuel combustion in a bubbling fluidized bed for CCS technologies" are greatly acknowledged.

Finally, my greatest appreciation goes to my parents, my beloved wife Vlaďka and my daughters Anička and Kačka. Thank you very much for all your support.

LIST OF FIGURES **8**
LIST OF TABLES **11**
NOMENCLATURE **13**
1 INTRODUCTION **15**
1.1 Motivation and scope of the dissertation 15
2 ASPECTS OF THE OXYFUEL COMBUSTION PROCESS **17**
2.1 General alternatives for CO_2 reduction 17
2.2 History and current status of the oxyfuel combustion 20
2.3 Possible configuration of the oxyfuel CFB combustion plant 23
2.4 Specification of oxyfuel combustion in bubbling fluidized bed 25
3 EMISSIONS OF SULPHUR OXIDES **28**
3.1 Sulphur in coal 28
3.2 Formation of sulphur oxides 29
3.3 Methods of sulphur oxides reduction 31
3.4 Dry additive method of desulphurization in fluidized bed boilers 32
3.4.1 Calcination of limestone 33
3.4.2 Sulphation reactions 34
3.4.3 Parameters affecting the SO_2 capture 35
3.5 Desulphurization under oxyfuel conditions 41
4 THE GOALS AND CONTRIBUTIONS OF THE DISSERTATION **43**
5 THEORETICAL ANALYSIS OF THE OXYFUEL COMBUSTION **44**
5.1 Methodology for stoichiometric calculations [III, IV] 44
5.1.1 Volume of oxidant V_O 45
5.1.2 Volume of flue gas 46
5.1.3 Volume of recirculated flue gas 46
5.1.4 Volume of total flue gas 47
5.1.5 Volume of fluidization medium 47

5.2 Theoretical application of oxyfuel combustion in a BFB....49
5.3 Effect of water vapour condensation in FGR....53
5.4 Effect of false air ingress on CO_2 concentration....54
5.5 Evaluation of sulphur dioxide emissions under oxyfuel combustion....55

6 EXPERIMENTAL SET-UP....57

6.1 30 kW laboratory bubbling fluidized bed combustor....57
6.2 500 kW pilot bubbling fluidized bed boiler....60
6.3 Fuel and additives characterisation....61
6.4 Experimental parameters and testing procedure....63
6.4.1 Experimental set up and testing procedure in MiniFluid under air conditions ...63
6.4.2 Experimental set up and testing procedure in MiniFluid and Golem under oxyfuel conditions....64
6.4.3 Uniform system of results presentation....66

7 VALIDATION OF THE MATHEMATICAL BALANCE....67

8 SO_2 CAPTURE IN MINIFLUID – EXPERIMENTAL RESULTS AND DISCUSSION....70

8.1 SO_2 capture in air-fired mode in MiniFluid combustor....70
8.1.1 Sulphur self-retention under air conditions....70
8.1.2 Effect of Ca/S ratio....72
8.1.3 Effect of bed temperature....74
8.1.4 Effect of oxygen concentration....77
8.2 SO_2 capture in oxyfuel mode in MiniFluid combustor....78
8.2.1 Sulphur self-retention....78
8.2.2 Effect of Ca/S ratio....79
8.2.3 Effect of bed temperature....80
8.2.4 Effect of oxygen concentration....83
8.3 Comparison of the results between air and oxyfuel combustion in MiniFluid ...85
8.4 Fly ash analysis....89
8.4.1 Balance of sulphur....89
8.4.2 Balance of calcium....91

9 SCALE-UP OF THE SO_2 CAPTURE EXPERIMENTS 92

9.1 Results of the experiments 92

9.1.1 Sulphur self-retention 92

9.1.2 Effect of Ca/S ratio 93

9.1.3 Effect of bed temperature 95

9.1.4 Effect of oxygen concentration 96

9.2 Fly ash analysis 97

9.3 Comparison of the results between MiniFluid and Golem 98

10 FINAL EVALUATION OF THE REASERCH RESULTS 103

10.1 Different views on the desulphurization evaluation 103

10.2 Summary of accomplished goals and tasks 105

10.2.1 Accomplishment of the main goal 105

10.2.2 Accomplishment of the individual tasks 106

10.3 Consequences for science and practice 108

10.4 Future work 109

11 CONCLUSION 110

12 BIBLIOGRAPHY 111

12.1 bibliography (excluding authors own publications) 111

12.2 authors Own publications 117

13 APPENDIX 119

13.1 SO_2 capture under air conditions 119

13.2 SO_2 capture in oxyfuel regime - MiniFluid 123

13.3 SO_2 capture in oxyfuel regime - Golem 127

13.4 Comparison of the results from MiniFluid and Golem 131

13.5 Different views on desulphurization efficiency 132

LIST OF FIGURES

Figure 2-1: Overview of carbon capture technologies.....17
Figure 2-2: Pre-combustion technology – IGCC system [10].....19
Figure 2-3: Simplified scheme for CFBC oxyfuel combustion [42].....23
Figure 2-4: The possible process scheme for CO_2 processing [43].....25
Figure 3-1: Equilibrium curve of calcination of limestone.....34
Figure 3-2: Influence of Ca/S ratio on SO_2 reduction [60].....36
Figure 3-3: Origin of the pores during calcination and creation of the $CaSO_4$ layer on the particle surface [61].....37
Figure 3-4: Effect of fly ash recirculation on SO_2 capture ratio [4].....41
Figure 5-1: A comparison of the volume flow of all streams of gases for combustion with air (A) and with oxygen (B) [I, II].....44
Figure 5-2: Effect of the amount of recirculated flue gas on adiabatic flame temperature and on volume of fluidized medium considering no condensation of water vapour in FGR [IV].....50
Figure 5-3: Effect of the amount of recirculated flue gas on adiabatic flame temperature and on volume of fluidized medium considering dry FGR (full condensation of water vapour in FGR) [IV].....50
Figure 5-4: Composition of the fluidized medium.....52
Figure 5-5: Composition of the flue gas.....52
Figure 5-6: Effect of FGR temperature on water vapour concentration.....54
Figure 5-7: The effect of false air ingress on CO_2 concentration in dry flue gas [IV].....55
Figure 6-1: Schematic diagram of the MiniFluid facility.....59
Figure 6-2: Photograph of the MiniFluid facility.....59
Figure 6-3: Picture of the control program in LabView.....59
Figure 6-4: Schematic diagram of the FBC boiler Golem [IX].....61
Figure 6-5: Photograph of the FBC boiler Golem.....61
Figure 6-6: Detail of the distributor.....61
Figure 8-1: Sulphur self-retention correlated with bed temperature under air conditions.....70
Figure 8-2: Sulphur self-retention correlated with bed oxygen concentration under air conditions.....70
Figure 8-3: Effect of different Ca/S molar ratio on SO_2 capture ratio – fitting of the measured points.....73

Figure 8-4: Effect of limestone addition on SO_2 capture represented as limestone to coal weight ratio 73
Figure 8-5: Correlation of SO_2 capture ratio with bed temperatures under air conditions – **limestone L1**....74
Figure 8-6: Correlation of SO_2 capture ratio with bed temperatures under air conditions – **limestone L2**....75
Figure 8-7: Correlation of SO_2 capture ratio with oxygen concentration in FG under air conditions – **L1** 77
Figure 8-8: Correlation of SO_2 capture ratio with oxygen concentration in FG under air conditions – **L2** 77
Figure 8-9: Experiments for different temperatures under oxyfuel conditions without any limestone addition....78
Figure 8-10: Experiments for different oxygen concentrations in FG under oxyfuel conditions without any limestone addition....78
Figure 8-11: Effect of different Ca/S molar ratio on SO_2 capture ratio – fitting of the measured points....79
Figure 8-12: Effect of limestone addition on SO_2 capture represented as limestone to coal weight ratio 80
Figure 8-13: Correlation of SO_2 capture ratio with bed temperatures under oxyfuel conditions – **limestone L1**....80
Figure 8-14: CO_2 concentration in wet flue gas for all experimental cases in MiniFluid combustor....81
Figure 8-15: Correlation of SO_2 capture ratio with bed temperatures under oxyfuel conditions – **limestone L2**....82
Figure 8-16: Correlation of SO_2 capture ratio with oxygen concentration in FG under oxyfuel conditions – **L1** 84
Figure 8-17: Correlation of SO_2 capture ratio with oxygen concentration in FG under oxyfuel conditions – **L2** 84
Figure 8-18: Comparison of sulphur self-retention under oxyfuel and air conditions [XIV]...85
Figure 8-19: Effect of Ca/S molar ratio on SO_2 capture ratio – comparison of air and oxyfuel conditions....86
Figure 8-20: Effect of limestone/coal weight ratio on SO_2 capture – comparison of air and oxyfuel conditions....86

Figure 8-21: Correlation of SO_2 capture ratio with temperature – comparison of air and oxyfuel combustion 87
Figure 8-22: Correlation of SO_2 capture ratio with oxygen concentration in FG – comparison of air and oxyfuel combustion 88
Figure 8-23: Correlation of SO_2 capture ratio with oxygen concentration expressed as oxygen excess – comparison of air and oxyfuel combustion 88
Figure 8-24: Sulphur and calcium content in fly ash in relation to the SO_2 capture ratio for limestone L1, oxyfuel conditions, MiniFluid 89
Figure 8-25: Sulphur and calcium content in fly ash in relation to the SO_2 capture ratio for limestone L2, oxyfuel conditions, MiniFluid 89
Figure 9-1: Sulphur self-retention correlation with temperature 92
Figure 9-2: Effect of different Ca/S molar ratio on SO_2 capture ratio – fitting of the measured points – results from Golem 94
Figure 9-3: Effect of limestone addition on SO_2 capture represented as limestone to coal weight ratio – results from Golem 94
Figure 9-4: Correlation of SO_2 capture ratio with bed temperatures under oxyfuel conditions – results from Golem – **limestone L1** 95
Figure 9-5: Correlation of SO_2 capture ratio with bed temperatures under oxyfuel conditions – results from Golem – **limestone L2** 95
Figure 9-6: Correlation of SO_2 capture ratio with oxygen concentration in FG under oxyfuel conditions – results from Golem – **L1** 96
Figure 9-7: Correlation of SO_2 capture ratio with oxygen concentration in FG under oxyfuel conditions – results from Golem – **L2** 96
Figure 9-8: Sulphur and calcium content in fly ash in relation to the SO_2 capture ratio for limestone L1, oxyfuel conditions, Golem 97
Figure 9-9: Sulphur and calcium content in fly ash in relation to the SO_2 capture ratio for limestone L2, oxyfuel conditions, Golem 97
Figure 9-10: Comparison of the results of sulphur self-retention 99
Figure 9-11: Comparison of the effect of Ca/S molar ratio on SO_2 capture ratio 99
Figure 9-12: CO_2 concentrations in wet flue gas and bed temperatures for each experiment - Golem 101
Figure 9-13: Comparison of the effect of fluidized bed temperatures 102
Figure 9-14: Comparison of the effect of fluidized bed temperatures for T-wall temperature in Golem 102

LIST OF TABLES

Table 2-1: The summary of the pilot scale and laboratory scale units with fluidized bed working in oxyfuel regime 22
Table 5-1: Volume concentration of the substances in different types of the oxidant 45
Table 5-2: List of equations for calculation the volume flows in the boiler [III], [IV] 48
Table 5-3: Parameters of the reference air combustion 50
Table 5-4: Calculation of the characteristic velocities 53
Table 6-1: Main parameters of the MiniFluid facility [VIII] 58
Table 6-2: Proximate and ultimate analysis of the used coal 62
Table 6-3: Sulphur distribution in the fuel 62
Table 6-4: Characteristic of the inert fluidized bed material 62
Table 6-5: Properties of limestone additives 63
Table 6-6: Matrix of the experiments for air combustion 64
Table 6-7: Matrix of the experiments for oxyfuel combustion 65
Table 7-1: Experimental data from MiniFluid and comparison with mathematical model 68
Table 7-2: Experimental data from Golem and comparison with mathematical model 69
Table 8-1: XRF analysis of elements in the ash, wt. % as oxides 71
Table 8-2: Amount of limestone addition in MiniFluid, g sorbent per 10 kg of coal 72
Table 8-3: Values of K constant obtained from correlation by equation 3-20 72
Table 8-4: Relative decrease from maximal SO_2 capture ratio for limestone L1 under air conditions 75
Table 8-5: Relative decrease from maximal SO_2 capture ratio for limestone L2 under air conditions 76
Table 8-6: Additional analyses of the additives 76
Table 8-7: Effect of different oxygen excess on SO_2 capture ratio 77
Table 8-8: Chemical composition of the used fuel ash related as oxides from the measurement without limestone – XRF analyses; all in % wt. 79
Table 8-9: Values of K constant obtained from correlation by equation 3-20 79
Table 8-10: Relative decrease from maximal SO_2 capture ratio for limestone L1 under oxyfuel conditions 82
Table 8-11: Relative decrease from maximal SO_2 capture ratio for limestone L2 83
Table 8-12: Effect of different oxygen excess on SO_2 capture ratio 84

Table 8-13: Comparison of the results from XRF analysis of ashes 90
Table 8-14: Balance of sulphur.....90
Table 8-15: Balance of calcium.....91
Table 9-1: Recalculation of Ca/S ratios according to the real conditions 93
Table 9-2: Values of K constant obtained from correlation by equation 3-20 94
Table 9-3: Effect of different oxygen excess on SO_2 capture ratio – results from Golem 96
Table 9-4: Chemical composition of the used fuel ash related as oxides from the measurement without limestone – XRF analyses 98
Table 10-1: Desulphurization evaluation – comparison of air and oxyfuel combustion for Ca/S ratio = 1.5 at different temperatures.....104
Table 10-2: Desulphurization efficiency and limestone utilization – comparison of air and oxyfuel combustion at different Ca/S ratios at constant temperature.....104

NOMENCLATURE

Greek symbols

α	excess of air/excess of oxidant	[-]
ϵ_{mf}	voidage (void fraction) at minimum fluidization	[-]
$\eta_{capture}$	SO_2 capture ratio	[%]
$\eta_{desulph.}$	desulphurization efficiency	[%]
$\eta_{limestone}$	limestone utilization	[%]
ρ_b	bulk density	[kg/m^3]
ρ_f	density of fluidization medium	[kg/m^3]
ρ_s	density of solid particle	[kg/m^3]
ω_i	volume concentration of given substance	[ppm;%]
ω''_{H_2O}	saturation partial pressure of water vapour for given temperature	[%]
ϕ_s	sphericity	[-]

Latin symbols

A_l	limestone specific surface area	[m^2]
C	coefficient respecting the flue gas condensation at volumetric calculations	[m_N^3/kg_{fuel}]
C_D	drag coefficient	[-]
c_i	mass concentration of a given substance	[mg/ m_N^3]
d_p	diameter of the particle	[m]
E	activation energy	[J/kmol]
EF^x_{mass}	emission factor of component x related to the mass of fuel	[mg/kg_{fuel}]
EF^x_{LHV}	emission factor of component x related to the LHV of fuel	[mg/MJ]
f_l	limestone conversion factor	[-]
g	gravitational constant	[m/s^2]
I_{ad}	adiabatic flue gas enthalpy	[kJ/kg_{fuel}]
k	reaction constant	[(1/s). (kmol/m^3)]
k_o	preexponential factor	[m/s; kg/ (m^2.s.Pa)]
K	coefficient for approximation of SO_2 capture ratio with Ca/S ratio	[-]
LHV	low heating value	[MJ/kg]
M_i	molar weight of substance i	[kg/kmol]
Q_{fm}	specific heat of fluidization medium	[kJ/kg_{fuel}]
Q_{fuel}	specific heat of the fuel	[kJ/kg_{fuel}]
Q_u	heat released in combustion chamber	[kJ/kg_{fuel}]
p_N	standard pressure	[Pa]
r	recirculation ratio	[-]
R	gas constant	[J/kmol.K]
$\dot{R}$	rate of reaction	[kmol/s]

R^2	determination index	[-]
Re_p	Reynolds number for given particle	[-]
S_m^r	specific sulphur content	[kg/kJ]
T	temperature	[°C; K]
T_{ad}	normalized adiabatic flame temperature	[-]
T_N	standard temperature	[°C; K]
u_{mf}	minimum fluidization velocity	[m/s]
u_t	terminal velocity	[m/s]
V_{FG}	volume of flue gas	[m_N^3/kg_{fuel}]
V_{FGR}	volume of recirculated flue gas	[m_N^3/kg_{fuel}]
V_{fm}	normalized volume of fluidized medium	[-]
V_{FM}	volume of fluidized medium	[m_N^3/kg_{fuel}]
V_{TFG}	total volume of flue gas	[m_N^3/kg_{fuel}]
V_O	volume of oxidant	[m_N^3/kg_{fuel}]
Z_C	heat loss of the boiler because of unburned carbon	[-]
Z_{CO}	heat loss of the boiler because of unburned carbon monoxide	[-]
Z_f	heat loss of the boiler because of radiation loss	[-]

Subscripts

w	wet
d	dry
min	minimum

Used abbreviations

ASU	air separation unit
BFB	bublling fluidized bed boiler
BFBC	bubbling fluidized bed combustion
Bio-CCS	carbon capture and storage using biomass
CCS	carbon capture and storage
CCU	carbon capture and utilization
CFB	circulating fluidized bed boiler
CFBC	circulating fluidized bed combustion
CLC	chemical looping combustion
EIA	Energy Information Administration
FBC	fluidized bed combustion
FG	flue gas
FGD	flue gas desulphurization
FGR	flue gas recirculation
FM	fluidization medium
GPU	gas processing unit
IGCC	integrated gasification combustion cycle
SCR	selective catalytic reduction

1 INTRODUCTION

Energy production from the combustion of fossil fuels is accompanied by the formation of gaseous emissions. For several decades, there have been discussions about climate change caused by the production of greenhouse gases, and efforts are being made to reduce their production as much as possible. The most important greenhouse gas being discussed in this time is carbon dioxide CO_2, the product of oxidation of carbon from fossil fuels.

It is possible to decrease the production of carbon dioxide during the electricity and heat production by replacing the fossil fuels with other alternative sources of energy, both renewable energetic sources and nuclear energy. Although renewable sources are being promoted in this time and they start to have more and more important role in an energy mix, they still do not have the adequate capacity to satisfy the energy consumption.

The fossil fuels have and in future decades will have the irreplaceable role in an energy mix and the role of coal will stay very important. Coal is the most frequently used source for heat and electricity production. According to the IEA statistics the coal production in 2015 was about 8.2 billion of tons and about 40 % of produced electricity in world comes from coal combustion [1].

About 47% of electricity produced in the Czech Republic comes from coal combustion. The Czech Republic accepted SET plane in 2007, which is a complex of steps leading to lowering greenhouse emission production in EU in order to start research of new so called clean technologies. The Czech Republic is also committed to the EU Directive known as Strategy 20 20 20, which includes reducing greenhouse gas emissions in 2020 by 20% compared to 1990.

1.1 MOTIVATION AND SCOPE OF THE DISSERTATION

CCS technologies (Carbon Capture and Storage, or Carbon Capture and Sequestration) are one of the main approaches for the reduction of carbon dioxide emissions from stationary energy sources. Oxyfuel combustion belongs to this group of technologies with the potential to become so called near zero CO_2 emission combustion technology [2]. Oxyfuel combustion is a process, which uses pure oxygen as the oxidant during combustion instead of air for fuel combustion. However, using just pure oxygen would lead to too high combustion temperatures and thus the recirculated flue gas must be used in order to supply sufficient amount of heat carrier and decrease the combustion temperatures. The result is a flue gas with high concentration of CO_2. Due to its relatively simple technology design and operation, the oxyfuel combustion can be considered as one of the most promising CCS technologies [3]. For the same reason, it can be

reasonably applied to smaller power production capacities, as opposed to other CCS technologies. Current oxyfuel research focuses mainly on pulverized coal combustion, or circulating fluidized bed combustion. Worldwide, there are several laboratory and pilot experimental facilities aimed at circulating fluidized bed and pulverized coal combustion. A few investigations have been made in the field of bubbling fluidized bed combustion, which is more suitable for lower power capacities and for wider range of fuels including low quality fuels.

One of the main advantages of the fluidized bed combustion is the possibility of sulphur dioxide removal directly in the furnace during combustion in a relatively easy and cheap way, by infusing an additive – limestone to the combustion chamber [4]. This method of direct flue gas desulphurization is known and well described method in air combustion. However, oxyfuel combustion is characterized by absolutely different combustion conditions and the desulphurization is highly affected. Lowering of SO_2 concentration is an important factor in the oxyfuel process, because SO_2 have impacts in the furnace, during ash collection, CO_2 compression and transport as well as storage.

In a boiler under oxyfuel firing combustion, the concentration of SO_2 is higher throughout the process and it causes the water wall corrosion in the furnace. Enhanced oxidation of SO_2 to SO_3 has an impact on ash deposits in the convective part. Additionally, it negatively affects the SCR, which needs to be installed for NO_x reduction, by formation of ammonium bisulphate, thus deactivating the SCR catalyst. In cooler sections, it forms liquid H_2SO_4 with high corrosion potential. SO_2 has negative impact on the CO_2 compression, and there are discussions about the transport, where the transport type and route will affect required SO_x regulations and economics. Some toxicological questions are associated with potential leakages from underground storage. Although no SO_2 legislation for pipeline or sequestration is currently drawn, it is necessary to know the process of desulphurization and to be able to work within the emissions limits which may be set. It is necessary to consider the risks between pipeline corrosion, toxicological risks of leakage, mineral reactions in sequestration and economic disincentives from over the stringent specifications. [5]

The facts mentioned above present clear evidence for the need to experimentally verify the possibilities of using a direct desulphurisation method for oxyfuel combustion in bubbling fluidized bed boilers and to determine the influences of individual operating parameters on desulfurization efficiency.

2 ASPECTS OF THE OXYFUEL COMBUSTION PROCESS

2.1 GENERAL ALTERNATIVES FOR CO_2 REDUCTION

Reducing production of CO_2 from fossil power generation is a subject of discussions among policy makers in association with the risk of global warming. However, today´s growing energy demand, mainly driven by the emerging economies, will keep the fossil fuels as the dominant energy source for the foreseeable future. General options for CO_2 emission reduction from coal-fired power generation are [3][6]:

- Improving efficiency of fuel conversion
- Decreasing energy consumption
- Replacement of hydrocarbon fuels with renewable and alternative sources, or use of low carbon fuels
- Promoting afforestation
- Capture and storage of CO_2 from conventional plants

CO_2 is a natural product from combustion of carbon-based fuels and the type of combustion directly affects the suitable method for CO_2 removal. The basic pathways applicable for CO_2 capture process – post-combustion, pre-combustion, oxyfuel combustion and chemical looping are shown in Figure 2-1.

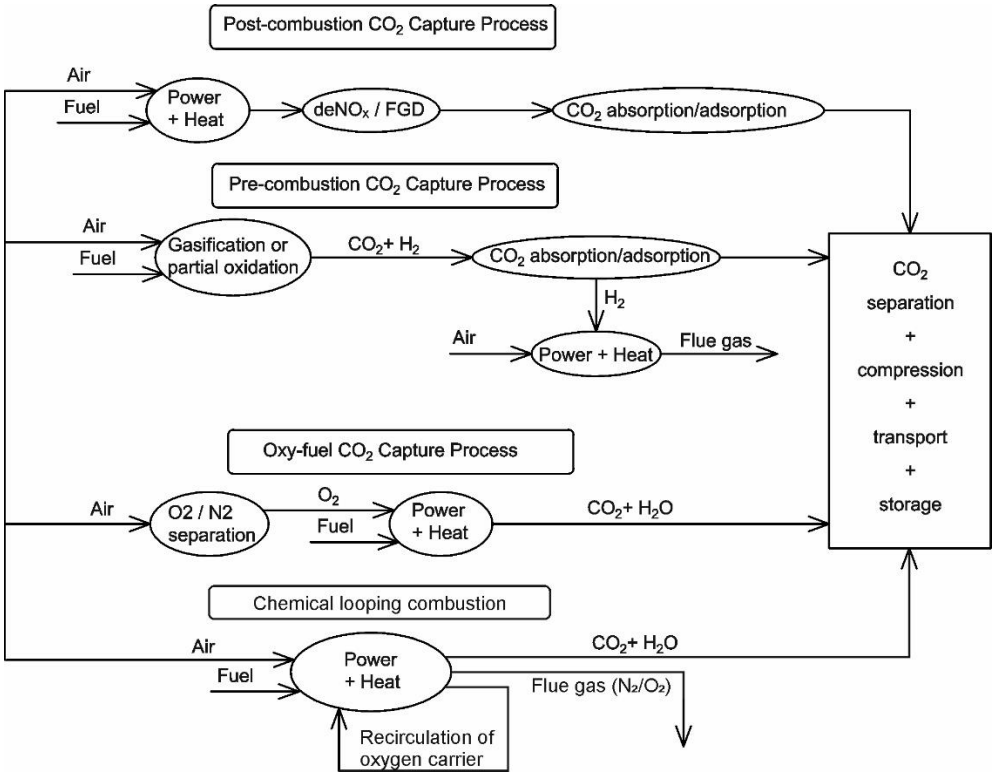

Figure 2-1: Overview of carbon capture technologies

Post-combustion processes

Post-combustion technologies are a good option for retrofit of recent coal-fired power plants. The CO_2 separation process is placed behind all technologies to the end of the flue gas way. Therefore, the whole original system of combustion process and systems for flue gas cleaning can stay unchanged or is just slightly optimized on the basis of used separation technology. All post-combustion technologies are based on separation of CO_2 at relatively low concentrations, usually not exceeding 15 % vol., using different kinds of chemical or physical processes.

The most common post-combustion processes are probably absorption processes using scrubbing of the flue gas with a liquid absorbent having higher selectivity for CO_2 than for N_2 - usually amines [7] or ammonia [8].

Adsorption is a process that involves the capture of molecules of liquid or gaseous substances on the surface of solids. Based on the types of the forces that bound the molecules to the surface of solid phase we distinguish two basic types of adsorption – physical adsorption (physisorption) and chemical adsorption (chemisorption). Typical physisorption processes uses zeolites or carbon-based sorbents. Among chemisorption processes belongs e.q. adsorption on natural limestone in the systems called Ca-looping cycles. Ca-looping cycles offers regeneration of the used sorbent that is carried out in the reactor based on oxyfuel combustion.

A wide variety of membrane based separations are under development using different kinds of membranes, polymeric membranes or membrane-adsorption processes. Among new advanced processes belong modified solid adsorbents (such as metal-organic frameworks, functionalized fibrous matrices) or structured fluid absorbents like CO_2 hydrates, liquid crystals or ionic liquids. [9]

Although, there are many approaches to post-combustion capture in theory, the only real option in today technology are scrubbing absorption processes using amines or ammonia.

Pre-combustion technologies

Pre-combustion technologies refer to the capture of CO_2 prior to completion of combustion process. In order to do it, the fuel must be converted to a form amenable for capture, typically to a gas from which the carbon is separated before combustion. Typical pre-combustion carbon capture system is called Integrated Gasification Combined Cycle (IGCC). It begins with gasification of the coal to produce synthesis gas (syngas). Gasification medium are oxygen (from the air separation unit) and steam. The syngas is going to cyclone for particulate removal. Syngas is than processed in water gas shift reformer, where the carbon monoxide is converted

to carbon dioxide and hydrogen using steam. The product stream continues to acid gas separation unit, which removes mostly sulphur-based compounds as well as CO_2, and optionally to a separate CO_2 removal unit. The product is hydrogen, which can be used in various power generation applications – in terms of IGCC system it is in gas turbine, but other applications are also possible e.g. gas boiler or fuel cell. The process is described in Figure 2-2. [10]

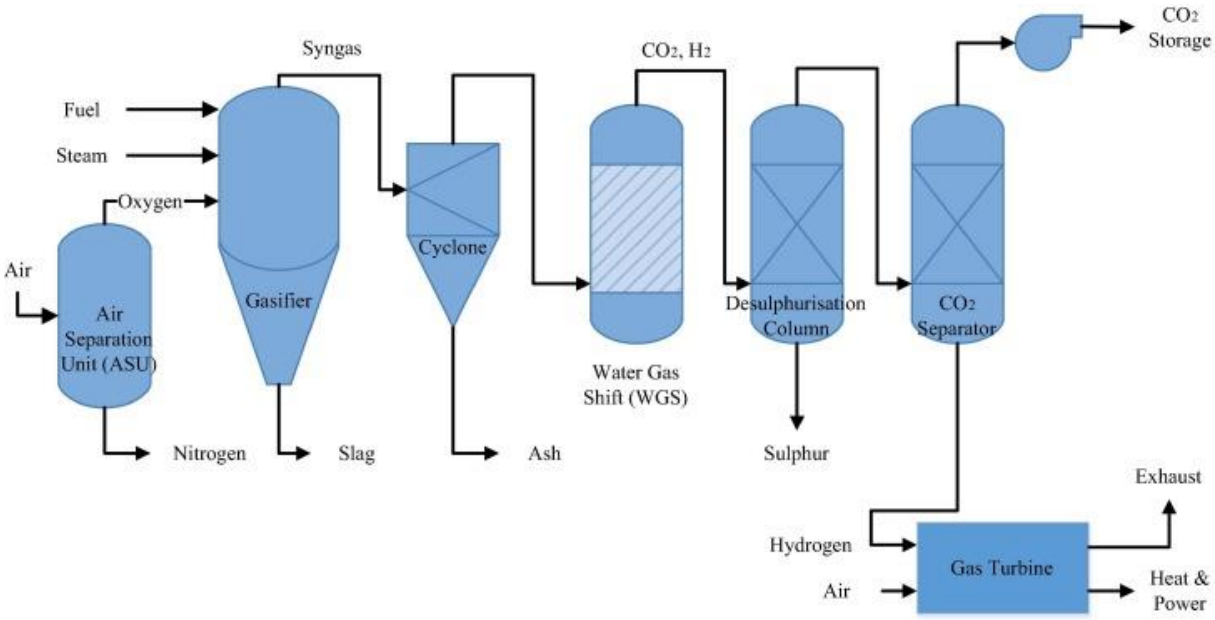

Figure 2-2: Pre-combustion technology – IGCC system [10]

IGCC system has less energy-intensive CO_2 separation process due to lower gas volume, higher pressure and higher CO_2 concentration. Another advantage is the generation of hydrogen rich gas. [10]

Chemical looping based CO_2 processes

Chemical looping combustion (CLC) is an alternative option for CO_2 capture. The CLC system uses two interconnected fluidized bed reactors – an air and a fuel reactor. Oxygen carriers in the form of metal oxide particles are circulated in these two reactors. In the air reactor, air is introduced and the oxygen carrier particles are oxidised by oxygen from air. The oxidised form of the oxygen carrier is then transported to the fuel reactor. In case of using solid fuels, two ways of the CLC processes are possible. In the indirect process, the gasification of the solid fuel precedes. The oxygen carrier than reacts with syngas. In the direct CLC process, the fuel is mixed with the oxygen in the fuel reactor. The oxygen carrier reacts with the gasification products of the solid fuel generated inside the fuel reactor. [6][11]

Oxyfuel combustion

Conventional combustion technologies use air for combustion. Air contains about 79 % of nitrogen, which passes through the process mostly as inert gas and dilutes CO_2 as the product of combustion. Oxyfuel combustion is based on usage oxygen as an oxidant for combustion. Flue gases then consist mainly of CO_2 and water vapour and subsequent CO_2 treatment is easier. On the other hand, the combustion in pure oxygen significantly increases the flame temperature and reduces the flue gas volume. This reduction has a negative impact on the heat flux and temperature profiles in a boiler. Oxyfuel combustion overcomes these problems by recycling the flue gas. Details about oxyfuel combustion in fluidized beds are discussed in following parts.

2.2 HISTORY AND CURRENT STATUS OF THE OXYFUEL COMBUSTION

Usage of oxygen or oxygen enriched air combustion has been for many years quite common in cement, glass and steel processing industries. The main margin of oxygen enrichment includes improved heat transfer, reduction of the fuel consumption or increased thermal efficiency and the focus is related more to the material science rather than combustion.

The basic scheme of combustion using oxygen with high amount of recirculated flue gas was firstly described by Abraham in 1982. The focus was related to get high concentrated source of CO_2 for enhanced oil recovery process [3]. The main oxyfuel combustion research focused on CO_2 capture and sequestration started in 1990 due to the concern of climate change and regulations given by Kyoto protocol and Intergovernmental Panel on Climate Change. Around the years 1992 to 2000 New Energy and Industrial Development Organisation (NEDO) in Japan carried out the first pilot plant studies [12]. In the same period, CANMET in Canada supported their first oxyfuel pilot plant – 0.3 MW vertical combustor facility [13]. Around the year 2000 Babcock and Wilcox Company built a 1.5 MW pulverized coal furnace [14].

Current research focuses on pulverized coal combustion, and there is also interest in circulated fluidized bed combustion. Several laboratory and pilot experimental facilities focusing on a circulating fluidized bed and pulverized coal combustion have been set up worldwide [3], [15]. The Schwarze Pumpe pilot power plant in Germany was a major project. It had power output of about 30 MW_{th} [16]. The plant is not in operation in this time. The Callide Power Station in Australia [17] is the facility with the highest power output until now, with an electric power output of 30 MW. Major facilities, with 30 MW_{th} pulverized coal and 30 MW_{th} circulating

fluidized bed boilers, were under investigation by CUIDEN in Spain [18], but the project has already been finished. A 3 MW_{th} full chain system has been constructed in China, and a 35 MW_{th} unit is ready for commissioning [19]. In addition, some commercial-scale oxyfuel power plants are currently under preparation: a 200 MW_e facility, by the Shenhua Group in China [20], and a 426 MW_e facility by Whiterose in the UK [21]. Other important projects are flexiburn facilities, which are able to operate under oxy-combustion and air combustion mode. They have been proposed by Foster Wheeler and by researchers from the Czestochowa University of Technology [22].

This work focuses on the oxyfuel combustion in bubbling fluidized beds. In order to see the current state of the art of oxyfuel combustion in fluidized bed generally, Table 2-1 was compiled summarizing the research activities. It can be seen that the current research is focusing more on combustion in circulating fluidized bed boilers. A few investigations have been made in the field of bubbling fluidized bed combustion, however it is more suitable for lower power capacities. The experimental facilities which are used in this thesis are also stated in the table.

Table 2-1: The summary of the pilot scale and laboratory scale units with fluidized bed working in oxyfuel regime

Organization	Size	Power output	Type of FB	Ref.
CIUDEN Technology Centre for CO_2 Capture and Transport, Spain *	Pilot scale Dem. unit	30 MW	CFB	[18], [23]
METSO, Tampere, Finland	Pilot scale	4 MW	CFB	[24]
Alstom, USA	Pilot scale	3 MW	CFB	[25]
Chinese Academy of Sciences, Peking, China	Pilot scale	1 MW	CFB	[26]
CANMET ENERGY, Canada	Pilot scale	0,8 MW	CFB	[27], [28]
Institut für Feuerungs - und Kraftwerkstechnik, Universität Stuttgard, Germany	Pilot scale	150 kW	CFB	[29]
CANMET ENERGY, Canada	Pilot scale	100 kW	CFB	[30], [31]
Czestochowa University of Technology, Poland	Pilot scale	100 kW	CFB	[32]
Technical University in Vienna, Vienna - Austria	Pilot scale	100 kW	CFB	[33]
VTT (Technical Research Centre of Finland), Jyväskylä, Finland	Pilot scale	30 - 100 kW	CFB	[2], [34]
Southeast University, School of Energy and Enviroment, Nanjing China	Pilot scale	50 kW	CFB	[35]
Czestochowa University of Technology, Poland	Lab scale	Units of kW	CFB	[36]
CTU in Prague, Prague, Czech Republic	Pilot scale	500 kW	BFB	Chapter 6.2
Center of Research of Energy and Consumption, CIRCE, University of Zaragoza, Spain	Pilot scale	95 kW	BFB	[37], [38]
CTU in Prague, Prague, Czech Republic	Pilot scale	30 kW	BFB	Chapter 6.1
ICB-CSIC, Spain	Lab scale	Approx. 3 kW	BFB	[39]
VTT (Technical Research Centre of Finland), Jyväskylä, Finland	Lab scale	1 kW	BFB/CFB	[34]
Monash University, Australia	Lab scale	Units of kW	BFB	[40]
Nagoya University, Japan	Lab scale	Units of kW	BFB	[41]
* The operation was cancelled				

2.3 POSSIBLE CONFIGURATION OF THE OXYFUEL CFB COMBUSTION PLANT

Oxyfuel combustion differs from air combustion in many ways. Designing an oxyfuel power plant calls for case-specific optimization. The most important factor is whether the plant is newly built or retrofitted.

A simplified process scheme for the oxyfuel CFBC is shown in Figure 2-3. The oxyfuel process differs in three main parts – air separation unit (ASU) used for oxygen production, gas processing unit (GPU) used for purification and separation of CO_2 and usage of flue gas recirculation (FGR) [42].

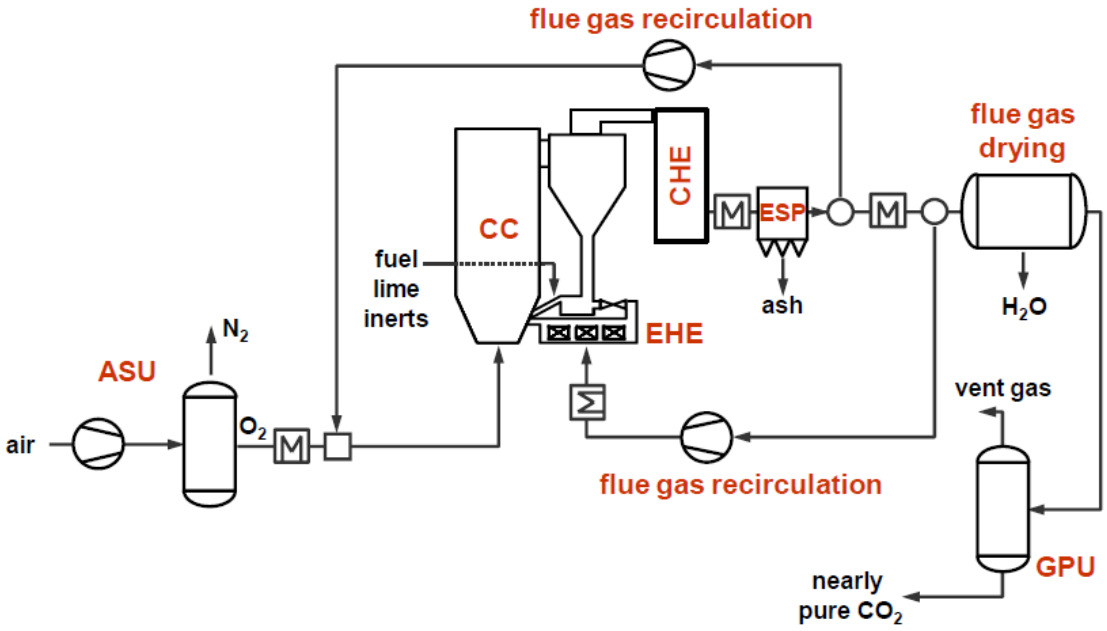

Figure 2-3: Simplified scheme for CFBC oxyfuel combustion [42]

Operation of ASU and purity of the oxygen

The air separation unit (ASU) provides the oxygen for combustion. Nowadays the only possibility of the oxygen production is by cryogenic distillation unit. No other technologies exist in such sizes to be able to produce sufficient amount of oxygen for typical industrial power plant sizes. Even for the biggest power plant units (500 MW_e) it is necessary to use two or three parallel ASU units. ASU consumes the highest amount of energy in the form of electricity and reduces the overall power plant efficiency by 7 to 9 %. [43]

It is also very important to ensure a sufficient amount of oxygen for the boiler in each moment of the boiler operation and follow the power load of the power plant. While ASU unit is able to reach the maximum ramp rate 3%/min, the boiler can be operated at a ramp up to 6%/min. ASU

unit should also operate in the range of 80 to 100% load, while under 80% of load losses the efficiency. These are the reasons for building a storage tanks having sufficient volume for synergy between the ASU and the boiler. [43]

The purity of the oxygen for combustion can be given by the relation between the lowest power requirements for liquefaction of flue gas and lowest power requirement for air separation. Nakayama [44] states the optimal O_2 purity of 97.5% for the1000 MW_e power plant as the optimum for the lowest overall power consumption of flue gas liquefaction and air separation. Others report optimum purities of 95% taking into account the effect of air ingress. The remaining impurities are argon (3-4%) and nitrogen (1-2%). [15], [43]

Location of the oxygen injection

The location of the oxygen injection to the furnace is an important factor that affects the optimum configuration of the process. Due to the safety reasons, no oxygen should be added to the primary recycle before entering the mills or drills in case of FBC combustion. Although CO_2 has inhibitory effect on explosions and it could be possible to raise the O_2 level in the mixture above 21%, the case of equipment failures in control valves, recycle fans, etc. are considered as security risks. In case of PC boilers, the method of oxygen injection and mixing is a question of the optimal burner design, taking into consideration satisfactory ignition, flame stabilization or optimization on NO_x formation. Generally, it is very important to minimize the risk of having pure oxygen present together with combustibles anywhere in the system. [43]

Flue gas recirculation

The combustion process in plant needs a reduced concentration of oxygen in the oxidant stream, which is made by flue gas recirculation. FGR is also used to control the flame temperature at acceptable limits for the boiler materials [43]. Figure 2-3 shows, the possible system of flue gas recirculation.

There are many other ways of positioning of recycle streams, depending on whether it is used for fuel supply, drying of the fuel, using in primary/secondary/tertiary stream etc. Two main possible ways are possible – dry and wet flue gas recirculation. Usage of dry FGR is usually necessary in case of pre drying the fuel. FGR stream must be dry in order to be able to carry the moisture. [43]

Even the oxygen concentration is set to reach the similar combustion temperatures as during air combustion, the combustion chemistry is different and due to the different physical properties of nitrogen and carbon dioxide the heat flux profile in the boiler is significantly affected. This

leads also into necessary optimization of the heating surfaces, where the biggest differences are supposed to change by more than 40% in the size, e.g. for economizer [45].

CO_2 processing

A required purity of the CO_2 for the process of compression, transportation and storage is another important factor that determine the configuration of the process. Compression of the gases is highly energy demanding and it is another important energy penalty, decreasing the electrical efficiency by 2 to3 %. The possible process scheme for CO_2 processing is shown in Figure 2-4.

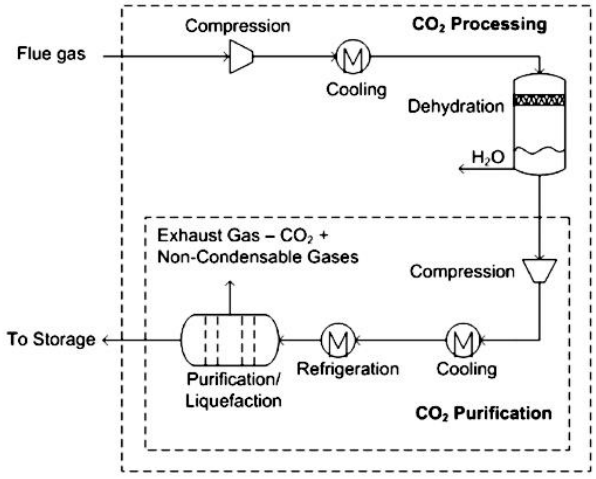

Figure 2-4: The possible process scheme for CO_2 processing [43]

After condensation of water vapour, the CO_2 stream will have purity 70 to 95 %. The purity of the stream depends on the amount of non-condensable gases. It is affected mainly by oxygen purity, oxygen excess and false air intake. The most important diluting gases are the nitrogen and argon from ASU and nitrogen from air ingress. [43], [46]

2.4 SPECIFICATION OF OXYFUEL COMBUSTION IN BUBBLING FLUIDIZED BED

Fluidized bed combustors can be classified to bubbling fluidized bed combustors (BFBC) and circulating fluidized bed combustors (CFBC). The BFBCs are characteristic by lower fluidization velocity, which is above minimum fluidization velocity but below terminal velocity (usually around 1 - 3 m/s, depending on the size and density of the particles). It has also low height of the bed with the evidently bounded surface of the fluidized bed. The majority of bubbling fluidized bed boilers works at lower temperatures than the ash softening temperature

(usually about the temperatures 800 – 850 °C. Particles are not agglomerated under normal conditions. In the BFBCs of higher power output it is necessary to cool the fluidized bed by a heating surfaces that are immersed directly in the bed.

In comparison with previous boilers, CFBC has higher gas velocity, higher than the terminal velocity (usually above 5 m/s). The fluidized bed is expanded in the whole volume of combustion chamber and is similar to pneumatic transport. For provision of stable continual regime it is necessary to use high efficiency cyclone. Cyclone separates majority of the bed particles from flue gas stream that continues through convective passes and recycles the particles back to the combustion chamber.

Although the CFB boilers are efficient and are used for higher power outputs, BFB boilers are justifiable for usage in lower power outputs around 50 MW and in case of using low quality fuels. This work focuses on research of oxyfuel combustion in BFBCs.

Oxyfuel combustion uses oxygen as an oxidant for combustion. Flue gases then consist mainly of CO_2 and water vapour, which is good for easier CO_2 capture, but the combustion in pure oxygen significantly increases the flame temperature and reduces the flue gas volume. This reduction has a negative impact on the heat flux and temperature profiles in a boiler. Oxyfuel combustion overcomes these problems by recycling the flue gas, which has two main reasons:

- It replaces the volume of nitrogen from air and thus provides a sufficient amount of heat carrier [3]
- for FB boilers, it provides a sufficient amount of fluidization medium [47].

Oxyfuel combustion differs from air combustion in several following aspects [3], [5]:

- Oxyfuel combustion is characterized by highly different volume flows of flue gases and oxidant/fluidization medium. The volume of flue gas after recycling is reduced by about 80% $_{vol}$.
- In order to reach the same adiabatic flame temperature it is necessary to reduce the oxygen concentration, by flue gas recirculation on typically 30%$_{vol}$, which is higher than for air combustion (21%$_{vol}$). More than 60% $_{vol}$ of flue gas must be recirculated.
- High concentration of CO_2 and water vapour causes higher emissivity of the flue gas stream. This leads to higher heat transfer in the furnace. In case of retrofitted boiler it is usually necessary to have oxygen concentration lower than 30% $_{vol}$.
- The density of the flue gas is higher during oxyfuel combustion, due to the higher molecular mass of the CO_2 (44 g/mol) compared to nitrogen N_2 (28 g/mol).

- Different properties of the fluidization medium in oxyfuel regime affect the fluidization regime.
- Typical air excess during coal combustion in air is about 20%. In case of oxyfuel combustion, the excess of oxygen is approx. 3-5% to achieve similar O_2 volume fraction in flue gas as in air combustion.
- Concentration of other emissions, without removing in furnace or in the recycle stream, are higher than in air firing.
- Oxyfuel combustion in combination with sequestration requires power for several significant unit operation, such as flue gas compression or oxygen production, that are not required in a conventional air fired plant. This leads to lowering the total efficiency of the plant. However, this loss is comparable with other CCS technologies.

3 EMISSIONS OF SULPHUR OXIDES

3.1 SULPHUR IN COAL

Sulphur is contained in each type of solid fuels and its content varies most commonly in the range from around 0.5 wt% up to 5 wt%. The coal with sulphur content up to 1 wt% is classified as low-sulphur coal, from 1 wt% to 3 wt% of sulphur are medium sulphur coal and coals with more than 3 wt% are known as high-sulphur coals. The superhigh-organic-sulphur coals also exist, having very high amount of organic sulphur, usually in the range between 4 wt% to 11 wt%. [48]

The amount of sulphur and the way how the sulphur is bounded, vary with the type of coal, its age and location of the source. Sulphur in coal has only negative impacts on the fuels quality. The main problem is the production of harmful sulphur oxides, but it also decreases the low heating value and it contributes to the easier self-ignition on the fuel depots.

Sulphur in coal is found in several forms and the problematic of sulphur type determination is very wide. The methodology of sulphur forms determination is summarized in [48]. The major forms are pyritic, organic, sulphates, and traces of elemental sulphur.

Pyrite FeS_2 is the predominant disulphide contained in coal. It is obtained in several forms and sizes in the forms of small grains ranging from the millimetres to the less than one micrometre, but can be also diluted in the form of small platy cleats, cell fillings, nodules or veins. Also some other types of sulphides can be found in coal as well, like ZnS or PbS. [48]

Organic sulphur is bounded to combustible matter by bond C - S and is impossible to be mechanically removed. It is in the form of thiols, sulphides and disulphides and thiophene. The molecular structure is still being under research and new structures are being found with new analytical instrumentations. [48]

The sulphate based sulphur is not usually considered as producing SO_2. It is chemically bounded to the ash in the form of SO_4^{2-} anions. The typical compounds of sulphates in coal are gypsum (calcium sulphate dehydrate), barium sulphate or wide variety iron or iron-aluminium sulphates. However, in some circumstances the sulphates can decompose to produce SO_2. Typical conditions are high temperatures above 1000°C and reduction environment.

Organic and pyritic sulphur account for the bulk of sulphur in coal. The fuel-bound sulphur is release to the gas phase during combustion, pyrites are released according to the reactions:

$$2\ FeS_2(s) \rightarrow 2\ FeS\ (s) + S_2(g) \qquad 3\text{-}1$$

$$2FeS(l) \rightarrow 2Fe + S_2 \qquad 3\text{-}2$$

$$S_2 + 2O_2 \rightarrow 2SO_2 \qquad 3\text{-}3$$

The content of sulphur in fuel is generally defined by the mass fraction in raw state of the fuel S^r [kg/kg] or in dry ash free state of the fuel S^{daf} [kg/kg]. Sometimes we can encounter specific sulphur content given by the relation 3-4 taking into consideration the amount of sulphur with low heating value of the fuel.

$$S_m^r = \frac{S^r}{LHV^r} \cdot 10^2 \qquad [kg/kJ] \qquad 3\text{-}4$$

3.2 FORMATION OF SULPHUR OXIDES

Two types of sulphur oxides arise during combustion – sulphur dioxide SO_2 and sulphur trioxide SO_3. Some other gaseous compounds can be also formed during combustion such as hydrogen sulphide, which arises or is released from organic sulphur compounds under sub-stoichiometric conditions but during typical air combustion conditions its concentration is negligible.

SO_2 is non-explosive, non-flammable, colourless gas, having pungent odour from concentrations around 3 ppm. It is thermodynamically favoured sulphur oxide at high temperatures above 1000°C and oxygen rich region [49]. Both SO_x compounds are toxic, they are also dangerous for whole combustion system, because they are causing both high-temperature and low-temperature corrosion. When releasing to the atmosphere, sulphur dioxide can be converted to sulphur trioxide, which later creates by reactions with water vapour sulphuric acid H_2SO_4. Sulphuric acid has damaging effect in atmosphere, it is usually marked as acid rain. Acid rains damage vegetation, are dangerous for water sources due to their acidification and have devastating effect on water organisms. Acid rains are also damaging a wide variety of building materials – mortar, marble, roofing slate.

Lower temperatures shifts the equilibrium towards SO_3, but the reaction rate is much lower than for SO_2 and during air combustion just 0.1 to 1% is oxidized to SO_3. Typical reactions for SO_3 formation are:

$$SO_2 + O^{\cdot} \rightarrow SO_3 \qquad 3\text{-}5$$

$$SO_2 + OH^{\cdot} \rightarrow HOSO_2^{\cdot} \qquad 3\text{-}6$$

$$HOSO_2^{\cdot} + O_2 \rightarrow SO_3 + HO_2 \qquad 3\text{-}7$$

Sulphur trioxide can be also formed by dissociation of sulphate. The factors influencing the formation of SO_3 are concentration of SO_2, temperature profile, residence time, concentration of O_2, fly ash composition, concentration of NO_2 and presence of catalysts.

Formation of SO_3 under oxyfuel conditions was studied e.g. by [49]. The outlet concentration of SO_3 was about 4 times higher in comparison with air combustion. The main reasons are – presence of SO_2 in oxidizing medium (from flue gas recirculation), higher concentration of O_2 in oxidizing medium and chemical effects caused by the change from N_2 to CO_2. The SO_3 concentrations were also studied in Schwarze Pumpe Oxyfuel Pilot Plant [50] where higher conversion from SO_2 to SO_3 was fuel dependant and ash properties played an important role. Higher conversion of SO_3 was determined for higher sulphuric coal [50].

SO_3 is more dangerous for corrosion, below 500°C it forms gaseous sulphuric acid H_2SO_4 by the reaction with water vapour, which can condensate on surfaces with lower temperature. SO_3 also supports particle formation, which promotes plugging of the last passages of the boiler (air preheater and economiser) but on the other hand it increases the efficiency of electrostatic precipitators. Although, SO_3 can cause problems with the boiler operation, only sulphur dioxide is subjected to emission limits and is being watched. [49]

Volume concentrations of SO_2 are significantly higher under oxyfuel conditions in comparison with air combustion. One of the reasons is the missing volume of nitrogen and generally lower volume of flue gas. Second reason is the FGR, which is an important part of oxyfuel combustion and has significant impact on sulphur retention in the boiler, because SO_2 may be returned to the furnace. [51]

According to [52] the SO_2 emission rate does not depend on the type of oxidizing medium. According to the experiments with different O_2/CO_2 gas mixture and air, the SO_2 emission rate was nearly the same. It leads to the conclusion that the sulphur conversion during coal combustion is controlled by equilibrium and not by the kinetics. The type of coal and its sulphur content is the most important parameter affecting SO_2 emission rates. [52]

Oppositely to above mentioned results, Czakiert [53] states slightly higher conversion of sulphur to sulphur oxides under oxyfuel conditions. This fact is attributed to the reactions of sulphur with different sulphur components, e.g. H_2S to SO_2. With increasing excess of oxygen decreases conversion to SO_2 which is probably caused by conversion of sulphur directly to SO_3 [53]. Similar results states also Hu [41].

Very important factor in production of sulphur oxides is self-retention of released sulphur oxides by neutralization of alkaline components obtained in fuel ash [49]. Combustion conditions in different types of combustors play important role – the behaviour differs among

pulverized coal and fluidized bed boilers. The most important element important for sulphur retention is calcium. In coals, it is usually present as calcite (limestone) or dolomite. The reaction mechanisms with limestone are thoroughly described in another section 3.4. Although the alkaline sulphates (Na/K) can be generated at low combustion temperature, the exact way in which alkaline sulphates are formed in boiler furnaces is poorly understood and calcium is supposed to be the most reactive specie for the SO_2 self-retention [54].

3.3 METHODS OF SULPHUR OXIDES REDUCTION

There are several possibilities of SO_2 emissions removing. Generally we speak about [55] :

- Decrease of fuel consumption
- Changing of high sulphuric fuels into a low sulphuric fuels.
- Decreasing of SO_2 by coal self-retention on the ashes.
- Desulphurization of fuel.
- Flue gas desulphurization.
- Desulphurization in fluidized bed combustion

First two methods are general approaches representing e.g. increase of energy efficiency of combustion facilities or decrease of heat consumption. Changing to lower sulphuric fuel is quite common approach, which can be seen typically in district heating plants, when the coal is changed by natural gas. However, this approach can be for many reasons problematic (e.g. local fuel capacities, economical reasons, technical difficulties).

Sulphur self-retention is a natural process depending on the type of coal, presence of calcium based compounds in ash and construction of the combustion facility.

Desulphurization of coal covers methods, which remove sulphur from coal just before combustion. These methods were under the main scope of research in 1970s and 1980s. The biggest problem for desulphurization of coal are several types of sulphur presented in coal. With increasing requirements on SO_2 emissions and usually very high energy demands and complicated process, these methods cannot complete with desulphurization of flue gas. Among the methods belongs e.g. mechanical separation of pyritic sulphur [56], method of Gravimelt [57], biological desulphurization of coal [56] or Meyers method of desulphurization [58].

Flue gas desulphurization are methods removing SO_2 after combustion processes. FGD is a relatively complicated process where it is necessary to remove relatively small concentrations of SO_2 from a large volume of flue gas. Generally it can be divided into wet, dry or semi-dry

methods. The most commonly used method for FGD in large power generation utility boilers is the wet limestone FGD system, but several others wet methods have been proven – e.g. wet lime and magnesium-lime FGD, seawater FGD, dual-alkali system or ammonia FGD system [59]. Among semi-dry methods belong spray dry FGD systems mostly used for relatively small to medium capacity boilers [59]. The above mentioned methods are flow through, i.e. the sorbent cannot be regenerated. However, methods using sorbents, which enables regeration, can be also used – e.g. sodium-sulphite process (Wellmann-Lord), magnesite process or sodium citrate process [56]. Even if the sorbents can be used in several cycles, the disadvantages of these processes (high energy consumption for regeneration of sorbents, high price of the sorbents or difficulties with the products) do not allow wider applicability of these methods.
Desulphurization of flue gases in fluidized bed boilers is a special type of dry FGD method, feeding the sorbents in-situ during combustion directly to the fluidized bed. A special chapter 3.4 is dedicated to this topic.

3.4 Dry additive method of desulphurization in fluidized bed boilers

The method of dry additive desulphurization is based on the reaction between the SO_2 and solid sorbent, which is added directly to the combustion process. This method of desulphurization is optimal for using in fluidized bed boilers. Among the main reason belongs the possibility of easy optimization of combustion temperature to the optimum value for desulphurization process. The second reason is the process of fluidization which brings high transfer of mass and higher resident time of sorbent in the combustion process. The most commonly used additives are limestone ($CaCO_3$) and dolomite ($CaCO_3 \cdot MgCO_3$). Although dolomite is more reactive, usage of limestone is widely spread mostly because of the price of the limestone and lower attrition in the boiler [60].
Firstly, it is necessary to define effect of desulphurization, which is in this work marked as **SO_2 capture ratio** and is given by the equation:

$$\eta_{capture} = \frac{C_{SO_2\ theoretical} - C_{SO_2\ desulphurized}}{C_{SO_2\ theoretical}} = 1 - \frac{C_{SO_2\ desulphurized}}{C_{SO_2\ theoretical}} \qquad 3\text{-}8$$

$C_{SO_2\ theoretical}$ is theoretical maximal concentration of SO_2 that could be reached by oxidation of all combustible sulphur in the fuel, $C_{SO_2\ desulphurized}$ is real measured concentration of SO_2.

The reaction of the sorbent and SO_2 can proceed via two different routes. The first way can be marked as indirect desulphurization going through two steps – calcination of limestone and sulphation reaction. The second way can be marked as direct sulphation of limestone and can be seen during higher CO_2 partial pressures (e.g. pressurized combustion or oxyfuel combustion). Both principles are described in following parts.

3.4.1 Calcination of limestone

The key factor for desulphurization in FBC under air conditions is calcination of limestone. Calcination is a thermal decomposition of calcium carbonate according to the endothermic reaction 3-9:

$$CaCO_3 \rightarrow CaO + CO_2 \qquad \Delta H = 182{,}1\ kJ/mol \tag{3-9}$$

In case of using dolomite as a sorbent, calcination occurs in two steps. First step is a thermal decomposition of the calcium carbonate and magnesium carbonate, which starts at temperatures around 600°C:

$$CaCO_3 \cdot MgCO_3 \rightarrow CaCO_3 + MgCO_3 \tag{3-10}$$

Another step is calcination of magnesium carbonate, which begins in lower temperatures around 760°C:

$$CaCO_3 + MgCO_3 \rightarrow CaCO_3 + MgO + CO_2 \tag{3-11}$$

Further calcination of calcium carbonate takes places according to the reaction 3-9. Magnesium oxide reacts with sulphur oxide just very slowly at typical FBC temperatures and can be considered as an inert part of additive.

Calcination is mostly influenced by fluidized bed temperature and CO_2 concentration. The equilibrium curve of limestone calcination is shown in Figure 3-1 and is defined according to the following relation [61]:

$$p_{CO_2,eq.} = 1.2 \cdot 10^7 \cdot e^{\left(\frac{E_a}{R \cdot T}\right)} \tag{3-12}$$

where E_a is activation energy and equals 159 000 kJ/kmol. The area of combustion on the right side of the equilibrium curve is the area where calcination of limestone occurs. On the left side of the equilibrium curve, the opposite reaction to the reaction 3-9 occurs which is called carbonation.

We can see that the area of typical air combustion (marked by orange colour in Figure 3-1) is in the area of calcination. The area of oxyfuel combustion is wider, depending on many factors, such as the case of wet or dry FGR or the type of used fuel and it is possible to get to the area were no calcination occurs. This problematic is closely discussed in chapter 3.5.

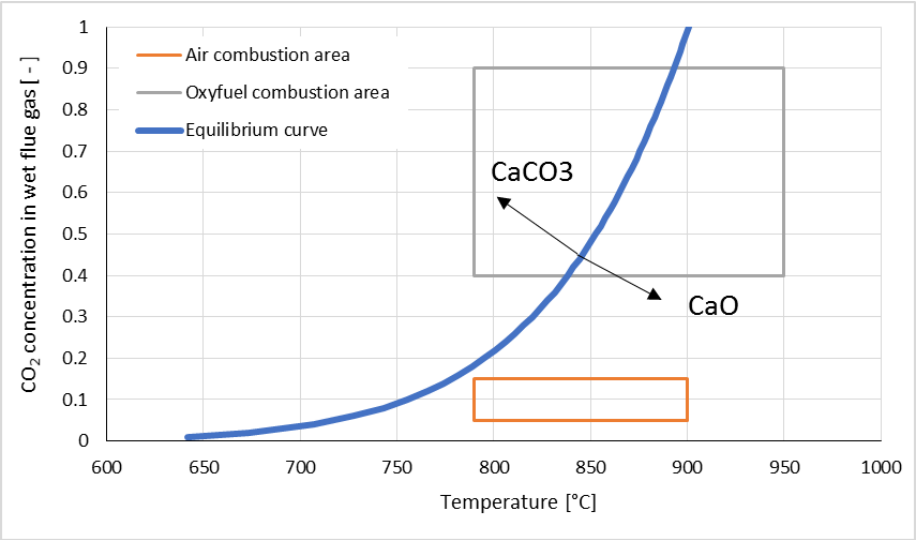

Figure 3-1: Equilibrium curve of calcination of limestone

3.4.2 Sulphation reactions

The desulphurization reaction (sulphation) can be summarized by equation 3-13 [62]:

$$CaO + SO_2 + \frac{1}{2}O_2 \rightarrow CaSO_4 \qquad \Delta H = -481\ kJ/mol \tag{3-13}$$

However, there are several possibilities of reaction CaO and SO_2 on $CaSO_4$. Some pathways were published by Anthony [62] (from equation 3-14 to 3-19). Till this time, no consensus was stated, which reaction takes the main part on the conversion. Different authors state different results on the various types of additives.

$$CaO + SO_2 \rightarrow CaSO_3 \tag{3-14}$$

$$CaSO_3 + \frac{1}{2}O_2 \rightarrow CaSO_4 \tag{3-15}$$

$$SO_2 + \frac{1}{2}O_2 \rightarrow SO_3 \tag{3-16}$$

$$CaO + SO_3 \rightarrow CaSO_4 \tag{3-17}$$

$$4CaSO_3 \rightarrow CaS + 3CaSO_4 \tag{3-18}$$

$$CaS + 2O_2 \rightarrow CaSO_4 \tag{3-19}$$

Calcium sulphate is the final product of the desulphurization reactions. It is a white, stabile solid, poorly soluble in water. In FBC it is mixed with the fluidized bed and it is impossible to separate it from ash. This fact leads to one of the main disadvantage – it increases the amount of solid residues after combustion.

Another disadvantage is a relatively low desulphurization rate while using stoichiometric Ca/S ratio. The Ca/S ratio in molar scale expresses the amount of calcium added to the fluidized bed to the amount of sulphur in fuel. For higher desulphurization it is necessary to use twice or three

times $CaCO_3$ more than the amount of created $CaSO_4$ (in molar scale). The reason is that the reactions are heterogeneous between gas and solid phase and diffusion plays important role in it. Sulphation is thus the controlling mechanism of desulphurization process.

3.4.3 Parameters affecting the SO_2 capture

The process of calcination and sulphation can be affected by several parameters. One of the most important parameter is the amount of used additive, usually expressed as molar Ca/S ratio. The other parameters can be divided into three general categories:

- Effects of the different additive properties
- Effects of the different parameters of the combustion process
- Effect of the boiler design

3.4.3.1 Ca/S ratio

Ca/S ratio represents in the molar scale the amount of calcium added to the fluidized bed related to the amount of combustible sulphur in fuel. In case of stoichiometric ratio, thus Ca/S=1, the SO_2 capture ratio does not exceed 50%. In order to increase the SO_2 capture it is necessary to increase the Ca/S ration. The dependence between the SO_2 capture ratio and the Ca/S is not linear as can be seen in Figure 3-2, but can be expressed by an inversely exponential function [60]:

$$\eta_{capture} = 1 - e^{-K\cdot\left(\frac{Ca}{S}\right)} \qquad 3\text{-}20$$

Coefficient K depends on the fuel type, limestone type, fluidized bed temperature and other operation parameters of the boiler and combustion process. In case of bubbling fluidized bed temperatures and common operation parameters of the boiler it equals approximately K=0.41 [60].

In order to predict the amount of limestone, which is necessary to reach some emission limit, it can be expressed as:

$$\mathrm{Ca/S} = -\frac{\ln\left(1 - \frac{\eta_{\mathrm{desulp}}}{100}\right)}{\mathrm{K}} \qquad 3\text{-}21$$

η_{desulp} expresses the required SO_2 capture ratio ,which is usually get by the value of the emission limit:

$$\eta_{\mathrm{desulph}} = 100 - \frac{\mathrm{C}_{\mathrm{SO_2 emission\ limit}}}{\mathrm{C}_{\mathrm{SO_2 theoretical}}} \cdot 100 \qquad 3\text{-}22$$

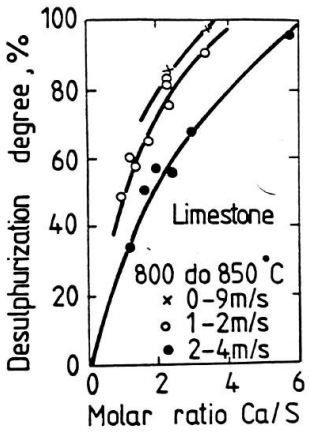

Figure 3-2: Influence of Ca/S ratio on SO_2 reduction [60]

3.4.3.2 Effect of the different additive properties

Limestone and dolomite are the most commonly used materials for desulphurization in fluidized bed boilers. Limestone is very common rock formed mostly of calcium carbonate. Most carbonate rocks origins from the deposited seawater. Limestones vary greatly in many properties. There are two types of limestone based on crystal forms – aragonite (orthorhombic) and calcite (rhombohedral). Majority of limestone used for desulphurization is in the form of calcite. Although there are differences between the geological type and chemical properties, there was founded no clear relationship in the limestone desulphurization performance. The only except was found for cretaceous type stone or chalk, which always shows very high sulphation capacities. It was also found that limestone obtained from different locations within the same quarry can exhibit different SO_2 adsorption properties. [62]

The most important parameters affecting the desulphurization performance in case of the additive properties are the size of the pores, limestone particle size distribution and chemical composition of the limestone.

The size of the pores

Reactivity of the sorbent is given by its porosity. Calcined limestone is highly porous thanks to the release of carbon dioxide from the porous system. The porosity later decreases by increasing volume and blocking the pores by created calcium sulphide layer. The process is shown in Figure 3-3.

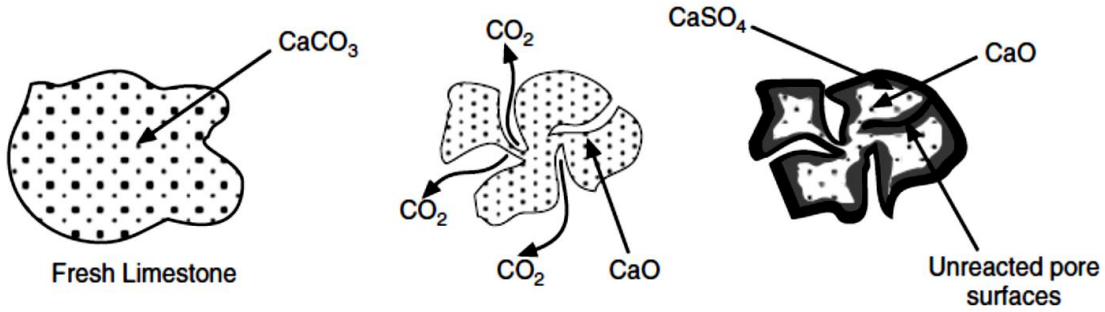

Figure 3-3: Origin of the pores during calcination and creation of the $CaSO_4$ layer on the particle surface [61]

Reactivity of the sorbent can be expressed by following equation:

$$\dot{R} = \frac{\pi \cdot d_p^3}{6} \cdot k \cdot C_{SO_2} \qquad 3\text{-}23$$

The above equation expresses the reactivity of the sorbent as a function of the volume of the sphere having the same diameter as the diameter of the sorbent particle d_p, as the concentration of the SO_2 and as the reaction constant k. Reaction constant is given by the Arrhenius equation:

$$k = k_0 \exp\left(\frac{-E}{RT} A_l f_l\right) \qquad 3\text{-}24$$

Where: $k_0 = 490\ g/cm^2 s$

$E = 7{,}33 \cdot 10^7 J/kmol$

A_l is a specific surface of the sorbent particle and f_l is a conversion factor for the limestone, which expresses the decrease of the sorbent reactivity by the pore blocking of the created calcium sulphide $CaSO_4$. [60]

It can be generally stated, that the younger type of limestone are usually more reactive than the older limestone, which is given by the higher porosity of the younger limestones. [62]

Particle size distribution of the limestone

Figure 3-3 describes the process of calcination and sulphation. The calcium sulphide creates relatively thin layer on the surface of the particle. The smaller are the particles, the bigger is the specific surface of the particles. From this point of view it can be stated, that the finer the particles are, the more sulphide dioxide can be adsorbed on its surface. However, the finer the particles are, the smaller is the residence time they spend in the combustion chamber before they are elutriated and the time for sulphation reaction is shortened. This leads to the statement that there exist some optimal size distribution, depending on the fluidization velocity, particle size distribution of the fluidized bed material, design of the combustion chamber, but also on

the economy of the pulverization of limestone. The optimal size of the sorbent for desulphurization is usually around 200 μm. [60] [63]

Chemical composition of limestone

The main chemical compound coming to the sulphation reaction is calcium carbonate $CaCO_3$, usually expressed as calcium oxide CaO. High percentage of the CaO does not necessarily mean a higher capacity for SO_2 capture. It is possible that some impurities may have a catalytic effect and influence the limestone capacity. Some studies investigated possible positive effect of Fe_2O_3. [4]

3.4.3.3 Effect of the different parameters of the combustion process

The dry additive desulphurization process consist of two main important steps. The first step is calcination of the limestone, the second is the process of sulphation. Both steps can be affected by the parameters of the combustion process – the temperature of the fluidized bed, pressure, fluidization velocity, height of the fluidized bed, concentration of the oxygen in the zone of reactions and the effect of the used fuel. All these parameters are discussed in this chapter.

Temperature

Temperature is the most affecting factor of the desulphurization process. The optimal temperatures for air combustion are in the region from 780 to 900°C. This temperature window is given by the essentiality of the limestone calcination. The calcination under 790°C is very slow and the possibility of desulphurization is thus very limited. The optimum temperature, for which the highest SO_2 capture ratio is reached can vary for different types of limestones. Different types of limestone have different sensitivity towards temperature.

The upper limit of the optimal temperature window is influenced by two factors. At first it is the fact, that the sulphation reaction is very fast and the layer of created calcium sulphate is very strong. This creates a huge unreacted core, and the capacity of sorbent is not satisfactory utilized, because the molecules of SO_2 cannot get deeper inside the pores. The second factor is, the possible reduction of newly-emerged $CaSO_4$ producing back SO_2. Anthony [62] states that the maximal SO_2 capture is reached at the temperatures where the desulphurization reactions competes with the reverse reduction reactions 3-25, 3-26 and 3-27. Above the optimum temperature, the SO_2 capture ratio decreases. CO concentration is an important factor for

desulphurization effect, because with increasing CO concentration mainly at higher temperatures (above 900°C) increases the effect of reverse reduction reactions.

$$CaSO_4 + CO \rightarrow CaO + SO_2 + CO_2 \quad 3\text{-}25$$

$$CaSO_4 + 4CO \rightarrow CaS + 4CO_2 \quad 3\text{-}26$$

$$3CaSO_4 + CaS \rightarrow 4CaO + 4SO_2 \quad 3\text{-}27$$

Pressure

Increasing of the combustion pressure has different effects for usage of limestone and dolomite. In case of using dolomite, the SO_2 capture ratio increases with increasing pressure. In case of using limestone, we get opposite effect. The main reason is insufficient calcination, which is decelerated by higher partial pressure of CO_2. SO_2 is than bounded throw the direct way of sulphation and creates just the thin layer on the surface of the particle. Using pressurized combustion favours dolomite as the suitable sorbent. [60], [63]

Fluidization velocity

Fluidization velocity is the factor, which affects very significantly the processes inside the fluidized bed. However, the effect on desulphurization can be hardly quantified, because fluidization velocity depends on many other parameters, such as excess of air or temperature. The main factor is the residence time of limestone particles in the fluidized bed. With increasing fluidization velocity the small particles starts to elutriate and the utilization of the sorbent is weak. On the other side the higher the velocity is, the better mixing occurs and also the attrition increases, which works in favour with the process of desulphurization. These two effects works against each other. The general statement is that, the effect of elutriation is higher and with increasing fluidization velocity decreases the SO_2 capture ratio. However this process can be eliminated by recirculation of the fly ash. [4]

Height of the fluidized bed

With increasing residence time of the sorbent in fluidized bed and increasing time of the contact between the particles and SO_2, increases also the SO_2 capture ratio. With increasing high of the bed the above mentioned parameters are improved thus the desulphurization is improved. [4]

Oxygen concentration in fluidized bed - air excess

Increasing concentration of oxygen in fluidized bed minimalizes the amount of reduction zones in fluidized bed, thus the reduction of calcium sulphide is lowered. Increasing excess of oxygen

also decreases the concentration of CO_2, which has a positive effect on calcination. Increasing excess of air thus increases the SO_2 capture ratio. [4]

Air staging

In order to lower the emissions of NO_x and CO the majority of boilers is constructed using a secondary or tertiary air supply. The reason is to create a reduction zone in fluidized bed to reduce the amount of NO_x. This has negative effect to desulphurization reactions. The leading factors are usually the emissions of NO_x, which must be lowered under the emission limit by the primary measures. Using SCR or SNCR would be economically unaffected. The lower SO_2 capture ratio must be than balanced by optimization of other parameters or by increasing the Ca/S ratio. [4]

Fuel composition

The composition of the coal can significantly influence the desulphurization rate. High volatile fuels burn faster and in case of loading such a fuel on the fluidized bed, the emission of SO_2 can be released very fast, which reduce the contact time with the sorbent in the fluidized bed.
The positive effect is the presence of calcium oxide in the ash of the fuel. Some types of the fuel could reached up to the 90% of self-desulphurization. [4]
The way how the sulphur is bounded is also very important parameter. While pyritic sulphur usually remains in the fluidized bed and is oxidized during char oxidation, organic bonded sulphur is released mainly in volatile through some intermediate products such as H_2S, COS and CS_2 and oxidize to SO_2, CO_2 and H_2O above fluidized bed. The contact time between the calcined limestone and SO_2 is the crucial factor for sufficient SO_2 capture. It can be expected that coals with higher pyritic content will account higher CaO utilization and higher SO_2 capture.
An individual topic is the effect of biomass co-combustion with coal on desulphurization rate, which is quite problematic. Although, biomass has low amount of ash, it contains compounds which can create some low temperature melting eutectics blocking the calcium oxide particles and negatively affecting the desulphurization. [64]

3.4.3.4 Effect of the boiler design

The optimized design of the boiler can improve the process of desulphurization. There were defined two main parameters – the effect of coal and limestone feeding system and presence of

fly ash recirculation. Both two parameters are important for BFB. CFB is characterized by a high circulation of the fluidized bed, sorbent and fuel and method of the coal feeding does not play any important role.

Coal and limestone feeding system

The way how the fuel and limestone are feed into the combustion chamber has also the effect on the desulphurization. The most optimal system of fuel and limestone feeding is the feeding inside the fluidized bed. However this is technically more difficult solution and majority of boilers uses loading of fuel on surface of the fluidized bed. The major problem is shorter contact time between SO_2 and the sorbent. Limestone feeding on the bed surface leads also to a lower sulphur retention, due to elutriation of fine limestone particles.

Fly ash recirculation

Possibility of fly ash recirculation is an option for higher limestone utilization – it moves BFBC boilers closer to CFBC boilers. Fly ash recirculation can improve the sulphur retention by more than 10%. Figure 3-4 expresses the effect of recirculation. Recirculation coefficient is a ratio between the mass flow rate of recirculated fly ash particles and coal. [4]

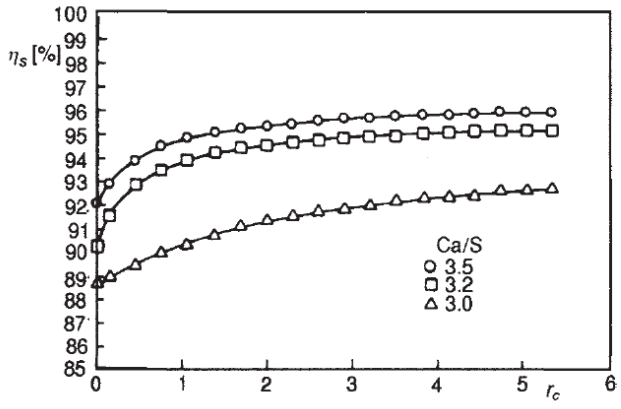

Figure 3-4: Effect of fly ash recirculation on SO_2 capture ratio [4]

3.5 DESULPHURIZATION UNDER OXYFUEL CONDITIONS

Desulphurization under oxyfuel conditions is strongly affected by the high partial pressure of CO_2. Concentration of CO_2 under oxyfuel conditions can vary in relatively high range – from around 40 to 90% depending on the amount of FGR and the type of FGR – wet or dry. Partial pressure of CO_2 is higher than the equilibrium CO_2 partial pressure at usual fluidized bed temperature which leads to stopping calcination. The area typical for oxyfuel conditions is

shown in Figure 3-1 by grey colour. This area reaches both left and right side of the equilibrium curve.

In case of no calcination occurs, many authors state a direct way of desulphurization. Direct sulfation reaction is presently not well known. There are only few suggestions presented in the literature. The following reaction steps can cover the reaction mechanism [65]:

$$CaCO_3 + SO_2 \rightarrow CaSO_3 + CO_2 \quad 3\text{-}28$$

$$2CaSO_3 + O_2 \rightarrow 2CaSO_4 \quad 3\text{-}29$$

$$2CaSO_3 + SO_2 \rightarrow 2CaSO_4 + S \quad 3\text{-}30$$

$$S + O_2 \rightarrow SO_2 \quad 3\text{-}31$$

The overall reaction can be expressed by following equation:

$$CaCO_3 + SO_2 + 0{,}5O_2 \rightarrow CaSO_4 + CO_2 \quad 3\text{-}32$$

The direct way of desulphurization is slower than the indirect way of desulphurization going through limestone calcination. Lower SO_2 capture ratio efficiency can be thus expected. On the other hand, the created layer of $CaSO_4$ on the surface of the limestone particle has greater porosity in comparison to the $CaSO_4$ layer on the surface of the calcined lime particle. This results to the lower diffusion resistance for SO_2 and greater utilization of the limestone, because the pores keep opened for a longer time and the molecules of SO_2 have greater possibility to get deeper into the particle. [66]

The $CaCO_3$ content is higher in the ashes from oxyfuel combustion in comparison to conventional air-firing ashes where the $CaCO_3$ content is usually nearly undetectable due to the calcination process that occurs [31]. The amount of $CaSO_4$ in ashes from oxyfuel combustion is lower compared to air combustion, which leads to the fact, that direct way of combustion shows lower SO_2 capture ratio [31].

According to the shape of the equilibrium calcination curve we can see, that the higher combustion temperatures must be set in order to reach calcination process under higher CO_2 concentration. This has been proven by the presence of unreacted CaO in ashes [31].

The higher optimal temperatures (above 900°C) for desulphurisation under oxyfuel combustion state also other authors. De Diego [67] and de las Obras-Loscartes [68] state the most optimal temperature for desulphurization in the range of 900 to 925°C. Oppositely Eriksson [34] states the most optimal desulphurization temperatures in the range of 800 to 830°C for south African coal and 870°C for Polish bituminous coal. Generally all author state that the optimal desulphurization temperatures for oxyfuel combustion are higher compared to optimal temperatures for air combustion.

4 THE GOALS AND CONTRIBUTIONS OF THE DISSERTATION

The dissertation thesis focuses on oxyfuel combustion in bubbling fluidized bed boilers and **the main goal is to study the process of direct desulphurization during oxyfuel combustion and compare it with the desulphurization process under air combustion.**

The most important contribution and novelty of the thesis is experimental verification of the desulphurization process during oxyfuel combustion in bubbling fluidized bed combustors under real combustion and operation conditions, which is in contrast to the majority of other research which has been made on this topic so far conducted mainly in laboratory conditions or with simulated atmospheres. In order to achieve the main goal of the thesis a suitable experimental facility has to be designed. Moreover the experiments will be run also on the already existing 500 kWt pilot bubbling fluidized bed boiler; this one has to be reconstructed and modified so that it is able to operate under oxyfuel regime. Using two experimental facilities gives another benefit in terms of the possibility of scaling up the results. The results from the experiments should show the pros and cons of the oxyfuel conditions on the desulphurisation process. The main factors influencing the desulphurization process will be defined and optimization of the process will be done.

The individual objectives of the dissertation thesis are summarized in the following points:

1) Theoretical analysis of oxyfuel combustion and its mathematical balance model with the specification on combustion in bubbling fluidized bed boilers and comparison with combustion under air conditions.
2) Design of the experimental facility with the power output about 30 kWt, suitable for working under air and oxyfuel combustion and modification of the bigger 500 kWt BFBC pilot boiler to be able to operate under oxyfuel regime.
3) Experimental validation of the mathematical balance model of oxyfuel combustion.

Previous steps are important and necessary in order to reach the main goal of the dissertation thesis which is defined as:

> **Describe and compare the process of SO_2 capture during bubbling fluidized bed combustion under air and oxyfuel conditions and study the effect of scaling up the experiments from lab-scale facility to pilot scale BFBC.**

5 THEORETICAL ANALYSIS OF THE OXYFUEL COMBUSTION

This chapter reports on a theoretical analysis of oxyfuel combustion, and contains a comparison with combustion using air. A suitable methodology is proposed for stoichiometric calculations and for computations of basic characteristic fluidization properties. The methodology presented here can be applied to calculations for combustion using air, using oxygen-enriched air, and also for full oxyfuel conditions. Oxyfuel combustion and air combustion use different volumes of all streams of gases, which is shown in Figure 5-1. All streams in this figure corresponds to the ratio of the real flows (normal cubic meters per kg of fuel).

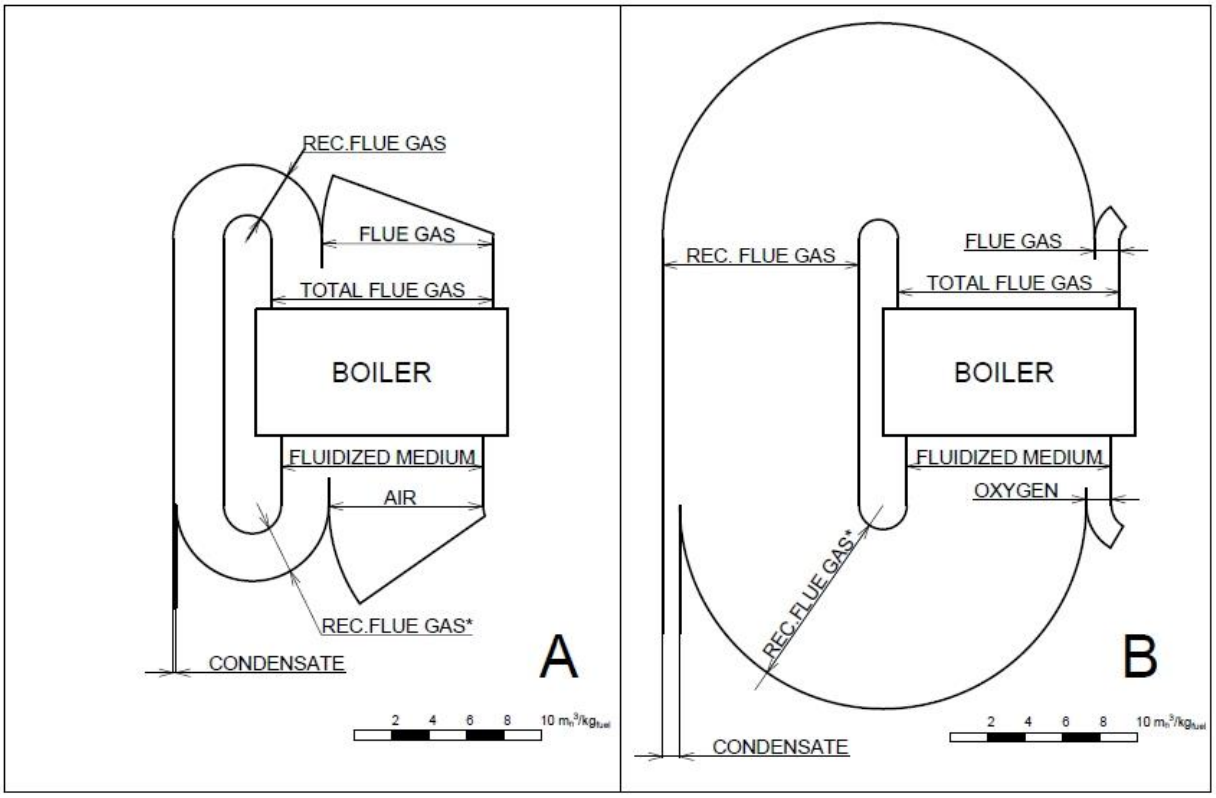

Figure 5-1: A comparison of the volume flow of all streams of gases for combustion with air (A) and with oxygen (B) [I, II]

5.1 METHODOLOGY FOR STOICHIOMETRIC CALCULATIONS [III, IV]

Stoichiometric calculations are volumetric calculations. They are used to determine the amount of oxidant required to burn a unit amount of fuel, and to determine the volume of the flue gases that arise. Stoichiometric calculations are based on chemical reaction equations and the balance of the amount of substance. In general, we consider two basic models here - a complete

combustion model, and an incomplete combustion model. The complete combustion model considers complete combustion of all combustible substances. The incomplete combustion model can calculate with only partial fuel burn out and with unburned carbon formation. Although the incomplete combustion model is more appropriate, the complete combustion is used in most model technical applications, and it is also used here. Relative difference between results using complete and incomplete approaches is typically less than 5 %. [69]

It should be also mentioned, that the effect of addition of $CaCO_3$ on the combustion stoichiometry and balance model was taken into consideration. $CaCO_3$ increases amount of ash and during its calcination produces additional CO_2. However, the differences in volumetric calculations do not exceed 2% in the case of the maximum added limestone (taking into account maximally Ca/S=5) and that is why the effect of $CaCO_3$ is not further used in balances.

By using this methodology it is possible to calculate the balances of all volume streams – volume of oxidant V_O, volume of flue gas V_{FG}, volume of recirculated flue gas V_{REC}, total volume of flue gas V_{TFG} and volume of fluidization medium V_{FM}.

5.1.1 Volume of oxidant V_O

The key step in stoichiometric calculation is to properly determine concentrations of the substances in the oxidant. The term oxidant in this meaning expresses air, oxygen or the mix of air and oxygen in case of partial oxyfuel combustion. Table 5-1 shows the concentrations of the substances for several possibilities of oxidants. Oxygen 1 means 100% pure oxygen which is used for the calculations. In practice it is supposed to use some economical optimum of oxygen purity, usually referred value is 95% [3], this corresponds to oxidant Oxygen 2. Table 5-1 also shows concentrations for two types of oxygen enriched air – Air+oxy 30 and Air+oxy 50, where the numbers corresponds to the oxygen concentrations. The concentration of water vapour in air, presented also in Table 5-1, corresponds to the 70% of relative moisture at 20°C.

Table 5-1: Volume concentration of the substances in different types of the oxidant

	Concentration				
	ω_{O_2}	ω_{CO_2}	ω_{N_2}	ω_{Ar}	ω_{H_2O}
Air	0.2062	0.0004	0.7685	0.0092	0.0157
Oxygen 1	1	0	0	0	0
Oxygen 2	0.95	0	0.05	0	0
Air+oxy 30	0.3	0.0003	0.6777	0.0081	0.0139
Air+oxy 50	0.5	0.0002	0.4841	0.0058	0.0099

At first, the minimum volume of oxygen, which is needed for complete combustion, is calculated (Table 5-2). The excess of air or oxidant is defined as the ratio of the real volume of oxidant which is used for combustion to the minimum volume of oxidant (equation 5-1).

$$\alpha = \frac{V_{O,W}}{V_{O,W,min}} = \frac{V_{O,D}}{V_{O,D,min}} \quad 5\text{-}1$$

It is important to mention, that using α for comparison between air and oxyfuel combustion can be little bit misleading. Due to the significantly reduced volume of flue gas at oxyfuel combustion, the excess of oxidant is lower. For example, concentration of O_2 in flue gas at 6% corresponds to α=1.39 for air combustion, but in case of oxyfuel combustion it equals α=1.055.

5.1.2 Volume of flue gas

The volume of flue gas is given by the sum of the components which are formed during combustion (CO_2, SO_2, N_2 from the fuel, H_2O) and the components which are contained in the oxidant but does not participate combustion process and goes through the process as inert (excess of O_2, N_2, Ar, H_2O) or come into the combustion process from air by its ingress (N_2, O_2, Ar).

The volume of water vapour in the flue gas is influenced by potential condensation of water vapour in the recirculated flue gas, which is explained later. This reduction is expressed by the coefficient C (see Table 5-2). If there is no condensation of water vapour the coefficient C equals 0.

5.1.3 Volume of recirculated flue gas

The flue gas recirculation (FGR) is a very important part of combustion in fluidized bed boilers. The air combustion uses FGR for controlling the temperature of the fluidized bed and for securing the proper fluidization. In the case of oxyfuel combustion, it is the key issue for reducing the temperature in the combustion chamber and for keeping the necessary amount of the fluidization medium flow. FGR is extracted after all heat exchanging parts of the boiler and the amount can be expressed with a proportional recirculation coefficient r [-], related as the ratio of the recirculated flue gas volume to the flue gas volume:

$$r = \frac{V_{REC,W}}{V_{FG,W}} \quad 5\text{-}2$$

By this definition, the value of "r" can be higher than 1, which is typically the case for oxyfuel mode. The "r" greater than 1 means that flow of the recirculated flue gas is higher than flow of the flue gas leaving the combustor out to the stack.

In case of cooling down of the recirculated flue gas under the temperature of the dew point (e.g. because of the low operation temperature of the FGR fan), the water vapour begins to condensate. The methodology of computation given in Table 5-2 includes the reduction of the water vapour due to its condensation.

If we introduce simplifying assumption that we have the ideal gas and that the absolute gas pressure is equal to 0.1 MPa, we can say that the water vapour concentration is equal to the partial pressure of water vapour. The maximum water vapour concentration ω''_{H_2O} at a given temperature will therefore be equal to the saturation pressure for this temperature. The effect of condensation is respected by the coefficient C (Table 5-2).

Coefficient C is a simplified method for evaluation of the flue gas condensation, respecting the partial pressure of water vapour only. It does not respect the effect of sulfuric acid dew point, which causes an increase of the flue gas dew point temperature. Sulfuric acid is formed by the reaction of sulphur trioxide with water vapour. If we consider the generally accepted fact, that approx. 1 % of all SO_2 in air fired mode to 5 % in oxyfuel mode is converted into SO_3, the maximum concentration of SO_3 is in tens to hundreds of ppm [70]. This amount is negligible in comparison with the concentration of water vapour, which is from about 15 % in air mode to 40 % in oxyfuel mode. This fact allows us to presume that the effect of the sulfuric acid condensation is negligible for the calculation of the coefficient C and for the total volume balance. [II]

If the gas temperature in the system does not fall below the dew point temperature (in the case of the oxyfuel mode below approx. 80 °C) there is no condensation and the volume of water vapour in the recirculated flue gas is calculated using the same relation as the calculation for other compounds (eq. 5-3) and total volume of wet recirculated flue gas is according to eq. 5-4:

$$V_{REC,H_2O} = r \cdot V_{FG,H_2O} \quad 5\text{-}3$$

$$V_{REC,W} = V_{REC,D} + V_{REC,H_2O} \quad 5\text{-}4$$

5.1.4 Volume of total flue gas

Total volume of flue gas is the real volume, which is released from the boiler (see Figure 5-1). It is the sum of the recirculated flue gas and flue gas, which arises from oxidant. This stream is going through the boiler and it is the main heat carrier.

5.1.5 Volume of fluidization medium

To correctly determine the flow properties of the fluidization medium, it is necessary to know the composition and the concentration of the individual components. Fluidization medium consists of the volume of recirculated flue gas and volume of oxidant (see Table 5-2).

Table 5-2: List of equations for calculation the volume flows in the boiler [III], [IV]

	Volume of oxidant	Volume of flue gas	Volume of recirculated flue gas	Total volume of flue gas in the boiler	Volume of fluidization medium
$V_{\dots,O_2}$	$\alpha \cdot 22.39 \cdot \left(\frac{C^r}{12.01} + \frac{H^r}{4.032} + \frac{S^r}{32.06} - \frac{O^r}{32}\right)$	$\frac{\alpha - 1}{\alpha} \cdot \omega_{O_2} \cdot V_{O,D}$	$r \cdot V_{FG,O_2}$	$V_{FG,O_2} + V_{REC,O_2}$	$V_{O,O_2} + V_{REC,O_2}$
$V_{\dots,N_2}$	$\alpha \cdot \omega_{N_2} \cdot V_{O,D,min}$	$\frac{22.4}{28.016} \cdot N^r + V_{O,N_2}$	$r \cdot V_{FG,N_2}$	$V_{FG,N_2} + V_{REC,N_2}$	$V_{O,N_2} + V_{REC,N_2}$
$V_{\dots,CO_2}$	$\alpha \cdot \omega_{CO_2} \cdot V_{O,D,min}$	$\frac{22.26}{12.01} \cdot C^r + V_{O,CO_2}$	$r \cdot V_{FG,CO_2}$	$V_{FG,CO_2} + V_{REC,CO_2}$	$V_{O,CO_2} + V_{REC,CO_2}$
$V_{\dots,Ar}$	$\alpha \cdot \omega_{Ar} \cdot V_{O,D,min}$	$V_{O,Ar}$	$r \cdot V_{FG,Ar_2}$	$V_{FG,Ar} + V_{REC,Ar}$	$V_{O,Ar} + V_{REC,Ar}$
$V_{\dots,SO_2}$	$\alpha \cdot \omega_{SO_2} \cdot V_{O,D,min}$	$\frac{21.89}{32.06} \cdot S^r + V_{O,SO_2}$	$r \cdot V_{FG,SO_2}$	$V_{FG,SO_2} + V_{REC,SO_2}$	$V_{O,SO_2} + V_{REC,SO_2}$
Total volume of dry gas $V_{\dots,D}$	$\sum_i V_{O,i}$	$\sum_i V_{FG,i}$	$\sum_i V_{REC,i}$	$\sum_i V_{TFG,i}$	$\sum_i V_{FM,i}$
$V_{\dots,H_2O}$	$V_{O,W} - V_{O,D}$	$V_{FUEL\,H_2O} + V_{O,H_2O} - C$	$V_{REC,W} - V_{REC,D}$	$V_{FUEL,H_2O} + V_{O,H_2O} + V_{REC,H_2O}$	$V_{O,H_2O} + V_{REC,H_2O}$
Total volume of wet gas $V_{\dots,W}$	$\kappa \cdot V_{O,D}$	$V_{FG,D} + V_{FG,H_2O}$	$\frac{V_{REC,D}}{1 - \omega_{H_2O}}$	$V_{TFG,D} + V_{TFG,H_2O}$	$V_{FM,D} + V_{FM,H_2O}$

Minimum volume of oxidant	$V_{O,min} = \frac{V_{O,O_2}}{\omega_{O_2}} = \frac{22.39 \cdot \left(\frac{C^r}{12.01} + \frac{H^r}{4.032} + \frac{S^r}{32.06} - \frac{O^r}{32}\right)}{\omega_{O_2}}$
Volume of water vapour arisen only by combustion of the fuel	$V_{FUEL,H_2O} = \frac{44.8}{4.032} \cdot H^r + \frac{22.4}{18.016} \cdot W^r$
Coefficient for reduction of water vapour in case of condensation	$C = \frac{r \cdot \left(V_{FUEL,H_2O} + V_{O,H_2O} - \frac{\omega''_{H_2O} \cdot V_{FG,D}}{1 - \omega''_{H_2O}}\right)}{r + 1}$
Values i	O_2, N_2, CO_2, Ar, SO_2

5.2 THEORETICAL APPLICATION OF OXYFUEL COMBUSTION IN A BFB

The above mentioned methodology of theoretical calculation was used for verification of oxyfuel combustion in BFB. Fuel used for the calculation is also used for experimental part of the work - it is Czech brown coal from the North Bohemia coal basin called Bílina. Its proximate and ultimate analyses are stated in chapter 6.3.

In order to predict the possibility of usage the oxyfuel combustion in BFB, two main conditions should be met:

- the produced heat in the furnace should be similar to the air combustion in order to ensure the stability and quality of the combustion and reaching the required fluidized bed temperature
- the hydrodynamic characterisation of the fluidized bed should be similar to air combustion in order to ensure stabile fluidization regime

The verification of the oxyfuel combustion was thus based on finding such a state, which could be comparable with the reference air combustion in terms of the similar fluidized bed temperature and in terms of ensuring sufficient amount of fluidized medium. This would allow to assume that the oxyfuel combustion is applicable also for the BFB technology. Important assumption for the verification is that we consider constant fuel load for air and for oxyfuel state. [V]

Due to the complicated theoretical calculation of fluidized bed temperature, the adiabatic combustion temperature (T_{ad1}) was chosen as one of the correlation parameters. It is possible to determine the adiabatic combustion temperature from the heat released in combustion chamber, which can be determined from the adiabatic flue gas enthalpy:

$$Q_u = I_{ad} = LHV^r \cdot \left(1 - Z_C - Z_{CO} - Z_f\right) + Q_{fuel} + Q_{fm} \qquad \left[\frac{kJ}{kg_{pal}}\right] \qquad 5\text{-}5$$

The second parameter used for verification was the volume of fluidization medium.

Air combustion with adjusted parameters listed in the Table 5-3 was assumed as a reference state. These parameters account to the real combustion conditions for combustion in BFBC and were verified in the experimental facilities used in this work. Stated FGR temperature is above the dew point temperature (condensation of the sulphuric acid is in these calculation neglected) and no water vapour is condensed in FGR.

Calculations for oxyfuel combustion were set in order to get the same oxygen concentration in flue gas as during the reference air combustion, thus for air excess 1.4 it corresponds to the 6% of oxygen in flue gas.

Table 5-3: Parameters of the reference air combustion

Excess of air	Recirculation coefficient	FGR temperature
40%	0,3	100 °C

Comparison was made by using two normalized parameters – normalized adiabatic flame temperature T_{ad} and normalized volume of fluidized medium V_{fm}:

$$T_{ad} = T_{ad1}/T_{ad0} \quad [-] \quad 5\text{-}6$$

$$V_{fm} = V_{fm1}/V_{fm0} \quad [-] \quad 5\text{-}7$$

The calculated reference air state values of T_{ad0} and V_{fm0} are $T_{ad0} = 1180°C$ and $V_{fm0} = 9{,}7\ m_n^3/kg_{pal}$. The only parameter which can be used for setting the oxyfuel regime is the amount of FGR referred by recirculation coefficient r. The effects of FGR on the studied parameters are stated in Figure 5-2 considering wet FGR, respectively in Figure 5-3 considering dry FGR in oxyfuel mode. [IV]

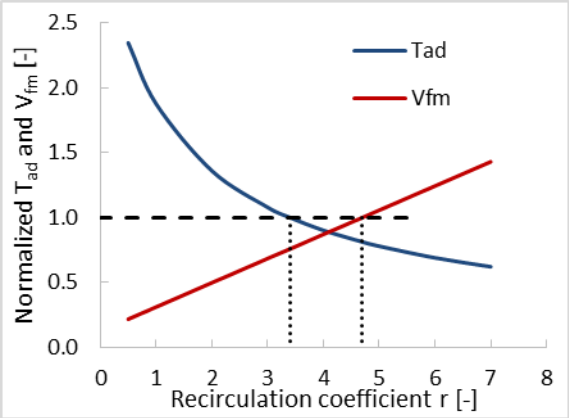

Figure 5-2: Effect of the amount of recirculated flue gas on adiabatic flame temperature and on volume of fluidized medium considering no condensation of water vapour in FGR [IV]

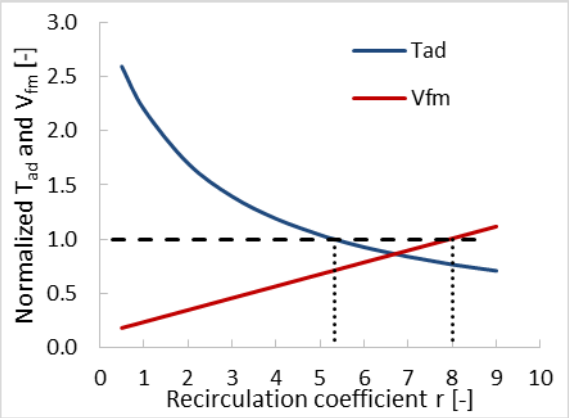

Figure 5-3: Effect of the amount of recirculated flue gas on adiabatic flame temperature and on volume of fluidized medium considering dry FGR (full condensation of water vapour in FGR) [IV]

Figure 5-2 and Figure 5-3 show the inverse effect of the FGR on adiabatic flame temperature and on volume of fluidized medium. With increasing amount of FGR (increasing coefficient r) decreases adiabatic flame temperature, while the volume of fluidized medium logically

increases. The dash line in Figure 5-2 and Figure 5-3 expresses the reference state of air combustion. It can be seen, that in the intersection of this dash line and the functions expressing the normalized values of T_{ad} and V_{fm} we get the values of recirculation coefficient with the same properties of the reference case. It can be seen that it is impossible to achieve equal oxy-combustion and air combustion regimes in terms of having simultaneously the same thermodynamic and hydrodynamic parameters, i.e. to keep the same thermal and fluidization conditions. The lower boundary limit is given by the recirculation coefficient $r = 3.4$ which defines equal adiabatic flame temperature. The O_2/CO_2 ratio (dry state) equals to 30/70 for this case and gives the same thermodynamic characteristic as air combustion. On the other side, the volume of fluidized medium is one quarter lower in comparison with air-combustion. This can lead to the insufficient fluidization, low fluidization velocity and problems with operation of the boiler. [IV]

In case of higher boundary limit (recirculation coefficient $r = 4.7$), we get the same volume of fluidization medium. The O_2/CO_2 ratio in fluidized medium (dry state) equals to 25/75 for this case and the adiabatic combustion temperature is 200°C lower in comparison with air-combustion. This leads to the strong decrease of fluidized bed temperature.

Figure 5-3 expresses the effect of FGR on adiabatic flame temperature and on volume of fluidized medium in case of using dry FGR, thus all water vapour in flue gas is condensed. The missing volume of water vapour is substituted by higher amount of recirculation. The boundary limits are $r = 5.3$ respectively $r = 8$ with the similar effect. [IV]

In order to keep the sufficient fluidization during oxy-combustion, it is necessary to check also the fluidization velocity, not just the volume of fluidization medium. The reason for this is given by different composition and thus different physical properties of the fluidization medium and recirculated flue gas. The composition of the streams is presented in Figure 5-4 and Figure 5-5. There are shown cases with FGR coefficient on the lower boundary, it means the situation with the same thermodynamic characteristic but with the lower amount of fluidization medium. [IV]

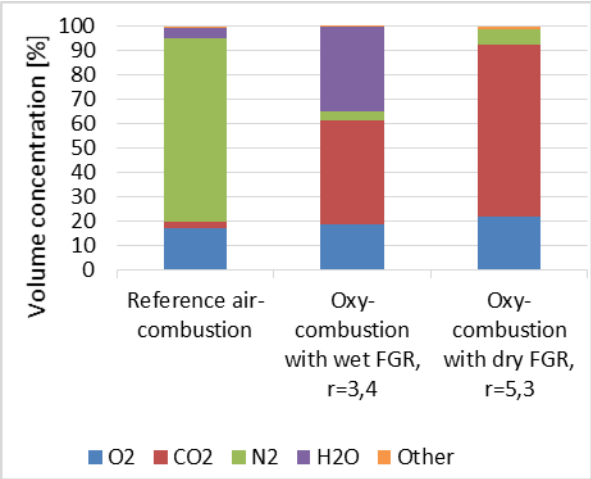

Figure 5-4: Composition of the fluidized medium

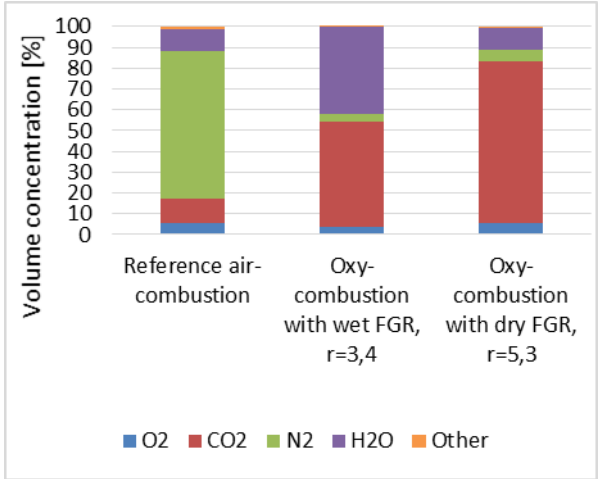

Figure 5-5: Composition of the flue gas

Two characteristic fluidization velocities were calculated – minimum fluidization velocity and terminal velocity. These values express the limit cases of the bubbling regime of fluidization. Minimum fluidization velocity u_{mf} is the velocity in which the buoyancy and the drag forces of the flowing stream counterbalances the gravity of the particles and the material starts to fluidize. The minimum fluidization velocity can be described by several correlations, but the most widely empirical correlation uses the combination of the Ergun correlation of the fixed bed pressure drop with the forces equilibrium of the solid particle. As a result we get the equation obtaining a quadratic dependence of u_{mf} [71]:

$$\frac{1{,}75}{{\varepsilon_{mf}}^3 \cdot \Phi_s}\left(\frac{d_p \cdot u_{mf} \cdot \rho_f}{\mu}\right)^2 + \frac{150\left(1-\varepsilon_{mf}\right)}{{\varepsilon_{mf}}^3 \cdot {\Phi_s}^2}\left(\frac{d_p \cdot u_{mf} \cdot \rho_f}{\mu}\right) = \frac{{d_p}^3 \cdot \rho_f \cdot \left(\rho_s - \rho_f\right) \cdot g}{\mu^2} \tag{5-8}$$

Terminal velocity of particle u_t is another important characteristic, describing the state, when the material starts to elutriate from the fluidized bed.

$$u_t = \left(\frac{4 d_p \left(\rho_s - \rho_f\right) g}{3 \rho_f C_D}\right)^{1/2} \tag{5-9}$$

C_D is the drag coefficient. There are several correlations for its calculation. For non-spherical particles we can use equation by Haider and Levenspiel [71].

$$C_D = \frac{24}{Re_p}\left[1 + (8{,}1716 e^{-4{,}0655\Phi_s}) {Re_p}^{0{,}0964+0{,}5565\Phi_s}\right] + \frac{73{,}69 (e^{-5{,}0748\Phi_s}) Re_p}{Re_p + 5{,}378 e^{6{,}2122\Phi_s}} \tag{5-10}$$

The fluidized bed material used for the experiments and for the calculation was the own ash of the used fuel. Its characteristic and the results from the calculation are stated in Table 5-4. The mean diameter was calculated according to the results from PSD analysis. The density and bulk density were measured, value of sphericity was estimated.

Table 5-4: Calculation of the characteristic velocities

Input values			
Mean diameter of the particle d_p	Density ρ_s	Bulk density ρ_b	Sphericity Φ_s
0.37 mm	2195 kg/m^3	787 kg/m^3	0.75

	Reference air combustion	Oxy-combustion with wet FGR, r=3.4	Oxy-combustion with dry FGR, r=5.3
Minimum fluidization velocity u_{mf} [m/s for 900°C]	0,177	0,173	0,175
Terminal velocity u_t [m/s for 900°C]	1,92	1,86	1,79

The results in Table 5-4 show only a minimal effect of different composition of the fluidization stream on minimum fluidization velocity. The effect on terminal velocity is very similar. In case of using dry FGR the difference is up to 7%, which alert us to the possible earlier elutriation of the material, however the effect is relatively weak.

From the theoretical point of view, we can draw a conclusion, that it is impossible to achieve equal oxy-combustion and air-combustion regimes in terms of simultaneously having the same thermodynamic and hydrodynamic parameters. Figure 5-2 and Figure 5-3 show the limit cases. For fluidized bed combustion it is necessary to ensure sufficient fluidization – in practice it means to use twice or three times higher velocity than the minimum fluidization velocity. The possible decrease of the temperatures can be minimalized by a higher fuel supply, thus increased power load of the bed.

5.3 EFFECT OF WATER VAPOUR CONDENSATION IN FGR

Concentration of water vapour in oxyfuel flue gas can vary in relatively large interval depending on the water content in the fuel and mainly on the flue gas recirculation temperature. The effect of temperature on water condensation can be expressed by coefficient C explained in chapter 5.1.3. This coefficient takes into consideration the maximum partial pressure of water vapour at given temperature. The effect of condensation of acid gases is in terms of these volumetric calculation neglected. The reason for this neglecting is that the volume of acid gases is much

lower (more than two orders lower) in comparison with water volume, although the concentrations of acid gases are higher in oxyfuel combustion due to the lower amount of flue gas. However the effect of acid gases cannot be neglected in terms of material selection and corrosion problems.

The effect of temperature in FGR on water vapour concentration is shown in Figure 5-6. We can see, that the H_2O concentration in flue gas without condensation is more than 40%. The condensation of such a flue gas starts at the temperature of 78°C at normal pressure. The diagram in Figure 5-6 expresses the decrease of the H_2O concentration in flue gas, respectively in fluidization medium, depending on temperature in flue gas recirculation. It can be also seen that with increasing condensation of H_2O it is necessary to increase recirculation ratio in order to keep the same amount of fluidization medium.

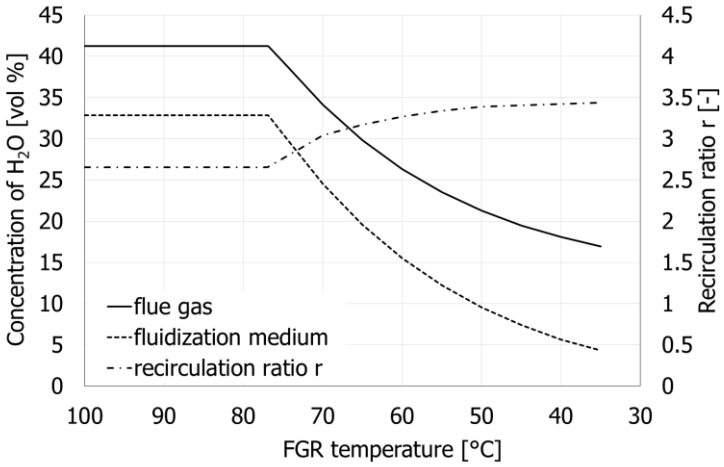

Figure 5-6: Effect of FGR temperature on water vapour concentration

5.4 EFFECT OF FALSE AIR INGRESS ON CO_2 CONCENTRATION

The main effort of oxyfuel combustion is to achieve as high CO_2 concentration as possible. Theoretically, the CO_2 concentration in dry flue gas should reach 90 to 95% CO_2, depending particularly on the fuel properties, excess of oxygen and purity of used oxygen. The purity of used oxygen is the question of the technical-economic optimization of ASU. The most important parameter affecting the CO_2 concentration is false air ingress into the combustor. Even relatively small amount of false air ingress decreases the CO_2 concentration. The numerically obtained dependence is presented in Figure 5-7. The false air ingress is related to the volume of oxygen flow into the combustor as well as to the volume of fluidization medium (FM). We can see that only about 5% of false air ingress related to the volume of FM decreases the output CO_2 concentration from 93% to 74% vol. in dry flue gas. [IV]

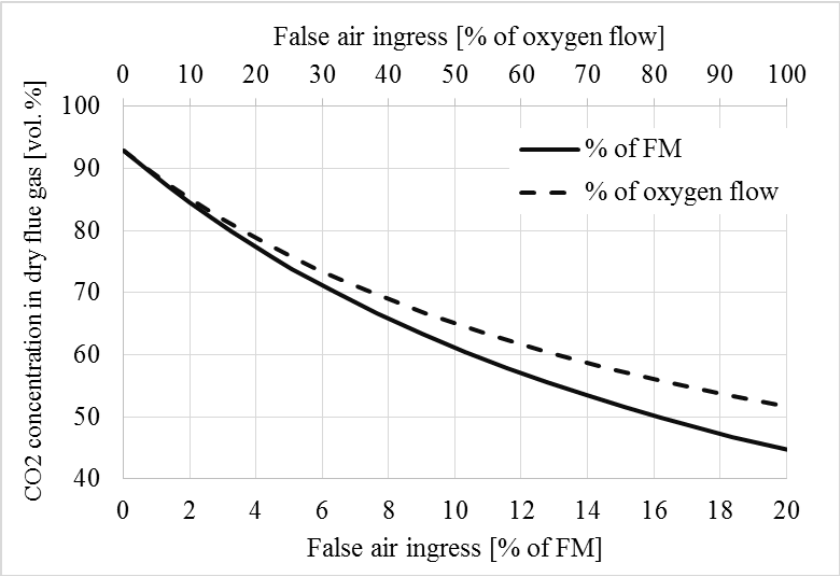

Figure 5-7: The effect of false air ingress on CO_2 concentration in dry flue gas [IV]

5.5 EVALUATION OF SULPHUR DIOXIDE EMISSIONS UNDER OXYFUEL COMBUSTION.

The most common analytical method for continuous measurement of SO_2 in a flue gas is on-line extraction and treatment of a flue gas sample and its analysis with the NDIR method. The results are obtained in volume fraction in dry flue gas. The common practice for comparison of the emissions is to calculate the mass concentration and refer it to the reference amount of oxygen. [VI], [VII]

$$c_{SO_2} = \omega_{SO_2,\text{measured}} \cdot \frac{M_{SO_2} \cdot p_N}{R \cdot T_N} \cdot \frac{21 - O_{2\,\text{ref}}}{21 - O_{2\,\text{measured}}} \qquad [\text{mg/Nm}^3] \quad 5\text{-}11$$

The reference amount of oxygen in flue gas for coal combustion is 6%. However, this practise can be used just for air combustion as the number 21 refers to the 21% of oxygen in air. Furthermore, the measured volume fraction of course depends on volume of the flue gas, which is about 80 % lower in oxyfuel combustion mode. Therefore, SO_2 emissions from oxyfuel combustion cannot be recalculated using the eq. 5-11. The most suitable way for comparison of emissions in oxyfuel combustion is application of emission factors. The emission factor is typically defined as the amount of a concerned pollutant emitted per the unit of burned fuel mass. [VI], [VII]. This is often referred to the mass-based emission factor and has units such as g of a pollutant per kg of burned fuel. An alternative representation is done by the amount

of a pollutant per MJ of calorific value of the fuel. The emission factor for each gas component X is defined [VII]:

$$EF_{mass}^{X} = V_{FG} \cdot c_X \qquad [\text{mg/kg}_{\text{fuel}}] \quad 5\text{-}12$$

Where V_{FG} is calculated specific volume of flue gas related to a unit of the combusted fuel. The emission factor related to the LHV of a fuel is then obtained as follows [VII]:

$$EF_{LHV}^{X} = \frac{EF_{mass}^{X}}{LHV} \qquad [\text{mg/MJ}_{\text{LHV}}] \quad 5\text{-}13$$

6 EXPERIMENTAL SET-UP

In order to fulfil the goals of the thesis and proceed the experimental part, it was necessary to design suitable lab-scale experimental facility having the size in order of tens of kW. This is bubbling fluidized bed combustor having the power output around 30 kW. This size of the facility is optimal for easy combustion control and for studying the optimization of the oxyfuel combustion process. Results from this experimental facility were later validated on bigger pilot plant facility – 500 kW bubbling fluidized bed boiler, which was reconstructed and optimized for oxyfuel combustion.

6.1 30 KW LABORATORY BUBBLING FLUIDIZED BED COMBUSTOR

The experimental facility "MiniFluid" was designed in order to cover relatively large field of various experiments. The facility is made of several modules, which are easily exchangeable and can be optimized for specific purposes. The facility can work both in cold regime without combustion in order to study e.g. fluidization properties of the fluidized bed materials but also in combustion regimes from air to pure oxyfuel combustion. The power output is about 20 to 30 kW depending on fuel load and fuel quality. Figure 6-1 shows the schematic diagram of the facility, Figure 6-2 is the photograph of the facility. [VIII]

The combustion chamber and freeboard part were designed with rectangular cross-section in order to copy the real scale BFB boilers. The combustor consists of windbox section (1), distributor (2), dense bed zone (3), transitional section with cross section enlargement and freeboard section (4). The main dimensions are shown in Table 6-1. The most important operational part of the facility is the primary fan, which ensures the air supply during air combustion but serves also as a recirculation fan (5).

The combustion air enters the windbox part at the bottom of the facility. Windbox serves for stabilization of the fluidization medium flow to have uniform load on the distributor. Distributor (2) is made of perforated plate. Above distributor the bed section zone (3) is placed. The height of the fluidized bed can be controlled by placing the side channel overflow (6), which ensures the constant height of the bed during the experiments. The side channel overflow can be placed at two positions 25cm and 35 cm above the distributor. The fuel feeding (7) is provided by a screw conveyor putting the fuel at the top of the fluidized bed. The flue gas then enters the freeboard section (4) with larger cross-section area, in order to slow down the stream and decrease elutriation of the particles. The secondary air (8) inlet is located at the beginning of freeboard section but is not used for oxyfuel combustion. For purposed of oxygen staging, a

secondary oxygen supply is attached at the same location. Flue gas later passes the cyclone (9) for fly ash separation and escapes the system by the flue gas fan to the stack. All parts are heat insulated by ceramic insulation.

The combustor is started by gas burner (10), which is placed to the windbox section and which warms up the fluidized bed. After reaching the ignition temperature, the fuel load is started. The gas burner is removed and the amount of fluidization air is increased to start fluidization. The system is always started on air combustion.

The fluidized bed temperature and oxyfuel regime are controlled by flue gas recirculation. FGR is taken just behind the cyclone and is set by opening and closing the flue gas recirculation valve (11). The recirculated flue gases passes the water-cooled heat exchanger (12). A condensate collector is placed beneath the cooler. After stabilization of the combustion process, the transition to the oxyfuel regime can begin. While the flue gas recirculation valve is fully opened, the primary air valve (13) is being closed and amount of oxygen supply is being increased. Oxygen is supplied from the bottle bundle and is introduced to the FGR tube. The amount of oxygen supply is set by the mass flow controller (14). In order to reduce the false air ingress during oxyfuel regime and reach the maximum CO_2 concentration, the reactor is properly sealed. All flanges between the sections are sealed by double sealing cords and all openings are sealed. Also the flue gas fan (15) is shut down during oxyfuel regime and the system works in a small overpressure.

Measured values are volume flow of air supply, volume flow of FGR, volume flow of oxygen supply, volume flow of secondary air supply, mass flow of the fuel, fluidized bed pressure drop and temperature profiles along the whole height of the reactor. Emission monitoring is continuous, flue gases are taken before the flue gas ventilator. Monitored emissions are O_2, CO, CO_2, NO_x and SO_2.

All the system is driven by LabView software, demonstration of the control program is shown in Figure 6-3.

Table 6-1: Main parameters of the MiniFluid facility [VIII]

Dimensions of the dense bed zone (L x W x H)	[cm]	15x22.5x40
Dimensions of the freeboard (L x W x H)	[cm]	20x30x150
Total height	[cm]	280
Power output	[kW]	20-30
Fuel consumption	[kg/h]	2-5
Working temperatures	[°C]	20-1100 (up to 300°C without combustion)

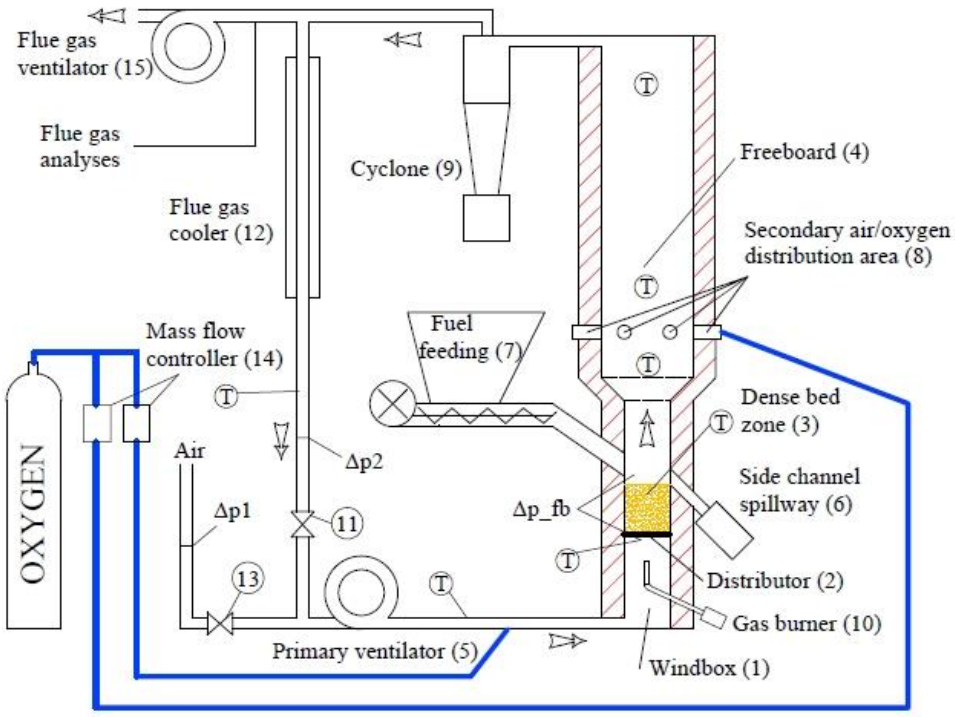

Figure 6-1: Schematic diagram of the MiniFluid facility

Figure 6-2: Photograph of the MiniFluid facility

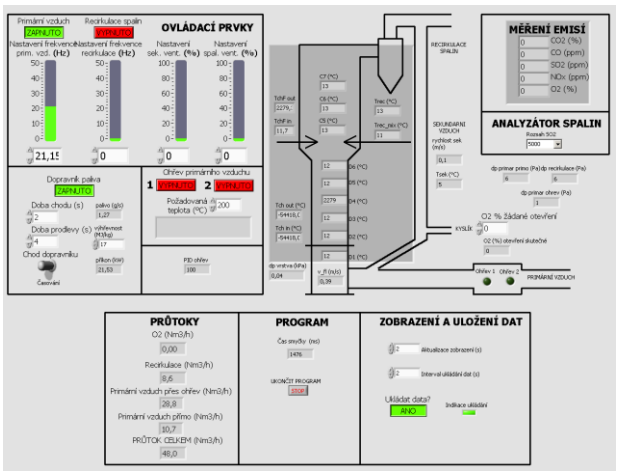

Figure 6-3: Picture of the control program in LabView

6.2 500 KW PILOT BUBBLING FLUIDIZED BED BOILER

Second facility, which was used for the experiments is a pilot scale experimental bubbling fluidized bed boiler having power output around 500 kW marked as "Golem". Although the maximal power output is 500 kW, majority of experiments was done on lower power output in case of decreasing the oxygen consumption. The boiler is designed as a vertical double pass boiler with a circular cross-section having a cross-over pass that connects the two vertical passes [IX]. The basic scheme is shown in Figure 6-4, photograph of the boiler is in Figure 6-5. The boiler is equipped with a V-shaped trough type fluidized bed distributor, and consists of 36 nozzles immersed in the fluidized bed, which are located on two parallel sides and are placed horizontally in three cascade rows (see Figure 6-6). The fluidization medium supply is separated to each parallel sides and to the middle trough, which is made of perforated metal plate. More details about the design of the distributor are given in [X].

The first pass of the boiler, including the fluidized bed distributor, is designed as an almost adiabatic combustion chamber. Typical height of the fluidized bed is between 50 and 60 cm. The fuel is fed to the boiler through screw conveyor. The combustion chamber has a firebrick lining, with a water cooling double wall on the outer side. The cross-over chamber is also cooled by water walls. A secondary pass is made as a fire tube heat exchanger. Fluidization air is supplied by a primary fan with controllable revolutions. Secondary air is supplied via a separate fan with the possibility of controllable revolutions. Secondary air is supplied to special distributors, from which it is led to the freeboard in four high levels and four places around the circumference of the first pass. This system enables high variability of secondary air distribution and optimization, however it was not used for oxyfuel experiments.

The flue gas is recirculated in the place behind the cyclone, and is supplied to the primary air duct. Similarly to the MiniFluid facility, only one fan is used commonly for primary air supply and FGR. The FGR ratio is regulated by valves opening. This system was proofed as the easiest solution for combustion regulation and for transition between air and oxyfuel regimes. The scheme of the facility is principally very similar to the scheme of MiniFluid (Figure 6-1). The difference is in placing the flue gas fan, which is placed before cyclone. The second difference is that recirculated flue gases are not additionally cooled but are oppositely heat insulated in order to avoid water vapour condensation in FGR piping.

The boiler was originally build for the air combustion purposes and it was reconstructed to meet the necessary requirements for oxyfuel regime. The fuel system was closed and sealed. All the openings, inspection ports and flanges were also sealed in order to avoid air ingress. Oxygen

for oxyfuel regime is supplied into the primary mixture after the primary fan and is controlled by mass flow controller.

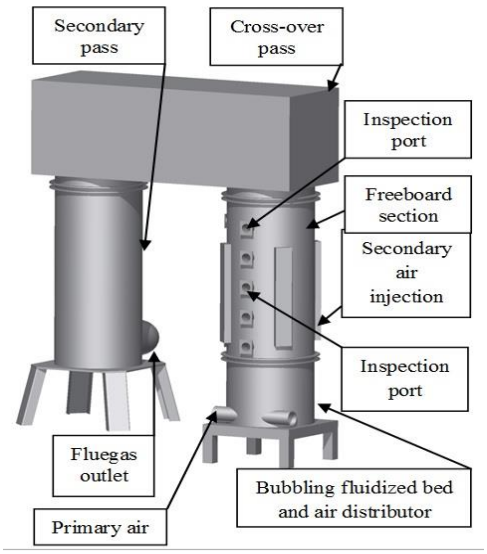

Figure 6-4: Schematic diagram of the FBC boiler Golem [IX]

Figure 6-5: Photograph of the FBC boiler Golem

Figure 6-6: Detail of the distributor

6.3 FUEL AND ADDITIVES CHARACTERISATION

Fuel

In order to keep stable combustion characteristics and good combustion quality and ensure the comparable results from the experiments, a single type of the fuel was chosen for all of the test. The coal is marked Bílina, type hp1 originating in the north-west Czech coal basin. It contains particle sizes from 0 to 10 mm according to the catalogue values, but it contains also particles around 20 mm. Particles above 10 mm cause fluidization problems in small experimental facility MiniFluid. That is the reason, why the coal was sieved before experiments in MiniFluid.

Along the whole period of experiments, several samples of coal were taken and proximate and ultimate analyses were done. The results are presented in Table 6-2. It was determined, that the coal did not change in elemental composition, but changes in water content, due to the gradual drying. The coal composition stated here shows the average values, but the differences in water content were covered in each evaluation of the measurement.

Table 6-2: Proximate and ultimate analysis of the used coal

	Properties "dry ash free"					Properties "as received"		
	C	O	H	S	N	A	W	LHV
	[wt %]	[wt %]	[wt %]	[wt %]	[wt %]	[wt %]	[wt %]	[MJ/kg]
Coal for Golem	72.3	18.9	6.3	1.33	1.13	9.3	25	18.5
Coal for Minifluid	72.3	18.9	6.3	1.33	1.11	10.6	14.9	21.8

For the desulphurization process it is also very important to know the sulphur distribution in the fuel. The percentage representation of the different sulphur types was get from the information from the producer of the fuel and is presented in Table 6-3. The sulphur content presented in the Table 6-2 covers just the combustible sulphur. The amount of sulphur in form of sulphates is taken as a part of the ash.

Table 6-3: Sulphur distribution in the fuel

S-pyrite (%)	S-free+organic (%)	S-sulphate (%)
53	36	11

Inert bed material

The inert material that forms the fluidized bed is ash originating from the used coal. Its physical characteristics are summarized in Table 6-4. The mean diameter was determined from the PSD analyses, density was measured by a pycnometer, bulk density was determined by volumetric method and sphericity was estimated from the literature references and previous experimental results. Voidage was calculated according to the values of density and bulk density.

Table 6-4: Characteristic of the inert fluidized bed material

	Mean diameter d_p	Density ρ_s	Bulk density ρ_b	Sphericity Φ_s	Voidage ε
	[mm]	[kg/m^3]	[kg/m^3]	[-]	[-]
Coal ash	0.495	2195	787	0.7	0.64

Limestone

Two sorts of limestone from different mines in the Czech Republic were used for the experiment with SO_2 capture. Their characteristics are shown in Table 6-5. The characteristic dimensions were got from the sieving analysis and the $CaCO_3$ content was got from the producers of the limestone. Limestones are marked as Limestone 1 and Limestone 2, later presented as L1 and L2.

Table 6-5: Properties of limestone additives

	Mean diameter d_p	Mode diameter d_{mod}	Median diameter d_{med}	$CaCO_3$
	[mm]	[mm]	[mm]	[%]
Limestone L1	0.29	0.22	0.31	99
Limestone L2	0.27	0.18	0.55	74

The samples are very similar in the size characteristics but differ in the purity. Limestone L1 is declared as very pure additive having just minimal amount of impurities. On the other hand, limestone L2 contains higher amount of impurities, mostly alumina-silicates.

Both experimental facilities do not have any special part for separate limestone addition. The process of limestone addition was done before each measurement by manual premixing the fuel with the given amount of limestone.

6.4 EXPERIMENTAL PARAMETERS AND TESTING PROCEDURE

6.4.1 Experimental set up and testing procedure in MiniFluid under air conditions

The overview of the experiments that were done in MiniFluid combustor under air conditions is presented in Table 6-6. Studying of all possible combinations would be very time demanding. In order to reduce the amount of experiments, the reference conditions were set. These reference conditions were derived according to the previous literature research (see chapter 3.4.3) and own experiences with desulphurization in Golem (see e.g. [XI], [XII]). The reference fluidized bed temperature was set at 840°C, oxygen concentration 6% and Ca/S molar ratio 1.5. The studied parameters were in following ranges:

- Effect of bed temperatures at 800°C, 840°C, 880°C and 920°C for Ca/S=1.5, 3 and 5 and for fixed oxygen concentration in flue gas 6%.
- Effect of oxygen concentration at 3%, 6% and 9% at Ca/S ratio 1.5 and for fixed fluidized bed temperature 840°C.
- The experiments were carried out for both sorts of limestone.

Each experiment consisted of stabilization of the combustion process at desired conditions and then keeping stable operation at these conditions for at least 30 minutes but in average about 1 hour at majority of measurements in order to make the results representative. The limestone was manually premixed with fuel prior to each experiment.

Table 6-6: Matrix of the experiments for air combustion

	T 800°C	T 840°C	T 880°C	T 920°C	O_2 3%	O_2 6%	O_2 9%	No Ca	Ca/S 1.5	Ca/S 3	Ca/S 5
T 800°C						X		X	X	X	X
T 840°C					X	X	X	X	X	X	X
T 880°C						X		X	X	X	X
T 920°C						X		X	X	X	X
O_2 3%		X						X	X	X	
O_2 6%	X	X	X	X				X	X	X	X
O_2 9%		X						X	X	X	
No Ca	X	X	X	X	X	X	X				
Ca/S 1.5	X	X	X	X	X	X	X				
Ca/S 3	X	X	X	X	X	X	X				
Ca/S 5	X	X	X	X		X					

6.4.2 Experimental set up and testing procedure in MiniFluid and Golem under oxyfuel conditions

The overview of the experiments that were done at oxyfuel conditions is presented in Table 6-7. In comparison with air combustion the temperature range which was studied was different starting at 840°C with the step of 40°C up to 960°C taken into account the specific behaviour of desulphurization process under oxyfuel conditions. The tested temperature range covers also the both sides of the equilibrium curve of limestone calcination presented in chapter 3.4.1. The effect of oxygen excess was studied also in three levels 3, 6 and 9%, however it has to be mentioned that the ratio of oxygen excess is different than under air combustion. The reference

conditions for oxyfuel combustion were set at 880°C fluidized bed temperature, oxygen concentration 6% and Ca/S molar ratio 3. The values of the parameters that were tested are:

- Effect of bed temperatures at 840°C, 880°C, 920°C and 960°C for Ca/S=1.5, 3 and 5 and oxygen concentration in flue gas 6%.
- Effect of oxygen concentration in the flue gas at 3%, 6% and 9% at Ca/S ratio 1.5 and 880°C.
- Above mentioned parameters were tested for both kinds of limestone.

Table 6-7: Matrix of the experiments for oxyfuel combustion

	T 840°C	T 880°C	T 920°C	T 960°C	O_2 3%	O_2 6%	O_2 9%	No Ca	Ca/S 1.5	Ca/S 3	Ca/S 5
T 840°C						X		X	X	X	X
T 880°C					X	X	X	X	X	X	X
T 920°C						X		X	X	X	X
T 960°C						X		X	X	X	X
O_2 3%		X						X	X	X	
O_2 6%	X	X	X	X				X	X	X	X
O_2 9%		X						X	X	X	
No Ca	X	X	X	X	X	X	X				
Ca/S 1.5	X	X	X	X	X	X	X				
Ca/S 3	X	X	X	X	X	X	X				
Ca/S 5	X	X	X	X		X					

Similarly to the air combustion the experiments lasted approximately about 1 hour at stabile operation conditions without changing the operation parameters. The experiments were set in full oxyfuel regime, it means that all combustion and fluidization air was replaced by the mix of FGR and oxygen. Oxygen was added from the bundle of bottles in case of MiniFluid measurements and in the form of liquid oxygen from cryogenic vessel in case of measurements in Golem. The oxygen for the experiments had high purity – more than 99% of O_2.

6.4.3 Uniform system of results presentation

In order to keep the same style of results presentation in the diagrams, the following rules are set:

- results from air combustion are referred by a solid line
- results from oxyfuel combustion are referred by a dash line
- results from measurements without limestone addition have green colour
- results from measurements with limestone L1 have blue colour, different Ca/S of L1 are distinguished by shades of blue
- results from measurements with limestone L2 have red colour, different Ca/S of L2 are distinguished by shades of red
- the points representing results from MiniFluid combustor have square shape
- the points representing results from Golem combustor have triangle shape.

7 VALIDATION OF THE MATHEMATICAL BALANCE

This chapter covers validation of the mathematical oxyfuel balance model with experimental results, which were obtained both on the MiniFluid and on Golem. This part also deals with the identification of oxyfuel regime and with the main aspects affecting the operation of the boiler under oxyfuel conditions.

The methodology of oxyfuel stoichiometric and balance calculations presented in chapter 5 allows good description of volumes and concentrations of the gases in different parts of the combustion process. In order to properly set the mathematical balance model to be comparable with experiments, it is necessary to input five parameters [II] [IV]:

- Proximate and ultimate analysis of coal
- Mass flow rate of the fuel
- Concentration of oxygen in dry flue gas
- Concentration of carbon dioxide in dry flue gas
- The volume flow rate of FGR

Proximate and ultimate analysis of coal is necessary for the basic stoichiometric calculations. Fuels used for experiments serves as an input for mathematical model and are described in Table 6-2.

Mass flow rate of the fuel must be known for obtaining real volume flows. Its determination in the MiniFluid facility was done by calibration of the amount of fuel supplied by a conveyor for a certain period of time. The fuel supply is controlled by setting the time of run and pause of the conveyor. In case of Golem, the fuel supply is obtained by measuring a mass decrement of the fuel storage using the electrical strain gauge.

Concentration of oxygen in flue gas is important for setting the excess of oxygen during combustion. It is measured continuously as a part of emission monitoring. Also the concentration of carbon dioxide is measured continuously, it is important in calculation for air ingress determination.

In order to balance the volume flows in the combustor, it is important to measure one of these volume flows – volume of flue gas or volume of FGR. Technically the most easily measurable flow rate is the flow rate of FGR. It is determined by the differential pressure on orifice plate.

The above mentioned parameters allows us to calculate whole stoichiometry and volumetric balances of the oxyfuel combustion process. The independent parameter, which can be used for comparison, is the oxygen volume flow into the combustor.

Representative experimental results used for validation of the mathematical balance model are presented in Table 7-1. Parameters marked with the superscript ^{M} are directly measured values, which are used as the input values for the calculation of the whole balance of the oxyfuel combustion process. All measured values presented in the table are mean values of the variables from one hour measurement under stable conditions.

Presented data from measurements are arranged according to the three different CO_2/O_2 ratios in the fluidization medium (measurements are marked as A, B and C referring to CO_2/O_2 ratios 64/36; 69/31 and 74/26). Different CO_2/O_2 ratios were set using different flow of FGR. The flow of FGR is given by the recirculation coefficient "r". It can be stated that with increasing "r" and simultaneously with constant oxygen flow increases also the concentration of CO_2 in the fluidization medium. For each CO_2/O_2 ratio, there are data from measurements with different fluidized bed temperatures.

Table 7-1: Experimental data from MiniFluid and comparison with mathematical model

	A1	A2	A3	B1	B2	B3	C1	C2	C3
CO_2/O_2 ratio	1.75			2.22			2.8		
CO_2/O_2 in fluidization medium (% vol)	64/36			69/31			74/26		
Bed temperature (°C) ^{M}	877	919	964	837	879	920	841	897	921
O_2 dry flue gas (%) ^{M}	8.5	6.1	5.8	6.8	6.6	6.4	5.7	8.3	5.9
CO_2 dry flue gas (%) ^{M}	87.0	89.2	90.6	88.9	90.8	90.9	87.9	84.0	88.4
Fuel feeding (kg/h) ^{M}	4.2	4.5	5.1	3.8	4.3	4.7	3.8	4.1	4.7
FGR temperature (°C) ^{M}	76	74	74	68	89	73	43	56	50
Fluidization velocity (m/s)	0.94	0.99	1.11	0.85	1.12	1.20	0.87	1.18	1.25
Recirculation coefficient r (-)	2.63	2.50	2.50	3.28	3.29	3.29	4.31	4.78	4.55
Measured oxygen flow (m^3_N/h) ^{M}	5.2	5.5	5.8	4.5	5.1	5.7	4.3	5.0	5.4
Calculated oxygen flow (m^3_N/h)	5.0	5.3	5.9	4.4	5.0	5.6	4.4	4.8	5.5
Relative deviation (%)	**5.2**	**4.4**	**-2.0**	**1.5**	**1.4**	**2.4**	**-0.9**	**2.7**	**-1.1**

Note: Superscript ^{M} refers to a measured value

It can be seen that the deviation between the calculated and measured oxygen flow is relatively low. The mean standard deviation along all measurements that were done in MiniFluid ranges around ±5%. Such a good accordance between measurement and calculation is important for the description of the oxyfuel process. [IV]

Results in the Table 7-1 also show the combined effect of fuel load and flue gas recirculation on combustion temperatures. In case of measurements with CO_2/O_2 ratio 66/34 (A1, A2, A3), we can see increase of fuel load by 21 % (from 4.2 to 5.1 kg/h) for temperature increase from 884 to 966 °C. Simultaneously we can see decrease of recirculation coefficient by 5 %, which plays also an important role in setting the fluidized bed temperature.

The Table 7-1 also illustrates the effect of FGR flowrate (or the "r" coefficient) on CO_2/O_2 ratio, while keeping constant bed temperature and power input in the fuel. When comparing e.g. cases A2-B3-C3 (all at 920°C), it can be seen that with a higher oxygen content in the fluidization medium a lower FGR flow is required to reach the same bed temperature at constant fuel feeding and oxygen flow into the combustor.

The same results were obtained from experiments in the Golem combustor, as shown in the Table 7-2.

Table 7-2: Experimental data from Golem and comparison with mathematical model

	G1	G2	G3
CO_2/O_2 ratio	2.06	2.37	2.61
CO_2/O_2 in fluidization medium (% vol)	67/33	70/30	72/28
Bed temperature (°C) ^{M}	883	881	883
O_2 dry flue gas (%) ^{M}	7	5	3.3
CO_2 dry flue gas (%) ^{M}	80	76.2	85.2
Fuel feeding (kg/h) ^{M}	52	39.1	44
FGR temperature (°C) ^{M}	200	136	138
Fluidization velocity (m/s)	1.44	1.07	1.18
Recirculation coefficient r (-)	3.17	3.28	3.45
Measured oxygen flow (m^3_N/h) ^{M}	57.6	44.9	49.5
Calculated oxygen flow (m^3_N/h)	57.4	38.8	42.9
Deviation (%)	**0.5**	**13.5**	**13.2**
Note: Symbol ^{M} marks measured value			

Measured and calculated values for Golem are more different. The average deviation between all measurements and mathematical balance model is around 7 % with maximal deviation about 15%. The main cause of the bigger differences in comparison with MiniFluid combustor is a size of the facility and lower accuracy of fuel feeding measurement. [XIII]

8 SO_2 CAPTURE IN MINIFLUID – EXPERIMENTAL RESULTS AND DISCUSSION

This chapter describes the results from experiments studying the sulphur dioxide capture and is carried out in MiniFluid. The first part focuses on results from air combustion. Second part deals with experiments under oxyfuel conditions.

8.1 SO_2 CAPTURE IN AIR-FIRED MODE IN MINIFLUID COMBUSTOR

The experiments in air mode were focused on studying of four important parameters, which significantly affect the sulphur capture process – effect of the used kind of limestone and amount of the limestone (expressed as Ca/S ratio) and two operation parameters of the boiler - fluidized bed temperature and oxygen concentration.

This chapter gives an overview of the most representative results, detailed data such as concentrations of other flue gas components (O_2, CO_2 and CO) and operational parameters of the experimental combustor (fuel load and fluidization velocity) are shown in Appendix 13.1 SO_2 capture under air conditions.

8.1.1 Sulphur self-retention under air conditions

The first investigated characteristics were focused on determination of the effect of self-retention of sulphur on the coal ash. The measurements were done using pure ash of the coal as the inert material of fluidized bed without limestone addition. Sulphur self-retention is possible in case of the presence of calcium in the ash. The sulphur self-retention in the ash correlated with bed temperature and oxygen concentration is presented in Figure 8-1 and Figure 8-2.

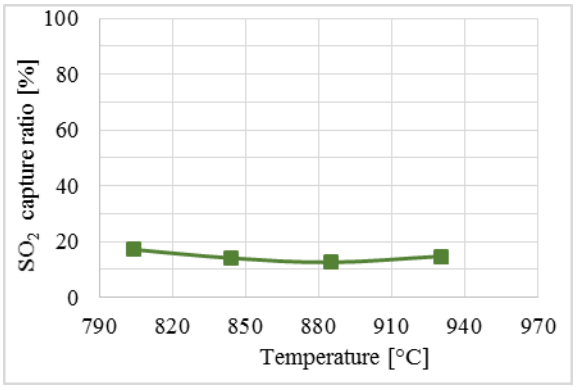

Figure 8-1: Sulphur self-retention correlated with bed temperature under air conditions

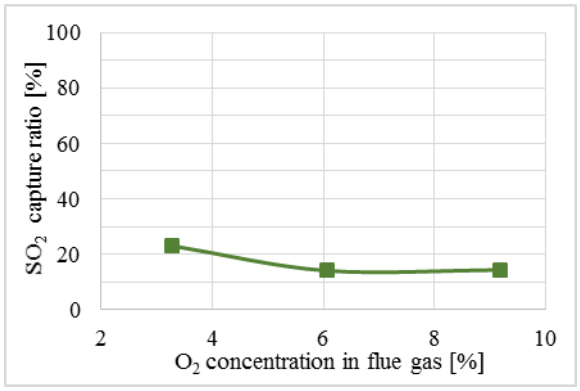

Figure 8-2: Sulphur self-retention correlated with bed oxygen concentration under air conditions

It can be seen that the SO_2 capture ratio without using any sorbent varies around 15%. The composition of the fuel ash according to the fuel supplier is given in the following Table 8-1. In order to exclude the possibility of additional limestone presence in the fluidized bed material, the fly ash samples after these measurements were analysed by XRF and no significant difference was found, as shown in the Table 8-1.

Table 8-1: XRF analysis of elements in the ash, wt. % as oxides

	SiO_2	Al_2O_3	Fe_2O_3	MgO	CaO	SO_3	Other comp.
Fuel supplier analysis	47.5	27.6	10.7	1.6	6.1	2.2	4.3
Average values from the XRF analysis	45.3	29.2	7.8	2	7	3.7	5

The amount of calcium from the XRF, expressed as CaO, is around 7 %. The amount of CaO was converted to Calcium as element and normalized taking into account unburned carbon content. The real amount of Calcium as an element in fuel ash is than about 7 % and calculated to the original fuel it is 0.8%. However, the XRF analysis does not give any answer, which chemical compounds are contained in the sample. The true chemical and mineral composition of the ash is not therefore known. However, the following consideration was done in order to estimate the real composition. Ca in a coal can be found as a part of its mineral matter. According to [72] there can be found these minerals containing Ca in coal – calcite ($CaCO_3$), dolomite ($CaMg(CO_3)_2$), ankerite ($Ca(Fe,Mg,Mn)(CO_3)_2$), calcium sulphate ($CaSO_4$), phosphorite ($Ca_5(PO_4)_3$), apatite ($Ca_{10}(PO_4)_6(OH,F,Cl)_2$) and calcium chloride ($CaCl_2$). There are other kinds of Ca containing minerals as well, but they are usually very rare in coal compositions. The XRF analysis of the ash showed that there is just very small amount of phosphorus and chlorine (both bellow 0.01wt%), so that calcium chloride, apatite and phosphorite does not play any important role in its composition. Ankerite transforms to calcite around 750°C and then it can be calcined similarly as calcite and dolomite. The amount of calcium sulphite can be determined according to the amount of sulphite sulphur contained in fuel. The analysis of the sulphur distribution in coal showed, that there is 11% of sulphur in the form of sulphite (see Table 6-3). According to the mass balance it can be determined that about 17% of calcium is in the form of $CaSO_4$.

From the above mentioned facts, it can be estimated that about 80% of Ca contained in the fuel is in the form of calcite, dolomite or ankerite that can calcine to CaO and can take part in the SO_2 capture reactions. This fact gives us a possibility to determine the “internal” Ca/S molar

ratio that equals for this composition **0.65**. This explains the sulphur self-retention, which is around 15% under air conditions. [XIV]

8.1.2 Effect of Ca/S ratio

The effect of Ca/S molar ratio was studied at three values– 1.5, 3 and 5. The real weight of limestone which was added to the fuel is presented in the Table 8-2. The Ca/S ratio corresponds to addition of limestone into the fuel and does not include Ca in the fuel ash. The fuel-limestone blends were always prepared prior to the experiments. The weights of the limestones were calculated for the sulphur content in the fuel according to the analysis of coal for MiniFluid and take into consideration different $CaCO_3$ content.

Table 8-2: Amount of limestone addition in MiniFluid, g sorbent per 10 kg of coal

	Ca/S = 1.5	Ca/S = 3	Ca/S = 5
Limestone L1	450	900	1500
Limestone L2	600	1200	2000

The results from measurements are shown in the Figure 8-3. All measurements were performed at constant operating parameters of the combustor – bed temperature 840°C, 6% of oxygen in dry flue gas, 4.4 kg/h of fuel load and 1.5 m/s fluidization velocity. The measured values of SO_2 capture ratio were correlated according to the equation 3-20 to calculate the parameter "K". The result from this correlation are shown in Table 8-3. The fitting procedure was done using the least squares method. We can see, that the correlation fits the measured data very well with determination coefficient R^2 of about 0.85 for limestone L2 and more than 0.90 for limestone L1. It has to be also mentioned that the Figure 8-3 contains two horizontal axes. The upper axis refers to the Ca/S ratio excluding Ca obtained in fuel ash. It means just added limestone. The axis at the bottom refers to the Ca/S molar ratio including the Ca in fuel. The points stated in the Figure 8-3 are the average values from the measurements. The green point represents the results of sulphur self-retention without adding any limestone. This point is logically common for both curves. [XIV]

Table 8-3: Values of K constant obtained from correlation by equation 3-20

	Limestone L1	Limestone L2
K [-]	0.31	0.42
R^2 [-]	0.905	0.846

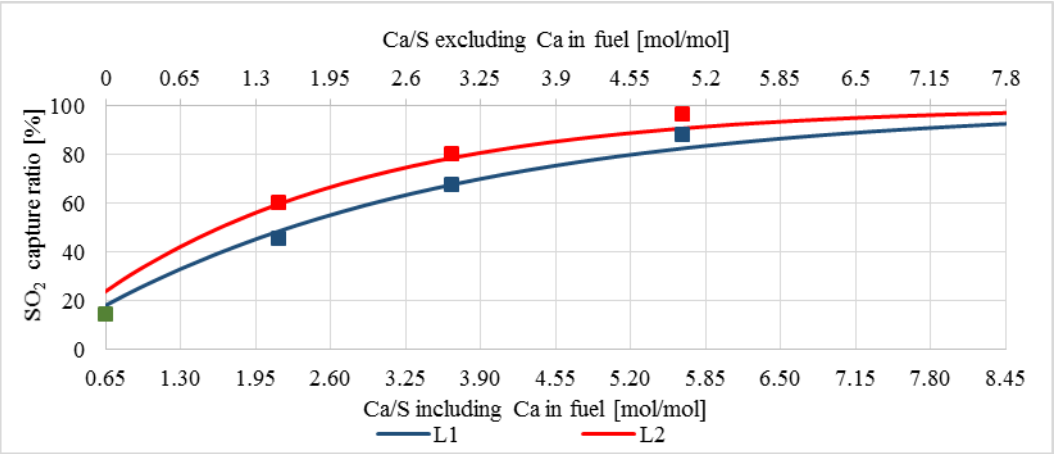

Figure 8-3: Effect of different Ca/S molar ratio on SO_2 capture ratio – fitting of the measured points

We can see, that limestone L2 gives about 15% higher SO_2 capture ratio in comparison with limestone L1 for Ca/S 1.5 and 3. For higher Ca/S ratios we see lowering difference between the limestones. Nevertheless, the dependences given in the Figure 8-3 are just one of the possible presentations showing the effect of added limestone on SO_2 capture. In practice it is more important to recalculate Ca/S ratio to the weight ratio between added limestone and used coal. Results of such calculation are presented in Figure 8-4. It can be seen, that due to the lower purity of limestone L2, the differences between the limestones performances are tightened, nevertheless, limestone L2 still reaches higher SO_2 capture ratio, mostly in lower amounts of limestone addition.

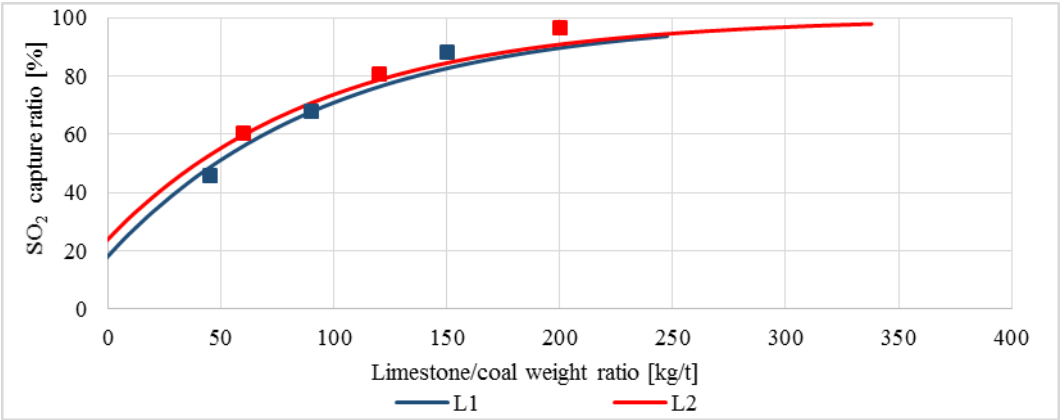

Figure 8-4: Effect of limestone addition on SO_2 capture represented as limestone to coal weight ratio

8.1.3 Effect of bed temperature

Another studied parameter affecting the SO_2 capture ratio was fluidized bed temperature. The results from measurements with limestone L1 are presented in Figure 8-5, with limestone L2 in Figure 8-6.

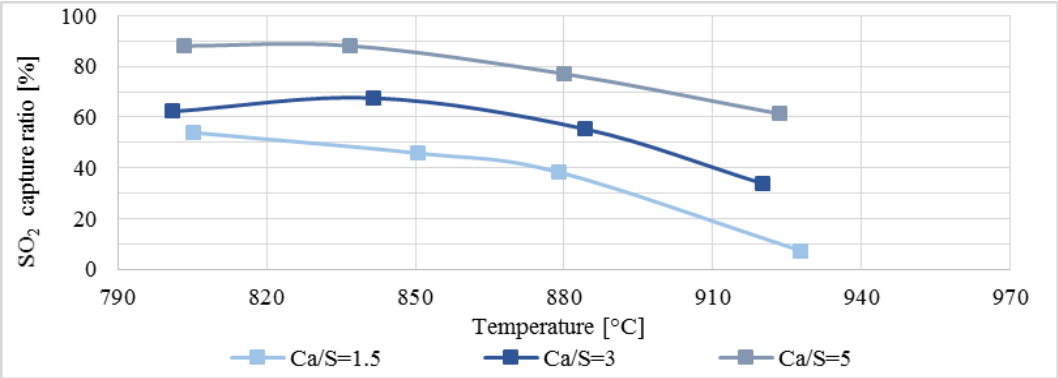

Figure 8-5: Correlation of SO_2 capture ratio with bed temperatures under air conditions – **limestone L1**

According to the literature research, the most optimal temperature for desulphurization in fluidized bed boilers is around 840°C. This fact was confirmed by the measurements for both limestones showing the highest SO_2 capture ratio also for temperatures from 800 to 840°C. Interesting results were got in case of using Ca/S=1.5. We can see that the highest SO_2 capture ratio was reached for the lowest studied temperatures around 800°C. Oppositely in case of the highest temperature (920°C), the SO_2 capture ratio fall below 10%. This value is even lower than in the case of self-retention experiments. The reason for this is probably given by combination of high concentration of CO in flue gas, which is more than 300% higher compared to the case of the highest SO_2 capture. See Table 8-4, that summarizes relative decrease from maximal SO_2 capture ratio reached for each Ca/S ratio of limestone L1 and contains also information about CO concentration.

Combination of such a high CO concentration and high temperatures favours reduction reaction of created $CaSO_4$, which then results in lowered overall SO_2 capture. This phenomenon is described in detail in chapter 3.4.3.3.

Table 8-4: Relative decrease from maximal SO_2 capture ratio for limestone L1 under air conditions

Ca/S [-]	Fluidized bed temperature [°C]	Relative decrease from maximal SO_2 capture ratio [%]	Concentration of CO [ppm]	Relative difference of CO [%] *
1.5	**802**	**0**	**160**	**0**
	849	15	300	+87.5
	879	28.8	266	+66.2
	929	86.4	640	+300
3	801	7.9	320	+72
	842	**0**	**186**	**0**
	884	18.2	216	+16.1
	920	50	251	+34.9
5	804	0	175	+88.2
	837	**0**	**93**	**0**
	880	12.5	218	+134.4
	924	30.4	70	-24.7
Reference case – given by maximal SO_2 capture ratio				
* Relative increase or decrease of CO concentration from reference case				

Results from measurements with limestone L2 show similar behaviour as results with limestone L1, they can be seen in Figure 8-6.

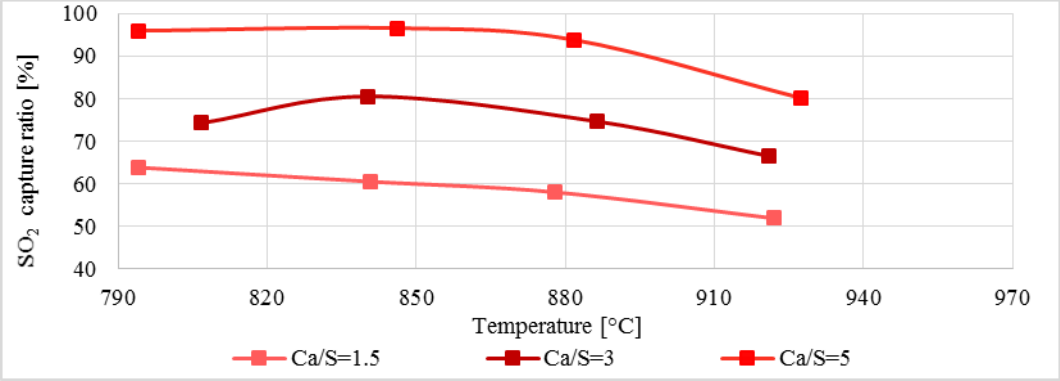

Figure 8-6: Correlation of SO_2 capture ratio with bed temperatures under air conditions – **limestone L2**

In case of Ca/S=1.5, the SO_2 capture ratio was the highest for 800°C and similar behaviour was seen for Ca/S=5. Table 8-5 summarizes the SO_2 capture differences for studied temperatures. We can see, that the differences in SO_2 capture in studied temperature interval were lower for L2, than the differences for L1. It means that limestone L1 is more sensitive to the bed temperatures. Maximal relative SO_2 capture diminution for limestone L2 was around 18%.

Table 8-5: Relative decrease from maximal SO_2 capture ratio for limestone L2 under air conditions

Ca/S [-]	Fluidized bed temperature [°C]	Relative decrease from maximal SO_2 capture ratio [%]	Concentration of CO [ppm]	Relative difference of CO [%] *
1.5	**794**	**0**	**164**	**0**
	841	5.2	234	+42.7
	878	9.1	160	-2.5
	922	18.7	799	+387.2
3	807	7.8	262	+66.9
	840	**0**	**157**	**0**
	886	7.3	92	-41.4
	921	17.5	97	-38.2
5	794	1	205	+23.5
	846	**0**	**166**	**0**
	882	3	91	-45.2
	927	17	77	-53.6

Reference case – given by maximal SO_2 capture ratio

* Relative increase or decrease of CO concentration from reference case

From Table 8-5, it can be seen that limestone L2 is less sensitive to the CO concentration. For example in comparison for Ca/S=1.5 we can see relative decrease in SO_2 capture just about 18.7 % for 920°C, although the CO concentration growth is nearly 4 times higher. The same situation for limestone L1 brought decrease in SO_2 capture by more than 86%. In case of Ca/S=5, the SO_2 capture ratio was the same for experiments at 800°C and 840°C.

Another difference between the limestones is, that limestone L2 reaches higher SO_2 capture than limestone L1, although the purity of L2 is lower. In order to explain this effect some additional analyses of the used limestones were done – analysis of the apparent density (mass divided by the volume of a material including permeable and impermeable voids presented in the material) and BET surface area. The results are presented in Table 8-6. There are big differences between the BET surfaces of the used limestones. Higher surface of the limestone L2 could be the reason for its higher SO_2 capture. However, as mentioned previously if the Ca/S ratio is recalculated to the weight ratio, the effect of higher calcium utilization for L2 is neglected and both limestones have very similar final results.

Table 8-6: Additional analyses of the additives

	Apparent density [g/cm^3]	BET surface [m^2/g]
Limestone L1	2.75	0.11
Limestone L2	2.46	14.5

8.1.4 Effect of oxygen concentration

Another studied parameter affecting the SO_2 capture ratio was oxygen concentration in flue gas. The results from the experiments are shown in Figure 8-7 and Figure 8-8. It can be seen that there is ambiguous dependence of SO_2 capture on air excess. In case of Ca/S=3 for both limestones, we see tendency of slightly decreasing SO_2 capture with increasing oxygen concentration. For Ca/S=1.5 there is no significant dependence. Table 8-7 shows also the effect of different oxygen concentration on CO emissions, which are significantly increased at lower air excess.

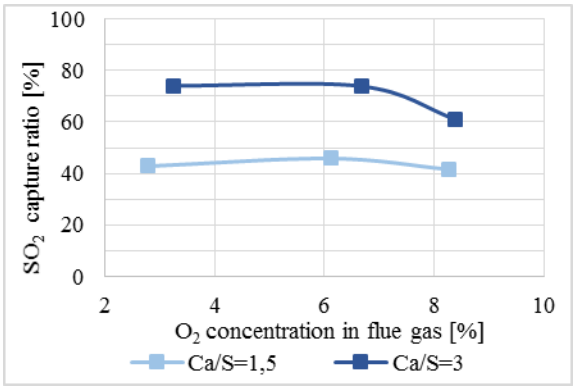

Figure 8-7: Correlation of SO_2 capture ratio with oxygen concentration in FG under air conditions – **L1**

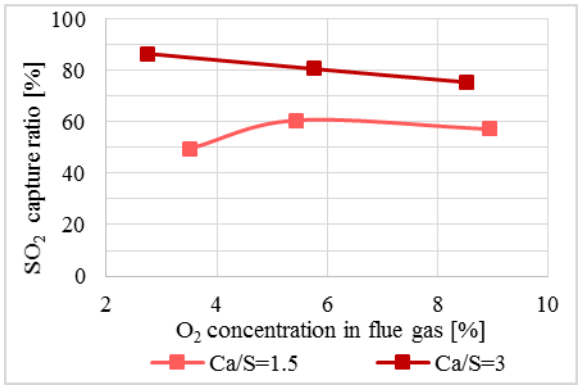

Figure 8-8: Correlation of SO_2 capture ratio with oxygen concentration in FG under air conditions – **L2**

Table 8-7: Effect of different oxygen excess on SO_2 capture ratio

Ca/S [-]	Oxygen concentration in FG [%]	Excess of oxidant [-]	Rel. decrease from maximal SO_2 capture ratio [%]	Concentration of CO [ppm]	Relative difference of CO [%] *
L1 1.5	2.8	1.15	6.5	1009	+235
	6.1	**1.40**	**0***	**301**	**0**
	8.3	1.63	10	202	-32.9
L1 3	**3.2**	**1.18**	**0***	**113**	**0**
	6.7	1.45	0.3	96	-15
	8.4	1.65	21.6	110	-2.6
L2 1.5	3.5	1.20	18.1	799	+241
	5.4	**1.34**	**0***	**234**	**0**
	8.9	1.72	6	119	-49.1
L2 3	**2.8**	**1.15**	**0***	**402**	**0**
	5.8	1.40	6.8	157	-60.9
	8.5	1.67	14.7	129	-68

Reference case – given by maximal SO_2 capture ratio

* Relative increase or decrease of CO concentration from reference case

8.2 SO_2 CAPTURE IN OXYFUEL MODE IN MINIFLUID COMBUSTOR

The desulphurization process under oxyfuel conditions was studied in similar way as under the air combustion mode. This chapter gives an overview of the results that has been done in oxyfuel regime in the MiniFluid facility related directly to the SO_2 capture. Detailed data from the measurements such as CO_2 concentration and fuel load are placed in Appendix 13.2 SO_2 capture in oxyfuel regime.

8.2.1 Sulphur self-retention

The firs experiments were focused on the evaluation of sulphur self-retention. The experiments were done in extended temperature range from 820°C to 950°C. Also the effect of different oxygen concentration in flue gas on SO_2 self-retention was studied. The results are shown in Figure 8-9 and Figure 8-10.

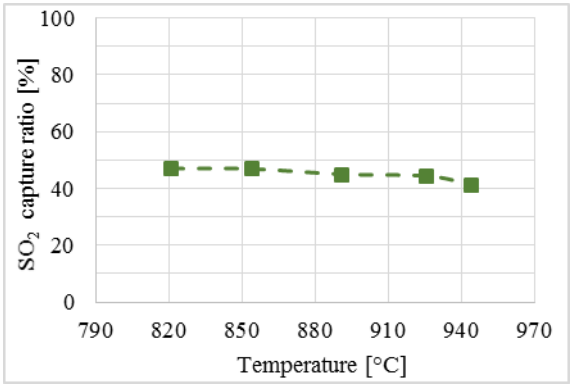

Figure 8-9: Experiments for different temperatures under oxyfuel conditions without any limestone addition

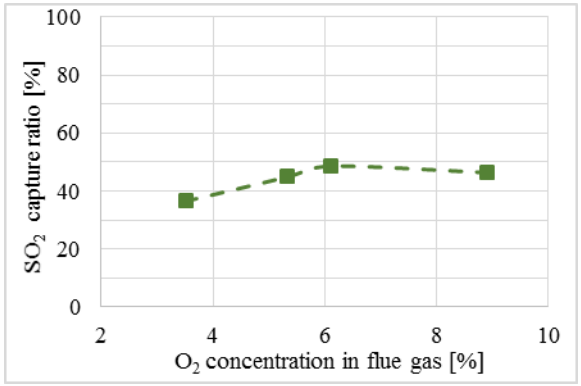

Figure 8-10: Experiments for different oxygen concentrations in FG under oxyfuel conditions without any limestone addition

It can be seen that the effect of sulphur self-retention is under oxyfuel conditions significantly higher. The SO_2 capture ratio is around 45% and varies with temperature only marginally. In comparison with air combustion the effect of sulphur self-retention is three times higher. The possible error due to the contamination of fuel by other limestone, or some limestone residues from other experiments was eliminated by performing XRF analyses of fly ash. These analyses showed just slightly higher amount of calcium as the measurements from air combustion without any limestone (see comparison in Table 8-8). The "internal" molar Ca/S ratio of the fuel thus slightly increases from the value 0.65 for air mode to **0.75** in oxyfuel mode.

Table 8-8: Chemical composition of the used fuel ash related as oxides from the measurement without limestone – XRF analyses; all in % wt.

	SiO_2	Al_2O_3	Fe_2O_3	MgO	CaO	SO_3	Other comp.
oxyfuel	42.2	28.4	7.5	2.5	9.4	4.8	5.2
air reference	45.3	29.2	7.8	2	7	3.7	5

In the Figure 8-10, there is remarkably lower SO_2 capture ratio at 3 % O_2. This can be attributed to an elevated CO level 2383 ppm compared to 856 ppm at O_2=6% (see A. Table 12 in Appendix 13.2). High CO concentration probably supports the reverse reactions of $CaSO_4$ with CO under low oxygen excess, as described by reactions 3-25 to 3-27 in the chapter 3.4.3.3.

8.2.2 Effect of Ca/S ratio

The effect of different Ca/S ratios was determined in the same way as in the air combustion experiments. The weight of limestone which was added to the fuel is the same as in Table 8-2. The other operation parameters were kept constant to see just the effect of different Ca/S ratios. The fluidized bed temperature during the experiments was 880°C, O_2 concentration in flue gas 6 % and fluidization velocity around 1.1 m/s. The results are shown in Figure 8-11. Figure 8-11 also includes the fitting curve according to the correlation from equation 3-20. The coefficient "K" and determination index R^2 are shown in Table 8-9.

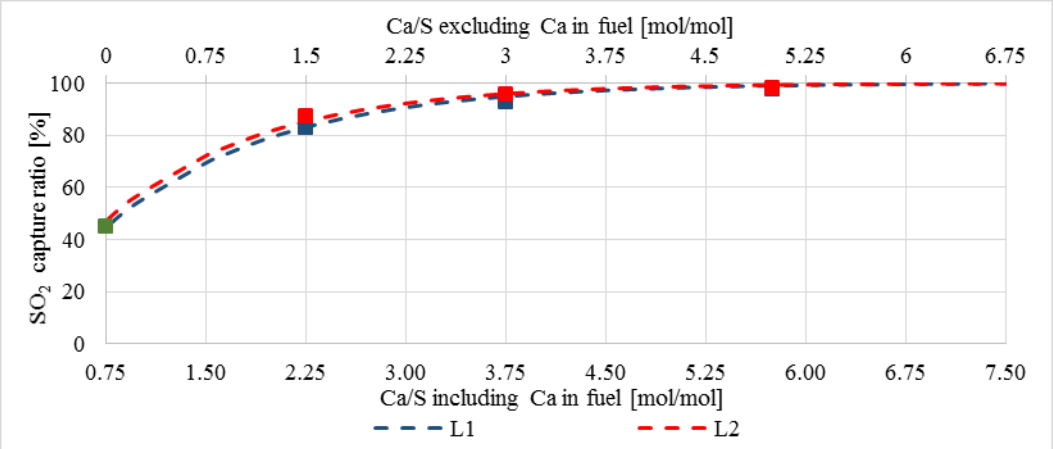

Figure 8-11: Effect of different Ca/S molar ratio on SO_2 capture ratio – fitting of the measured points

Table 8-9: Values of K constant obtained from correlation by equation 3-20

	Limestone L1	Limestone L2
K [-]	0.79	0.85
R^2 [-]	0.99	0.99

We can see similar desulphurization behaviour of both sorts of limestone. Just slightly higher SO_2 capture can be seen for Limestone L2, although the $CaCO_3$ content is about 25 % lower compared to limestone L1. If the $CaCO_3$ content is taken into account and the molar Ca/S is converted to mass ratio, the characteristic changes and limestone L1 starts to be more favourable (see Figure 8-12). This effect is significant up to the weight consumption around 150 kg per ton of coal where the difference disappears and both sorts of limestone show nearly the same capture ratio.

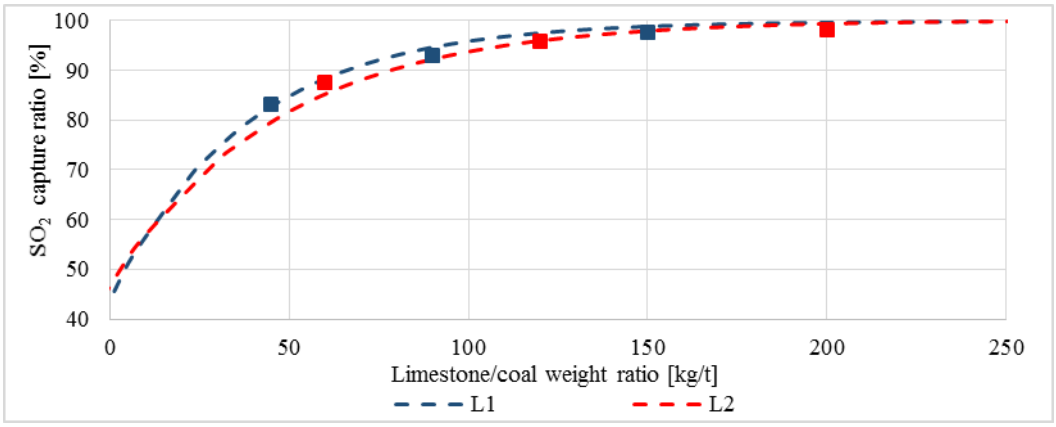

Figure 8-12: Effect of limestone addition on SO_2 capture represented as limestone to coal weight ratio

8.2.3 Effect of bed temperature

The results for different fluidized bed temperatures are presented in Figure 8-13 and Figure 8-15. The additional results of the concentrations of other flue gas components (O_2, CO_2 and CO) and operational parameters of the experimental combustor such as fuel load and fluidization velocity are shown in Appendix 13.2.

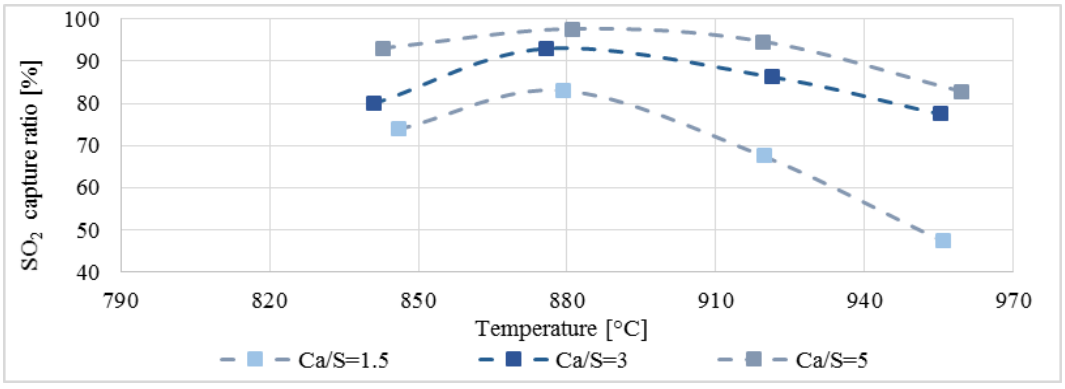

Figure 8-13: Correlation of SO_2 capture ratio with bed temperatures under oxyfuel conditions – **limestone L1**

Results from measurements with limestone L1 (Figure 8-13) show clear temperature dependence having the maximum SO_2 capture ratio around 880°C, which is about 40°C higher in comparison with air combustion. Higher optimal temperatures were proven also by other authors [2, 68, 73]. Higher temperatures move the reaction conditions to the right site of calcination equilibrium curve (see Figure 3-1). It means that the calcination proceeds as written in the equation 3-9 and desulphurization process goes through the indirect way similarly to the desulphurization under air conditions. The decrease of SO_2 capture ratio at temperatures around 840°C is on the other side caused by the fact, that the process of calcination is suppressed by high partial pressure of CO_2 and the process of desulphurization goes mainly through the direct sulphation. However, this reaction pathway is generally slower and with lower conversion according to authors [65, 74]. Actual CO_2 concentration in wet flue gas for all measurements in the equilibrium graph is shown in Figure 8-14.

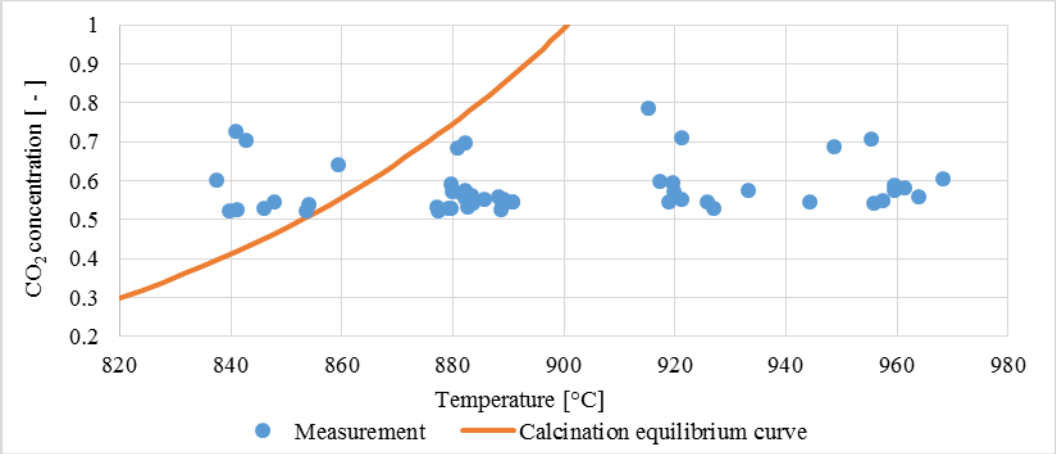

Figure 8-14: CO_2 concentration in wet flue gas for all experimental cases in MiniFluid combustor

It can be seen that all the measurements at the bed temperature below 860°C are on the left hand side of the equilibrium curve, resulting in fall of the SO_2 capture ratio between 880°C and 840°C. The most important decrease in comparison between 840°C and 880°C was in case of measurement with Ca/S=3, which was around 15% relatively, see Table 8-10. This decrease was probably caused not just by the effect of direct way of desulphurization but also by its combination with the effect of reduction reactions of $CaSO_4$ by increased CO emissions.

The most important differences of SO_2 capture ratio were in the case of changing the temperature from 880°C to 960°C for Ca/S=1.5, which was more than 40%. The reason for such a decrease can be attributed to approximately twice higher CO concentration compared to the reference case. On the other hand, this behaviour was not observed for Ca/S=5, where the

SO_2 capture ratio drops about 15 % at 960°C in comparison to the reference case, corresponding to about 4 times higher CO concentration.

Table 8-10: Relative decrease from maximal SO_2 capture ratio for limestone L1 under oxyfuel conditions

Ca/S [-]	Fluidized bed temperature [°C]	Relative decrease from maximal SO_2 capture ratio [%]	Concentration of CO [ppm]	Relative difference of CO [%] *
1.5	846	11.1	504	0
	879	**0**	**505**	**0**
	920	18.8	542	+8
	956	43	1307	+159
3	841	14.7	368	+126
	876	**0**	**163**	**0**
	921	24	392	+140
	955	28	446	+174
5	843	4.7	326	+6.6
	881	**0**	**303**	**0**
	920	3	308	+1.6
	960	15.2	1137	+275
Reference case – given by maximal SO_2 capture ratio				
* Relative increase or decrease of CO concentration from reference case				

The results from measurements with limestone L2 are presented in Figure 8-15. Other details about the SO_2 capture ratio are given in Table 8-11 and Appendix 13.2.

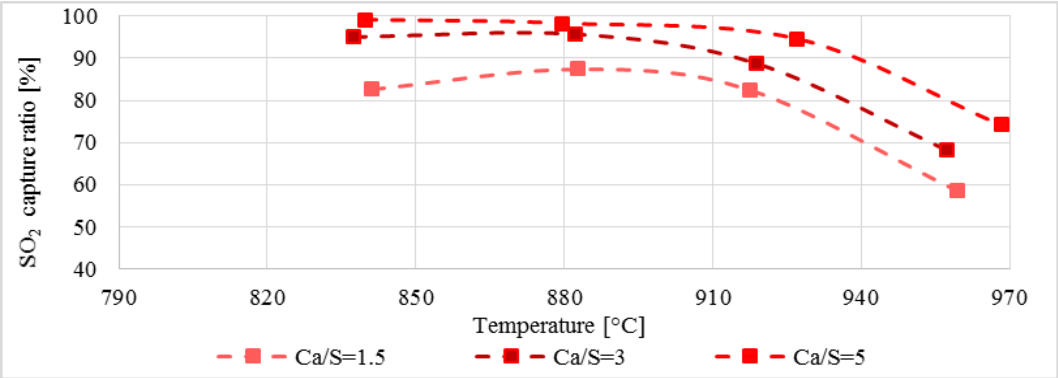

Figure 8-15: Correlation of SO_2 capture ratio with bed temperatures under oxyfuel conditions – **limestone L2**

Limestone L2, shows little bit different behaviour under oxyfuel conditions. Although the bed temperatures are around 840°C and they are on the left of the calcination equilibrium, the achieved SO_2 capture does not significantly change compared to 880°C+ cases, which are on the right hand side of the equilibrium curve. This means that the direct sulphation mechanism

is in this case not significantly less efficient in SO_2 capture compared to the calcination. Possible explanation for such a different behaviour between the L1 and L2 could be a difference in the BET surfaces, which is about a magnitude of order larger for limestone L2 (see Table 8-6). This fact could explain high SO_2 capture ratio also in the zone of temperatures, where the calcination is suppressed. Such a large surface area compensates the low rate of direct sulphation reactions, which finally results in the same limestone utilization.

The effect of higher temperatures is also slightly different between the used limestones. Limestone L2 has relatively small decrease in capture efficiency between the temperatures 880°C and 920°C. In case of Ca/S ratio 3 the decrease is about 7%, while the decrease for the same operation parameters for limestone L1 is 24%. However, the change in the temperatures from 920 to 960°C is similar to limestone L1.

Table 8-11: Relative decrease from maximal SO_2 capture ratio for limestone L2

Ca/S [-]	Fluidized bed temperature [°C]	Relative decrease from maximal SO_2 capture ratio [%]	Concentration of CO [ppm]	Relative difference of CO [%] *
1.5	841	5.5	401	+9.3
	883	**0**	**367**	**0**
	917	5.6	481	+31
	959	33.1	828	+126
3	837	0.7	521	-14.6
	882	**0**	**610**	**0**
	919	7.2	1120	+83.6
	957	28.9	1150	+88.5
5	840	-0.8	738	-21,7
	880	**0**	**943**	**0**
	927	3.7	860	-8.9
	968	24.5	390	-58.6

Reference case – given by maximal SO_2 capture ratio

* Relative increase or decrease of CO concentration from reference case

Interesting behaviour of Limestone L2 was found out in case of the measurement with Ca/S =5 at the highest temperatures. SO_2 capture ratio decreased by about 24% against reference case despite of the fact that the CO emissions were more than half in comparison with measurements at lower temperatures. This refers to higher effect of thermal degradation of the pores of the sorbent than the effect of reduction by CO as a reason for lower SO_2 capture ratio.

8.2.4 Effect of oxygen concentration

Experiments studying the effect of different O_2 concentration are presented in Figure 8-16 and Figure 8-17. It can be seen that with increasing amount of oxygen concentration, the SO_2

capture ratio increases as well. The increase is more significant for limestone L1, which is probably more dependent on composition of combustion atmosphere.

The oxygen concentration has two effects on desulphurization chemistry. The first effect is that with increasing oxygen concentration the CO_2 concentration decreases and the equilibrium of calcination changes. The second effect is indirect, higher excess of oxygen ensures more efficient combustion with lower CO emissions. As mentioned in previous parts and also in literature research (e.g. in [75]) CO can react at high temperatures with $CaSO_4$ and reduces it back to SO_2 and CaO (reactions 3-25 to 3-27) and thus decreases the SO_2 capture. Both effects are shown in Table 8-12. The reference state to which are the other states related to are with O_2 concentration at 6%. It can be seen that with increasing excess of oxygen in flue gas the concentration of CO_2 and CO decreases. In case of limestone L2, the effect of different oxygen excess was small having the difference from reference measurement at 6% of oxygen just ±1.5% relatively.

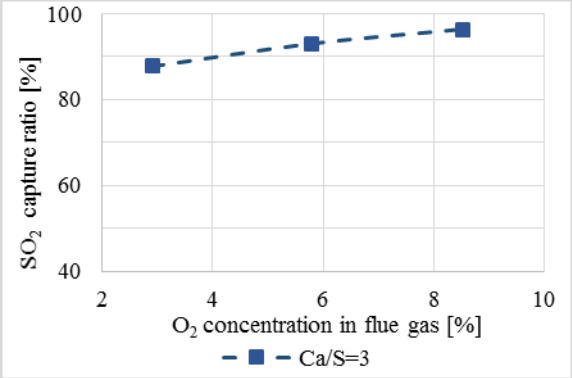

Figure 8-16: Correlation of SO_2 capture ratio with oxygen concentration in FG under oxyfuel conditions – **L1**

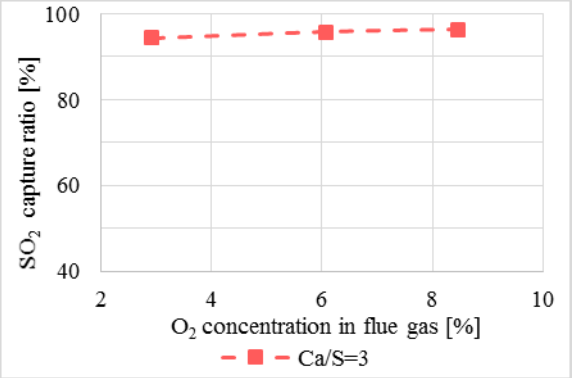

Figure 8-17: Correlation of SO_2 capture ratio with oxygen concentration in FG under oxyfuel conditions – **L2**

Table 8-12: Effect of different oxygen excess on SO_2 capture ratio

Ca/S [-]	O_2 in FG [%]	Excess of oxidant [-]	Rel. difference of SO_2 capture ratio [%]	CO_2 in dry FG [%]	Concentration of CO [ppm]	Relative difference of CO [%] *
L1 3	2.9	1.027	5.6	92.1	603	+270
	5.8	**1.056**	**0**	**88.6**	**163**	**0**
	8.5	1.084	-3.5	86.6	120	-26.4
L2 3	2.9	1.027	1.5	92.5	3036	+398
	6.1	**1.057**	**0**	**89.9**	**610**	**0**
	8.5	1.083	-0.6	87	516	-15.4
Reference case						
* Relative increase or decrease of CO concentration from reference case						

8.3 COMPARISON OF THE RESULTS BETWEEN AIR AND OXYFUEL COMBUSTION IN MINIFLUID

Sulphur self-retention

Comparison of sulphur self-retention in air and oxyfuel mode is shown in Figure 8-18. The figure clearly shows that the sulphur self-retention is significantly enhanced under oxyfuel combustion. The difference can be attributed particularly to the higher SO_2 concentrations in oxyfuel mode, allowing a higher conversion of the sulphation reaction and higher water concentration in flue gas probably enhancing conversion of the calcined sorbent to $Ca(OH)_2$.

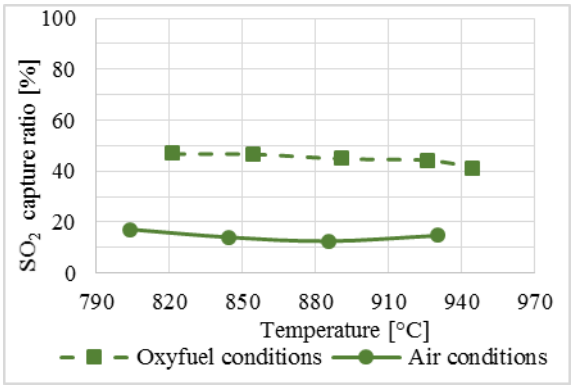

Figure 8-18: Comparison of sulphur self-retention under oxyfuel and air conditions [XIV]

Effect of Ca/S ratio

The most important parameter affecting the SO_2 direct capture is the stoichiometry of the added sorbent. With increase of Ca/S ratio, the SO_2 capture ratio increases according to the inversely exponential function in eq. 3-20. Figure 8-19 shows the difference between air and oxyfuel mode for both used sorbents, Figure 8-20 then represents the results in limestone/coal weight ratio. It can be seen that under oxyfuel regime, the SO_2 capture is significantly enhanced.

For example, in order to reach 80% SO_2 capture in air mode we need to set the Ca/S ratio to 3.75 for limestone L2, and nearly to 5 for limestone L1. In the case of oxyfuel mode, the required Ca/S ratio decreases to 1.85 and 2 for limestone L2 and limestone L1 respectively. In practice, this means saving of about 90 kg of limestone L1 or around 75 kg of limestone L2 per ton of coal. As for the sulphur self-retention, the higher SO_2 capture can be possibly attributed to generally higher SO_2 relative concentration and to conversion of calcined sorbent to $Ca(OH)_2$ by reaction with water vapour. The $Ca(OH)_2$ formation is more favoured in oxyfuel combustion due to significantly higher water vapour concentration.

The differences between used sorbents are similar, limestone L2 shows higher SO_2 capture, however after recalculation from Ca/S molar ratio to the weight ratio, limestone L1 shows higher SO_2 capture. Changing to oxyfuel mode, difference between the sorts of limestone disappears. [XIV]

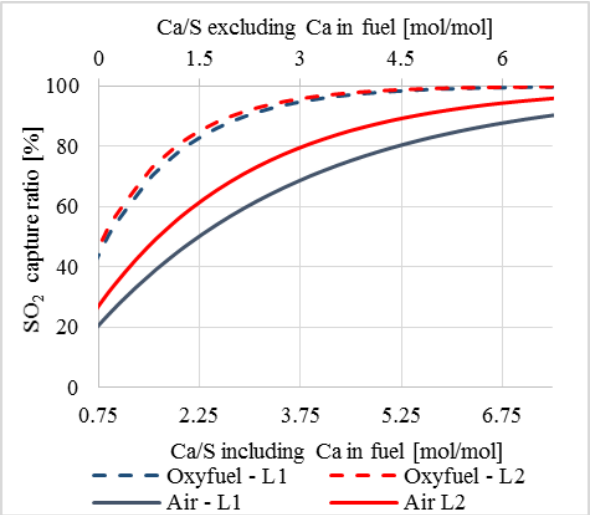

Figure 8-19: Effect of Ca/S molar ratio on SO_2 capture ratio – comparison of air and oxyfuel conditions

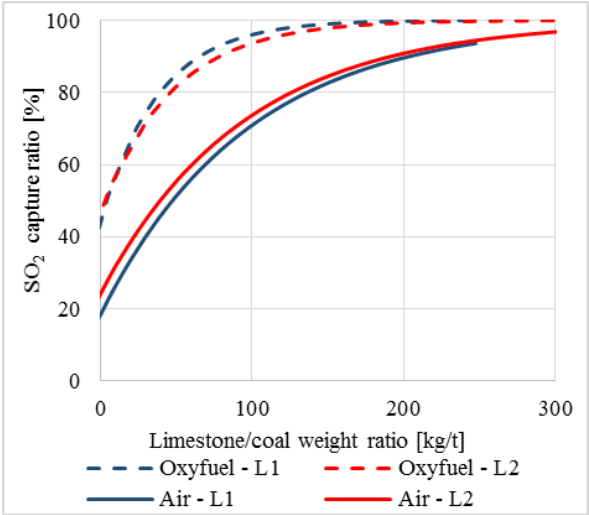

Figure 8-20: Effect of limestone/coal weight ratio on SO_2 capture – comparison of air and oxyfuel conditions

Effect of fluidized bed temperatures

Concerning the bed temperature, the optimal temperature interval for SO_2 capture is from 800°C to 850°C for air combustion and from 870°C to 890 °C for oxyfuel combustion. The temperature profiles of SO_2 capture are shown in Figure 8-21.

The optimal temperatures for desulphurization are affected by calcination equilibrium and reduction of the $CaSO_4$ by CO, mostly at high bed temperatures. Generally, the SO_2 capture always proceeds through the indirect pathway in air mode, since the CO_2 concentrations are very low and the working point is always on the right hand side of the equilibrium curve (see Figure 3-1). In the oxyfuel mode, the temperature threshold to switch from direct to indirect pathway is at about 840°C. This explains the shift of the optimum temperature window to higher level in the oxyfuel mode.

Significant differences between the sorbents L1 and L2 were observed in oxyfuel mode at the lowest temperatures, which were on the left side of the calcination equilibrium curve, as can be seen in Figure 8-21. Expected decrease of SO_2 capture was observed for the L1 sorbent only, while for L2 remains the capture degree roughly unchanged. This L2 behaviour can be

particularly attributed to a higher BET surface of this sorbent, which contributes to a higher reaction rate of the indirect sulphation.

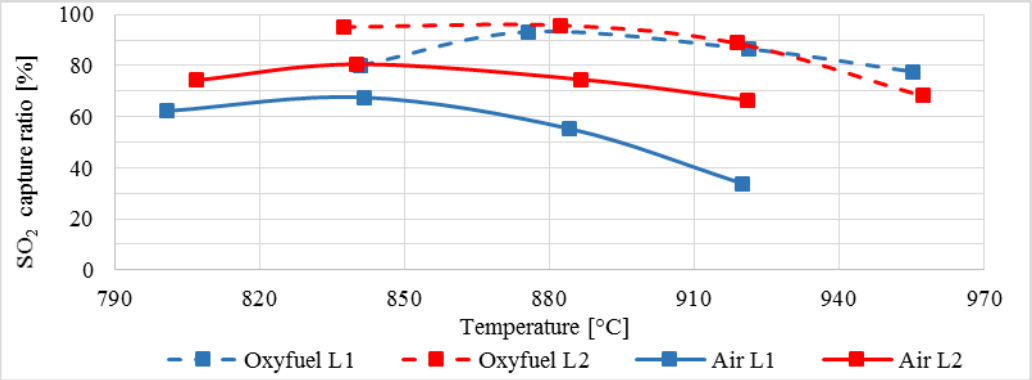

Figure 8-21: Correlation of SO_2 capture ratio with temperature – comparison of air and oxyfuel combustion

Effect of oxygen concentration

Another studied operating parameter affecting SO_2 capture ratio is oxygen concentration in flue gas. The results are shown in Figure 8-22 and Figure 8-23. It can be seen that the effect of oxidizer concentration is different for air and oxyfuel mode. Oxyfuel combustion shows slightly increasing tendency of SO_2 capture with increasing oxygen concentration. The reason is probably given by the fact that with increasing concentration of oxidizer decreases the concentration of CO_2, which shifts the calcination reaction towards the products. Important is also the effect of lower CO concentration at higher concentrations of oxidant. The effect in case of air combustion is opposite. Increase of O_2 concentration brings decrease of SO_2 capture ratio, which does not fully comply with the theory. Increase of O_2 concentration in air combustion increases also fluidization velocity that in turn decreases the residence time of limestone in the zone of appropriate temperature. The fluidization velocities are shown in the tables in appendix - A. Table 10 and A. Table 11 for air combustion and A. Table 22 and A. Table 23 for oxyfuel combustion). With the factor of fluidization velocity interrelates also the distribution of sulphur in the fuel. The tested fuel has more than 50% of sulphur bonded in the form of pyrite (Table 6-3). Pyrite causes that sulphation take place directly in the bed. The other forms of sulphur – organic and free are a part of volatiles and are released in freeboard. With increasing fluidization velocity the entrainment of the fine particles of limestone and coal increases and the process of desulphurization takes place more in freeboard section of the boiler with shorter time for reaction.

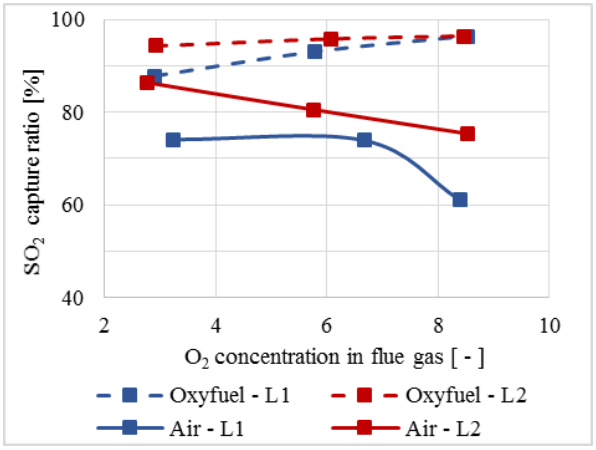

Figure 8-22: Correlation of SO_2 capture ratio with oxygen concentration in FG – comparison of air and oxyfuel combustion

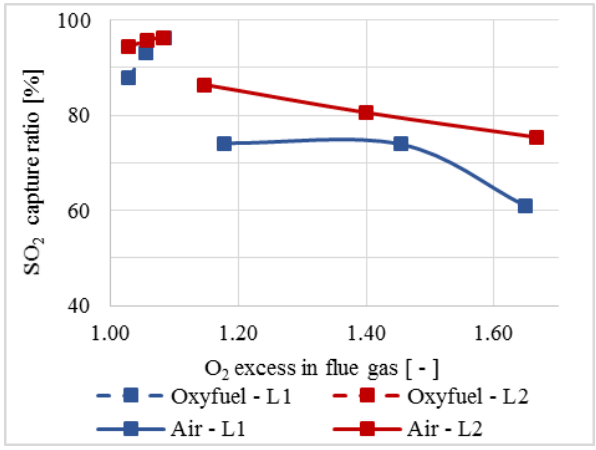

Figure 8-23: Correlation of SO_2 capture ratio with oxygen concentration expressed as oxygen excess – comparison of air and oxyfuel combustion

8.4 FLY ASH ANALYSIS

During the measurements in MiniFluid the samples of fly ash were taken from the fly ash discharger placed under the cyclone. The cyclone was discharged before and after each measurement. It is therefore possible to match the samples with the particular measurement cases. The XRF analyses was performed on the taken samples and the results of sulphur and calcium content were related to the SO_2 capture ratio. Results are shown in Figure 8-24 and Figure 8-25.

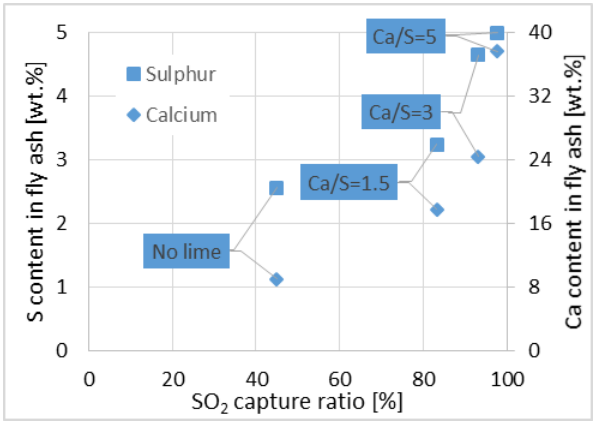

Figure 8-24: Sulphur and calcium content in fly ash in relation to the SO_2 capture ratio for limestone L1, oxyfuel conditions, MiniFluid

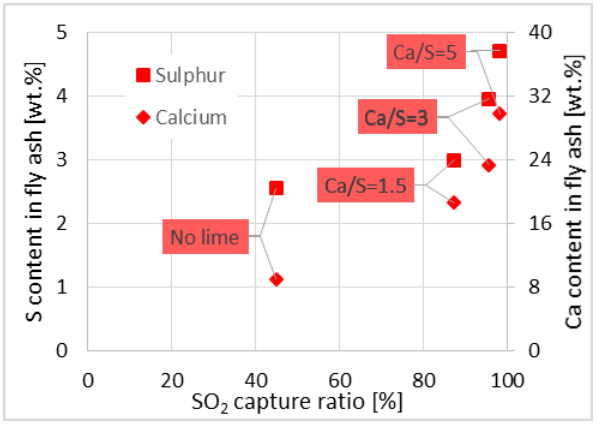

Figure 8-25: Sulphur and calcium content in fly ash in relation to the SO_2 capture ratio for limestone L2, oxyfuel conditions, MiniFluid

It can be seen that the amount of Ca increases with Ca/S ratio and the amount of captured sulphur also corresponds with this trend. For Ca/S = 0, there is only the calcium originating in the source fuel.

8.4.1 Balance of sulphur

In most of the cases only the fly ash samples captured in the cyclone were taken. Extraction of representative samples from the fluidized bed during the combustor operation for each case is highly complicated and was not carried out. Nevertheless, one sample of the fluidized bed material was taken during the measurement with limestone L1 at Ca/S=3 and bed temperature 920°C in the MiniFluid combustor, allowing a single comparison of the bed and fly ash samples. The results of XRF analyses of both ash samples are shown in Table 8-13.

Table 8-13: Comparison of the results from XRF analysis of ashes

	Si	Al	Fe	Mg	Ca	S	Other elements
Mass fraction – fly ash [%]	25.9	18.4	9.4	1.6	36.5	2.9	5.3
Mass fraction – bed ash [%]	27.4.	18.5	7.2	1.1	35.3	5.4	5.1

Based on the data in Table 8-13, sulphur mass balance can be done. For this specific case, a larger amount of sulphur was found in the fluidized bed while the amount of calcium remained roughly the same. In order to correctly express the amount of captured sulphur and calcium and relate it to kg of used fuel, it was necessary to determine the amount and distribution of ash produced in the combustor for certain time. This was done using the information about the pressure drop of the fluidized bed that was continuously measured. The ash accumulation in the fluidized bed was therefore determined from the growth of the pressure drop. Also the amount of captured fly ash in the cyclone was weighted for this specific measurement. The pressure drop at the beginning of the first measurement was 0.98 kPa and after four hours of measurement increased to 1.33 kPa. This corresponds to the increase of fluidized bed by ash for about 1.2 kg. The total amount of ash captured in cyclone was 2.2 kg. The ash balance is then following – 35 % remains in the fluidized bed, 65 % is entrained and then captured in the cyclone.

The sum of the sulphur in the ash of the fluidized bed, sulphur in fly ash and sulphur leaving the combustor as SO_2 was compared with the amount of sulphur supplied in the fuel. The results are shown in Table 8-14.

Table 8-14: Balance of sulphur

Sulphur in fly ash	2.34	g/kg_{fuel}
Sulphur in fluidized bed	2.48	g/kg_{fuel}
Sulphur from SO_2 emission	1.24	g/kg_{fuel}
Σ	6.1	g/kg_{fuel}
Sulphur in fuel	9.3	g/kg_{fuel}
Relative difference	-34	%

It can be seen from the table that most sulphur was captured in the ash of the fluidized bed in this measurement. The total sum of the sulphur is lower than the amount of sulphur in the fuel. However, the difference of 34 % can be considered to be a satisfactory accordance, taking into

account that the XRF analysis was performed only once and the tested samples were in amount of milligrams along with uncertain knowledge whether they are representative.

8.4.2 Balance of calcium

The balance of calcium was made in a similar way. The sum of added calcium and calcium naturally present in the fuel was compared with the amount of calcium in the ash samples, as shown in Table 8-15. The balance of calcium matches with satisfactory relative difference 6.5%. As for the sulphur balance, the same uncertainty of the analysis must be considered.

Table 8-15: Balance of calcium

Calcium added to the fuel	33.03	g/kg_{fuel}
Calcium from fuel	8	g/kg_{fuel}
Σ	41.03	g/kg_{fuel}
Calcium in fly ash	27.4	g/kg_{fuel}
Calcium in fluidized bed	16.3	g/kg_{fuel}
Σ	43.7	g/kg_{fuel}
Relative difference	+6.5	%

9 SCALE-UP OF THE SO_2 CAPTURE EXPERIMENTS

9.1 RESULTS OF THE EXPERIMENTS

This chapter summarizes the results from oxyfuel experiments made on Golem. The presented results are the average values from the minimally one hour measurements at stabilized conditions. Closer discussion of the results and comparison with results from MiniFluid are stated in following chapter 9.3.

The measurements performed on Golem were done using the same type of coal, but having higher water content (see Table 6-2). The amount of used limestone stayed the same as for measurements in MiniFluid (Table 8-2), but due to the different water content the values of molar Ca/S ratios were slightly changed. The real Ca/S ratios are given in the Table 9-1.

9.1.1 Sulphur self-retention

Similarly to the previous measurements performed on MiniFluid, the effect of sulphur self-retention was studied. The results from temperature dependence are shown in Figure 9-1. The effect of increasing oxygen excess in flue gas on sulphur self-retention was not studied. It can be seen that the effect of temperature is weak with the maximal efficiency around the temperatures of 880°C and it decreases with higher temperatures. The effect of decreasing sulphur self-retention can be explained by increasing CO concentrations, which cause reduction reactions with $CaSO_4$ (details about the particular emissions in Appendix 13.3) and negative effect of thermal degradation of CaO at high temperatures.

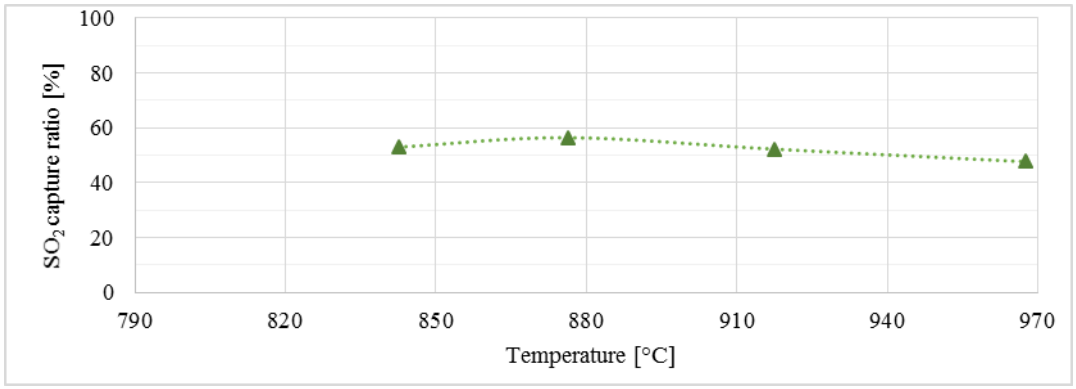

Figure 9-1: Sulphur self-retention correlation with temperature

9.1.2 Effect of Ca/S ratio

Another studied parameter was the effect of Ca/S ratio. Due to the fact, that the coal used in Golem had slightly different chemical composition of ash and different water content in comparison with coal used in MiniFluid, the inner Ca/S ratio changes. It was determined that the inner molar Ca/S ratio for the fuel used in Golem is 0.85 (more details about the coal ash composition are stated in Table 9-4).

It is important to mention, that the weight of limestone (Table 8-2) which was added to the fuel stayed the same as was used in all previous experiments, but due to the different water content in the fuel was slightly changed the molar Ca/S. The real molar Ca/S ratios were recalculated according to the new analysis of the coal and are shown in Table 9-1.

Table 9-1: Recalculation of Ca/S ratios according to the real conditions

Limestone L1				
Molar Ca/S ratio – reference amount	0	1.5	3	5
Real molar Ca/S ratio in Golem	0	1.65	3.3	5.5
Real molar Ca/S ratio including Ca in the fuel	0.85	2.5	4.15	6.35
Weight of added $CaCO_3$ (kg per 1t of coal)	0	45	90	150
Limestone L2				
Molar Ca/S ratio – reference amount	0	1.5	3	5
Real molar Ca/S ratio in Golem	0	1.65	3.3	5.5
Real molar Ca/S ratio including Ca in the fuel	0.85	2.5	4.15	6.35
Weight of added Ca (kg per 1t of coal)	0	60	120	200

The main results of the Ca/S ratio correlated with SO_2 capture are shown in Figure 9-2. The operation parameters that were set during the measurement were 840°C and oxygen concentration 6% in dry flue gas, the fluidization velocity was around 1.3 m/s. Detailed measurement data is listed in Appendix 13.3. The measured points of SO_2 capture ratio were approximated by equation 3-20, the results are shown in the Figure 9-2 as dashed lines. The results of coefficient K, including the values of determination coefficient R^2 giving the accuracy of approximation, are shown in Table 9-2. The value of SO_2 capture by the coal ash self-retention is indicated as green point in the Figure 9-2.

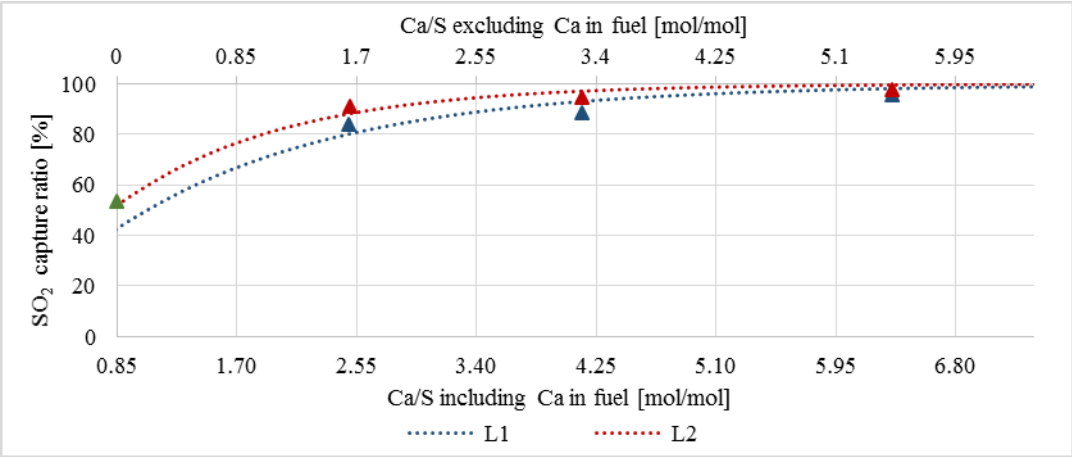

Figure 9-2: Effect of different Ca/S molar ratio on SO_2 capture ratio – fitting of the measured points – results from Golem

Table 9-2: Values of K constant obtained from correlation by equation 3-20

	Limestone L1	Limestone L2
K [-]	0.65	0.96
R^2 [-]	0.89	0.99

Another insight on the limestone characteristics can be seen by representation of the results as Ca/S weight ratio, which is displayed in Figure 9-3. The effect of the purity of the limestones neglects different limestones performance and both limestones start to show similar results of desulphurization, with smoothly higher desulphurization rate for limestone L2. The difference is mainly visible in lower Ca/S ratios.

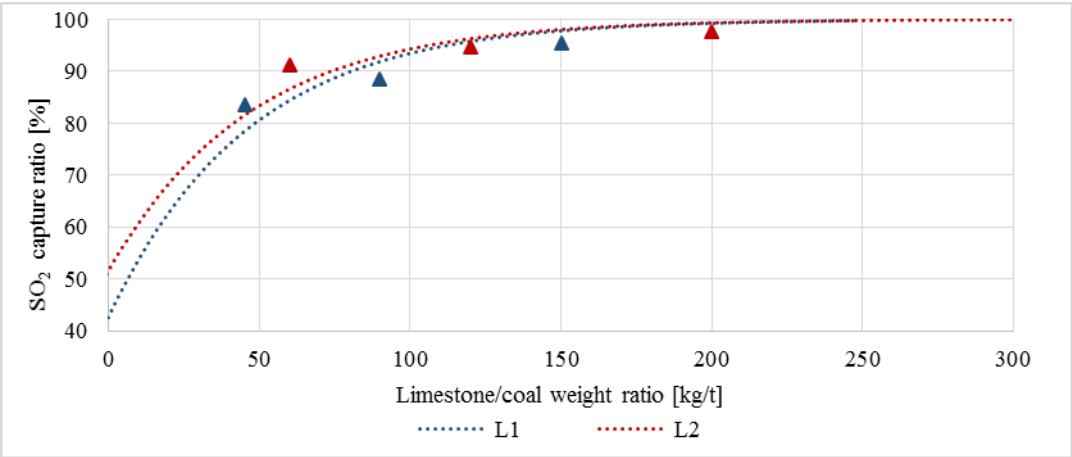

Figure 9-3: Effect of limestone addition on SO_2 capture represented as limestone to coal weight ratio – results from Golem

9.1.3 Effect of bed temperature

The methodology of measurements in Golem was similar to the methodology of measurements in MiniFluid and corresponds to the matrix of experiments presented in chapter 6.4.2. The difference between MiniFluid is in fact, that the bed temperature is measured using two thermocouples and the resulting bed temperature is given by their arithmetic average. The results of the experiments for different fluidized bed temperatures for limestone L1 are shown in Figure 9-4 and for limestone L2 in Figure 9-5. The maximum SO_2 capture ratio was found around the temperature 840°C, thus at the bottom part of the studied interval. In order to see the behaviour also below this temperature, an additional experiment for the bed temperature at 800°C was done, during the experiments with limestone L1 at Ca/S=5. This measurement shows decrease in SO_2 capture at the temperature below 840°C.

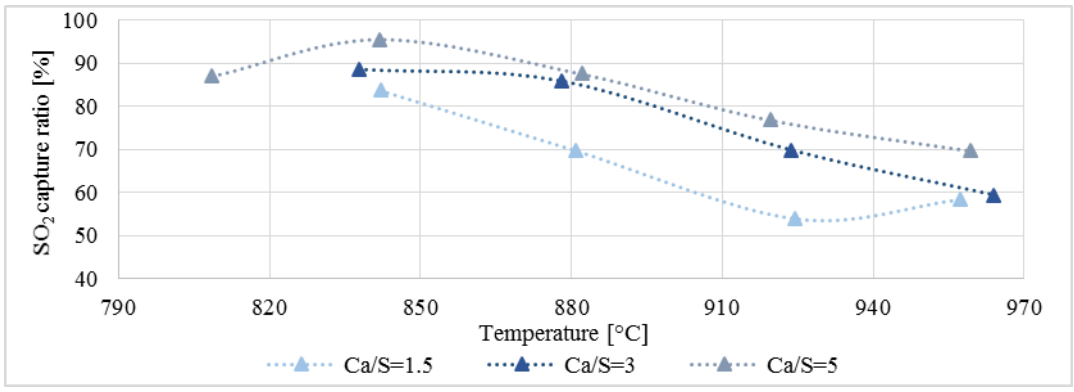

Figure 9-4: Correlation of SO_2 capture ratio with bed temperatures under oxyfuel conditions – results from Golem – **limestone L1**

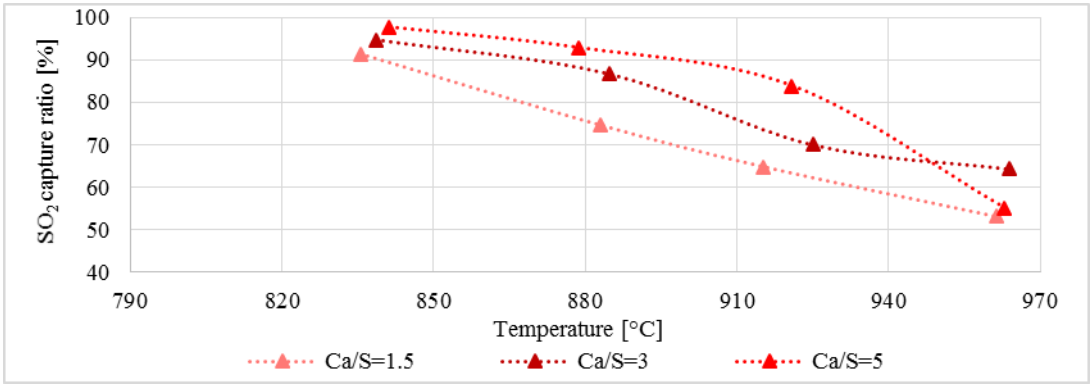

Figure 9-5: Correlation of SO_2 capture ratio with bed temperatures under oxyfuel conditions – results from Golem – **limestone L2**

Closer discussion about the results and comparison with the results from MiniFluid are stated in following chapter 9.3.

9.1.4 Effect of oxygen concentration

Figure 9-6 and Figure 9-7 show the results from measurements for different oxygen concentrations in flue gas. The behaviour of limestone L1 was measured at Ca/S=1.5, limestone L2 was studied at Ca/S=3. All the measurements were done at the same temperature 880°C. It can be seen, that for both limestones L1 and L2 the SO_2 capture increases with increasing oxygen excess, which is the same trend that was observed during MiniFluid measurments. Table 9-3 shows the effect of different O_2 concentrations also in the context with CO_2 and CO concentration. CO_2 does not correlate with oxygen as expected, since there is always a certain degree of false air ingress. Therefore, in some experimental cases a lower oxygen concentration does not correspond to a higher CO_2 concentration. The most important parameter negatively affecting the SO_2 capture is a higher CO concentration, supporting decomposition of the $CaSO_4$ product. Due to the low oxygen excess, the combustion quality rapidly changes. One of the example can be seen in Figure 9-6, the reason for decreased SO_2 capture ratio at the lowest oxygen concentration is probably caused by higher CO concentration which is about three times higher comparing with reference case (see Table 9-3).

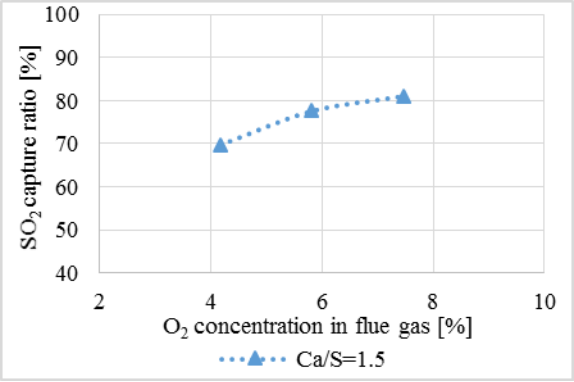

Figure 9-6: Correlation of SO_2 capture ratio with oxygen concentration in FG under oxyfuel conditions – results from Golem – **L1**

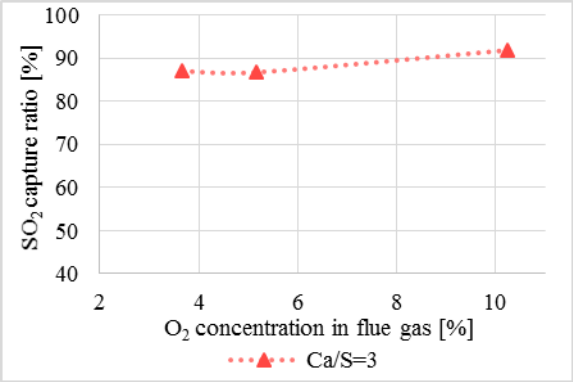

Figure 9-7: Correlation of SO_2 capture ratio with oxygen concentration in FG under oxyfuel conditions – results from Golem – **L2**

Table 9-3: Effect of different oxygen excess on SO_2 capture ratio – results from Golem

Ca/S [-]	O_2 in FG [%]	Excess of oxidant [-]	Rel. differences of SO_2 capture ratio [%]	CO_2 in dry FG [%]	Concentration of CO [ppm]	Relative difference of CO [%] *
L1 1.5	5.0	1.045	10.1	79.5	3503	+281
	5.9	**1.064**	**0**	**77.4**	**920**	**0**
	7.6	1.084	-4.4	75.6	585	-36.4
L2 3	3.7	1.038	-0.3	81.0	3 147	+42.5
	5.2	**1.054**	**0**	**81.3**	**2 208**	**0**
	10.2	1.115	-6.1	75.5	513	-76.7
Reference case						

* Relative increase or decrease of CO concentration from reference case

9.2 FLY ASH ANALYSIS

Similarly as for the measurements on MiniFluid also during the measurements on Golem the samples of fly ash were taken from the fly ash discharger placed under the cyclone. The cyclone was discharged before and after each measurement and the samples were assigned to the particular measurement cases. The results of sulphur and calcium content in fly ash were related to the SO_2 capture ratio. Results are shown in Figure 9-8 and Figure 9-9.

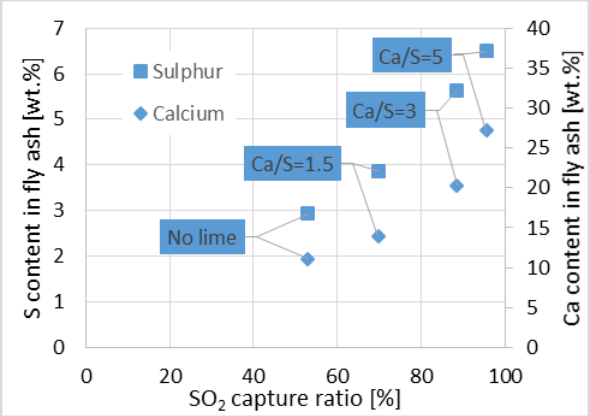

Figure 9-8: Sulphur and calcium content in fly ash in relation to the SO_2 capture ratio for limestone L1, oxyfuel conditions, Golem

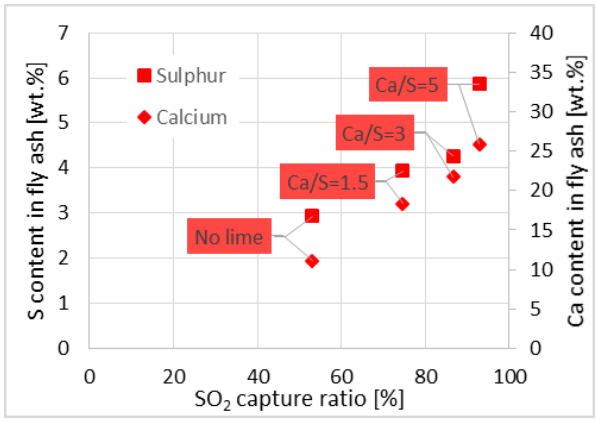

Figure 9-9: Sulphur and calcium content in fly ash in relation to the SO_2 capture ratio for limestone L2, oxyfuel conditions, Golem

Figures shows relatively high amount of calcium during measurements with no limestone addition. The fact about the relatively high calcium content in the fuel has been already mentioned in previous parts of this thesis.

It is also important to mention, that due to the complicated process of fluidized bed removal the samples of fluidized bed were not taken, thus the balance of the sulphur and calcium could not be made for measurements on Golem.

9.3 COMPARISON OF THE RESULTS BETWEEN MINIFLUID AND GOLEM

This chapter evaluates the effect of scale up from laboratory (MiniFluid, 30 kW) to pilot scale combustor (Golem, 500 kW). Naturally, there are significant differences in operation of the combustors, mainly due to the different design of them. As mentioned in chapter 7, the larger facility Golem suffers more from air ingress, resulting in lower CO_2 concentration at the outlet from the combustor, associated with higher presence of nitrogen as a result. However, the concentration of CO_2 does not drop under 75% in dry flue gas. Also the fluidization velocity is slightly higher in Golem (around 20% in general) and the dimensions of the combustion chamber and freeboard are proportionally different in both facilities. However, it can be concluded that the effect of the monitored parameters on SO_2 capture has the same trends in both facilities, and generally the transfer of experimental results between the scales is possible.

Effect of sulphur self-retention

In comparison with the results from MiniFluid, we can see a slightly higher SO_2 capture ratio reaching up to 55% just by the sulphur self-retention. In order to identify the reason of such behaviour, the samples of fly ash, which were taken during the measurements, were taken on the XRF analyses. The results from the XRF analysis from measurements with no limestone addition are presented in Table 9-4. In order to see the difference with the same measurements in MiniFluid there are added also the results from this measurements.

Table 9-4: Chemical composition of the used fuel ash related as oxides from the measurement without limestone – XRF analyses

	SiO_2	Al_2O_3	Fe_2O_3	MgO	CaO	SO_3	Other comp.
Mass fraction – ash from Golem [%]	36	29.9	8.6	2.8	11.3	6.1	5.3
Mass fraction – ash from MiniFluid [%]	42.2	28.4	7.5	2.5	9.4	4.8	5.2

It can be seen, that the chemical composition of fly ash was different in calcium content, which was higher for the coal used in Golem. Such a difference could explain the reason of slightly higher sulphur self-retention compared to the MiniFluid experiments, which does not exceed 7 percentage points. Concerning the sulphur self-retention, the scale-up differences are shown in Figure 9-10.

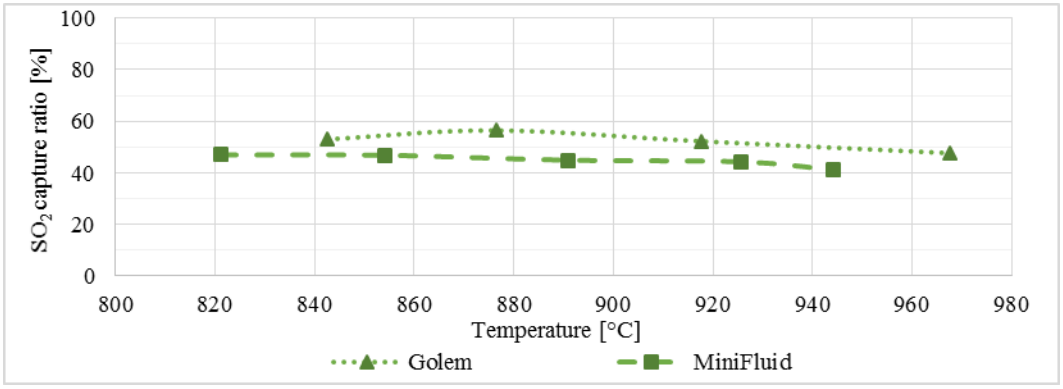

Figure 9-10: Comparison of the results of sulphur self-retention

Effect of different Ca/S ratios

Figure 9-11 compares the effect of Ca/S ratio for both facilities. It can be seen that limestone L2 has very similar results in both facilities, the curves in Figure 9-11 are nearly the same and covers each other.

On the contrary, in case of using limestone L1, bigger differences are seen. In general, limestone L1 achieves lower SO_2 capture efficiency when used in larger scale combustor Golem. Also the XRF analyses of fly ash show that the calcium content was lower by approximately 5 to 10 percentage points (Figure 9-8 and Figure 9-9).

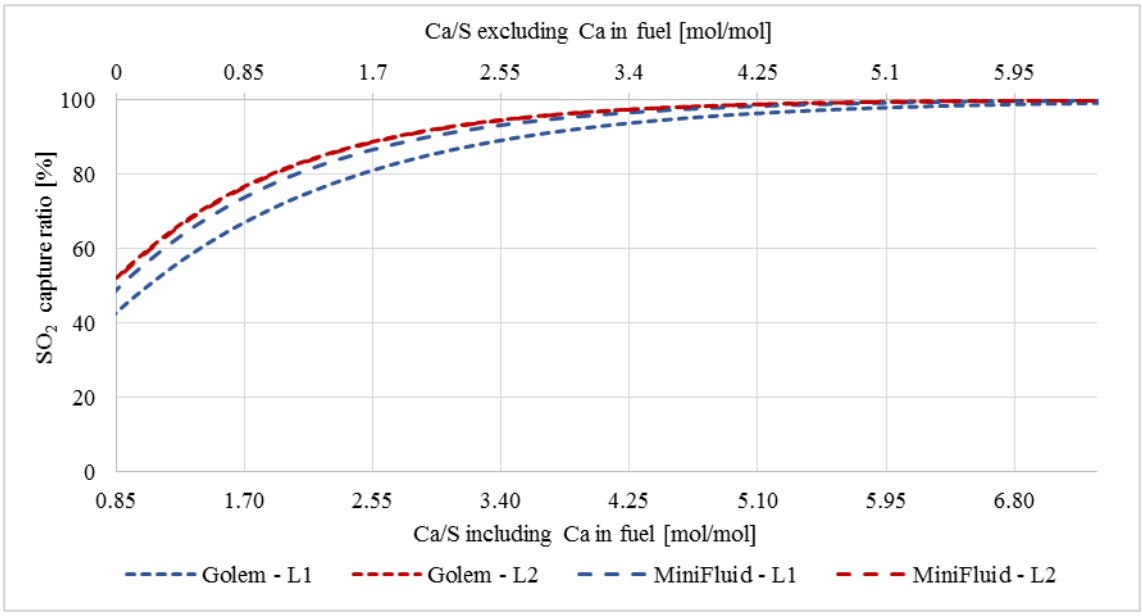

Figure 9-11: Comparison of the effect of Ca/S molar ratio on SO_2 capture ratio

Effect of bed temperatures

The results from the experiments studying the effect of bed temperatures on SO_2 capture ratio in Golem (Figure 9-4 and Figure 9-5) shows different behaviour compared to the same experiments carried out in the MiniFluid. The maximum SO_2 capture ratio is at about 40°C lower than in case of the measurements in MiniFluid.

In order to find out the reason of such behaviour, the closer insight into to measurement process was done. The temperature of the fluidized bed was determined as an average value of two temperatures measured by the thermocouples immersed in the fluidized bed. Placing of the thermocouples can be seen in Figure 6-6. Although the fluidized bed is known for very good heat exchange, the temperature differences between the thermocouples were for some measurements more than 40°C. One of the reason for this difference is the fact, that one thermocouple is placed closer to the fuel input to the fluidized bed. The second thermocouple is placed in the centre. In order to see how much this temperature difference can change the interpretation of the results, the Figure 9-12 is added to see the measurements in calcination equilibrium context. The values of CO_2 concentrations for each experiment are displayed in relation to the three temperatures – temperature from the centre of the fluidized bed (T-centre), temperature of the fluidized bed placed closer to the wall, where the fuel is added (T-wall) and average of these two (T-average). The T-average is currently used for control of the combustor. It can be seen that in case of the T-wall temperature interpretation, the measurements for lower border of the studied temperature interval are moved closer to the calcination equilibrium curve and are moved to the place of indirect desulphurization process.

The measurements which are placed on the left side of the limestone calcination equilibrium curve in diagram with T-wall temperature are the measurements with limestone L2.

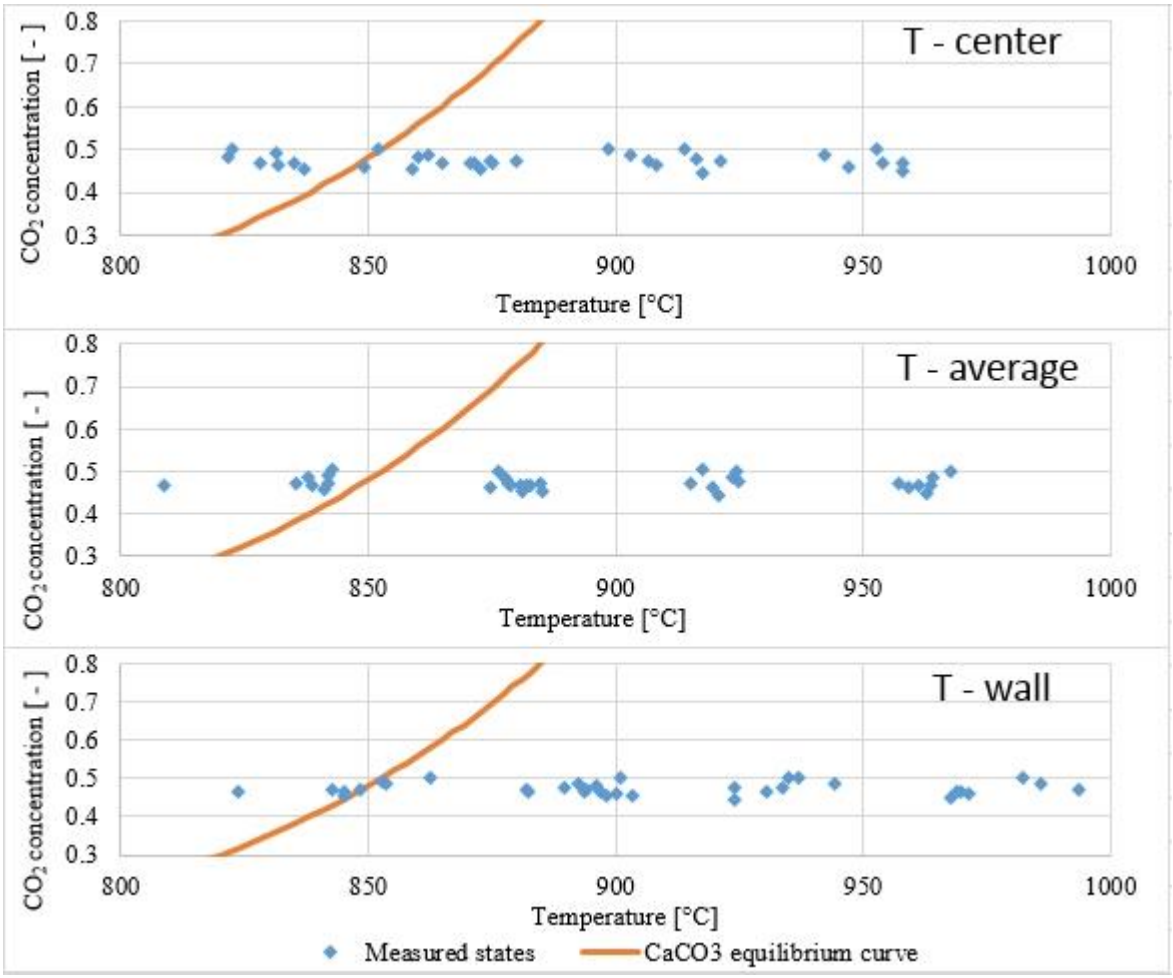

Figure 9-12: CO_2 concentrations in wet flue gas and bed temperatures for each experiment - Golem

Figure 9-12 also shows that the concentration of CO_2 in flue gas were lower for measurements in Golem in comparison with the values from MiniFluid. The CO_2 concentrations were in the range from 45 to 50 % in wet gas, in opposite to the MinuFluid measurements where the CO_2 concentration were always above 50%. There are two reasons for lower CO_2 concentrations for measurements on Golem. One reason is a higher air ingress which dilutes the CO_2 concentrations. Although, the concentration of nitrogen in flue gas is not measured, it can be assumed that the remaining volume to 100% is in majority the nitrogen. Comparing the air ingress between Golem and MiniFluid it is about 20% of nitrogen in dry flue gas for Golem against just about 5% of nitrogen in MiniFluid. The second reason is that the flue gas recirculation was always wet in Golem, it means, the FGR temperature did not decrease bellow 130°C and there was no condensation of water vapour in FGR, resulting in higher water vapour concentrations. This is different to MiniFuid where the FGR temperatures were lower and water vapour condensation in FGR occurred, which causes lowering the water vapour concentration

by more the 50% (depending on the temperature). Higher water vapour concentration in Golem is also caused by higher water content in the fuel used in Golem.

It is important to mention, that the maximal reached SO_2 capture ratio is nearly the same in both combustors, but the optimal temperature differs. However the temperature dependence is stronger in Golem and SO_2 capture ratio significantly decreases out of the optimal temperatures. The example is shown in Figure 9-13, where the correlation of temperature influence at Ca/S=3 is compared. The presented results in Figure 9-13 are given for the T-average bed temperature in Golem, the results for higher bed temperature (T-wall temperature) in Golem are added in Figure 9-14. It can be seen that the results in Figure 9-14 are closer to the results from MiniFluid, however the differences are still significant. The reason for lower SO_2 capture ration in Golem can be attributed to the significantly higher CO concentration in Golem, which are higher across all measurements and also to the higher fluidization velocity reducing the residence time in the fluidized bed.

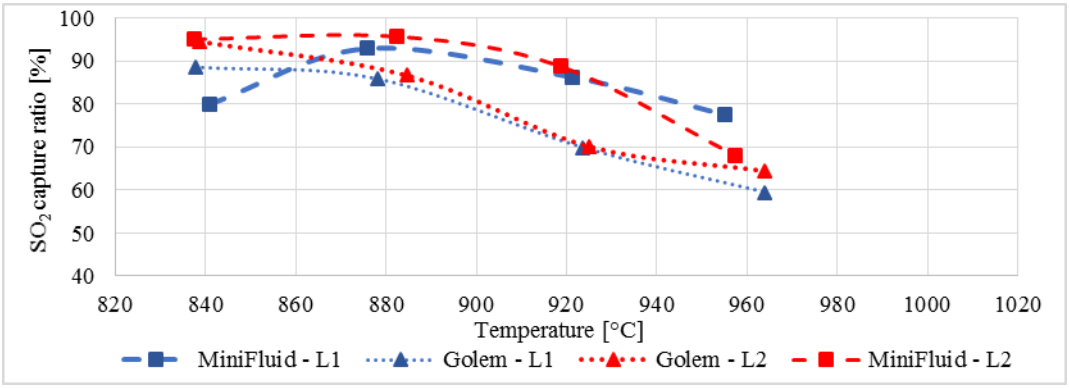

Figure 9-13: Comparison of the effect of fluidized bed temperatures

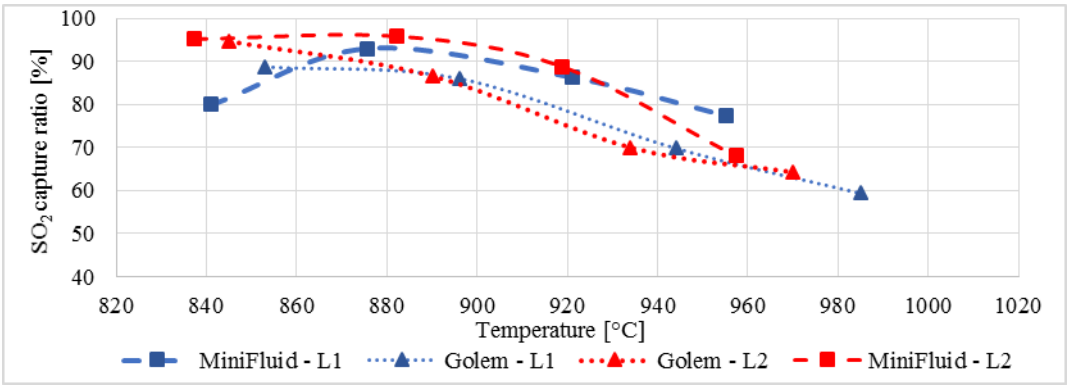

Figure 9-14: Comparison of the effect of fluidized bed temperatures for T-wall temperature in Golem

10 FINAL EVALUATION OF THE REASERCH RESULTS

10.1 DIFFERENT VIEWS ON THE DESULPHURIZATION EVALUATION

Until now, all the results were expressed as SO_2 capture ratio defined according to the equation 3-8 (stated here again for easier comparison as equation 10-1). The variable $C_{SO_2\ theoretical}$ is by the definition a maximum theoretical SO_2 concentration, which would be reached in case of oxidation of all the combustible sulphur contained in fuel. However, it is also possible to define the amount of captured SO_2 by the equation 10-2 expressing the desulphurization efficiency of used limestone. This relation characterizes just the effect of added limestone, disadvantage of this approach is that the sulphur self-retention must be experimentally determined.

Another possibility how to characterise the desulphurization process is the limestone utilization. This parameter is defined by equation 10-3, where EF_{SO_2} is emission factor in g/kg_{fuel}, M_{SO_2}, M_S, M_{Ca} are the molar weights of the particular substances for calculation between molar and weight ratios and m_{Ca_total} is the sum of the amount of calcium added to the fuel related in g per kilogram of fuel and the amount of calcium naturally presented in fuel ash. m_{Ca_total} is determined from equation 10-4. Here, $m_{limestone}$ corresponds to the weight of added limestone to the fuel and ω_{CaCO_3} expresses the purity of the limestone (amount of $CaCO_3$).

$$\eta_{capture} = \frac{C_{SO_2\ theoretical} - C_{SO_2\ desulphurized}}{C_{SO_2\ theoretical}} \qquad 10\text{-}1$$

$$\eta_{desulp.} = \frac{C_{SO_{2self-retention}} - C_{SO_2\ desulphurized}}{C_{SO_2\ self-retention}} \qquad 10\text{-}2$$

$$\eta_{limestone} = \frac{(EF_{SO_2\ theoretical} - EF_{SO_2\ measured}) \cdot \frac{M_S}{M_{SO_2}}}{m_{Ca\_total}} \cdot \frac{M_{Ca}}{M_S} \qquad 10\text{-}3$$

$$m_{Ca\_total} = \frac{m_{limestone} \cdot \omega_{CaCO_3} \cdot \frac{M_{Ca}}{M_{CaCO_3}} + m_{Ca\ in\ fuel}}{1000 + m_{limestone}} \cdot 1000 \qquad 10\text{-}4$$

Table 10-1 shows the results of desulphurization efficiency and limestone utilization correlated for different bed temperatures at constant Ca/S ratio 1.5. In case of comparison between SO_2 capture ratio and desulphurization efficiency, we can see, that the relative difference is bigger for oxyfuel combustion, which is given by significantly higher sulphur self-retention at oxyfuel combustion. In case of limestone utilization we can see, that it also copies the trends of SO_2 capture ratio. The highest limestone utilization reached under air combustion was around 25%

for limestone L1 and 28% for limestone L2. In the oxyfuel mode, the limestone utilization is generally in average more than 10 percentage points higher.

Table 10-1: Desulphurization evaluation – comparison of air and oxyfuel combustion for Ca/S ratio = 1.5 at different temperatures

		Air			Oxyfuel		
	Bed temp. [°C]	$\eta_{capture}$ [%]	$\eta_{desulp.}$ [%]	$\eta_{lime.total}$ [%]	$\eta_{capture}$ [%]	$\eta_{desulp.}$ [%]	$\eta_{lime.total}$ [%]
L1	T800°C	53.9	44.3	25.5	-	-	-
	T840°C	45.8	36.9	21.7	73.9	53.9	32.9
	T880°C	38.4	29.5	18.1	83.2	71.2	37.0
	T920°C	7.3	0.0*	3.5	67.6	45.2	30.1
	T960°C	-	-	-	47.4	10.5	19.8
L2	T800°C	63.8	56.0	28.4	-	-	-
	T840°C	60.5	53.7	26.9	82.7	69.3	36.8
	T880°C	58.0	51.7	25.8	87.4	78.5	38.9
	T920°C	51.9	43.2	23.1	82.5	70.4	36.7
	T960°C	-	-	-	58.5	33.5	26.0

* zero value means that the desulphurization reached just the value of sulphur self-retention

The effect of increasing Ca/S ratio on limestone utilization at constant bed temperature 840°C (air) and 880°C (oxyfuel) is shown in Table 10-2. As expected, with increasing Ca/S ratio the degree of limestone utilization decreases. In case of Ca/S 5 it is less than 20%. The negative effect of a high Ca/S ratio is, that it significantly increases amount of ash. In case of the highest amount of added limestone to the fuel, the amount of ash increases from 10.6 % to 22.2 % in the fuel. This fact of course increases operational cost and should be taken into consideration.

Table 10-2: Desulphurization efficiency and limestone utilization – comparison of air and oxyfuel combustion at different Ca/S ratios at constant temperature

		Air			Oxyfuel		
	Ca/S	$\eta_{capture}$ [%]	$\eta_{desulp.}$ [%]	$\eta_{lime.total}$ [%]	$\eta_{capture}$ [%]	$\eta_{desulp.}$ [%]	$\eta_{lime.total}$ [%]
L1	1.5	45.8	36.9	21.7	83.2	71.2	37.0
	3	67.6	62.3	20.0	93.0	88.0	25.9
	5	88.1	86.2	17.9	97.6	95.9	18.7
L2	1.5	60.5	53.7	26.9	87.4	78.5	38.9
	3	80.5	75.8	24.9	95.8	92.8	26.9
	5	96.6	96.0	18.9	98.2	97.0	18.5

Detailed information about limestone utilization is given in the appendix 13.5.

10.2 SUMMARY OF ACCOMPLISHED GOALS AND TASKS

10.2.1 Accomplishment of the main goal

Describe and compare the process of SO_2 capture during bubbling fluidized bed combustion under air and oxyfuel conditions and study the effect of scaling up the experiments from lab-scale 30 kW facility to pilot scale 500 kW BFBC.

The main parameters affecting the SO_2 capture were defined and studied – the amount of the limestone expressed as Ca/S ratio and two operation parameters of the boiler - fluidized bed temperature and excess of oxygen. In total about 120 experimental runs were performed at MiniFluid and about 60 runs at Golem. **It was found that it is possible to reduce SO_2 concentration in BFBC bellow 100 ppm at oxyfuel conditions which can be considered as a sufficiently low concentration for further processing of CO_2 such as compression and storage.**

The most general conclusion from the experiments is that SO_2 capture ratio is significantly higher at oxyfuel combustion under equal operating conditions compared to air conditions. The highest differences between air and oxyfuel conditions were observed in measurements at low Ca/S ratios. One of the reasons is the fact that SO_2 concentration in oxyfuel conditions is significantly higher (about 5 times higher). Higher concentration then leads to higher rate of desulphurization reactions. In the case of the highest examined Ca/S ratios the differences were lower (just about 3 percentage points for limestone L2 at Ca/S=5 and 8 percentage points for L1).

Two different sorts of limestone were used and several differences were found. Limestone L2 has significantly higher surface area and shows higher SO_2 capture ratio in both air and oxyfuel regimes.

In terms of temperature dependence, it has been observed that in the case of air combustion, the optimum temperature for desulphurization is in a range from 800°C to 840°C, which corresponds to the general knowledge about dry additive desulphurization method. In case of oxyfuel combustion, the optimum temperatures are higher, particularly around 880°C. Higher temperatures correspond to a higher limestone calcination temperature due to higher partial pressure of CO_2 in the flue gas. Especially in the case of using limestone L1, the SO_2 capture ratio significantly decreases in the zone where direct sulphation occurs. Oppositely limestone L2 has much flatter dependence on combustion temperatures. It was found that limestone L2

works in oxyfuel regime also in the zone of direct sulphation, i.e. in the zone were calcination of limestone is suppressed.

The experiments were also carried out on larger experimental facility – Golem. The results show a similar behaviour in the case of sulphur self-retention. However, in other measurements the differences were higher. The main difference is in stronger dependence of SO_2 capture ratio on temperature. The maximal SO_2 capture ratio was at the similar level as for MiniFluid combustion but it was achieved at a lower combustion temperatures, particularly about 850°C. The difference between the two devices was in CO_2 concentration, which was about 10 percentage points lower in the case of combustion in Golem. Such a decrease of CO_2 concentration causes, that limestone can calcine already at temperature 850°C. This is opposite to MiniFluid combustion, where the calcination was suppressed at this temperature. Another difference is the significantly decreasing SO_2 capture ratio with rising temperature. The reason is probably attributable to the fact that in the case of combustion in Golem, there was a significantly higher concentration of CO, which in combination with the high temperature causes the reduction of $CaSO_4$.

10.2.2 Accomplishment of the individual tasks

In order to fulfil the main goal of the dissertation thesis the individual tasks were necessary to be solved:

1) *Theoretical analysis of oxyfuel combustion and its mathematical balance model with the specification on combustion in bubbling fluidized bed boilers and comparison with combustion under air conditions.*

The theoretical analysis of the oxyfuel combustion process contained modification of the stoichiometric balance calculation known from air combustion to oxyfuel conditions. The calculation was specified for the combustion in BFB and was calculated both for air and oxyfuel conditions. **It was determined that it is impossible to achieve equal oxyfuel and air combustion regimes in terms of simultaneously having the same thermodynamic and hydrodynamic parameters.** Oxyfuel combustion is characterized by about 5 times lower volume of flue gases and in order to ensure sufficient fluidization it is necessary to increase the FGR. On the other hand, FGR works as the heat carrier which decreases the fluidized bed temperature. The possible decrease of the temperatures can be minimalized by a higher fuel supply, thus increasing power load of the boiler. The detailed results are stated in chapter 5.

2) *Design of the experimental facility with the power output about 30 kWt, suitable for working under air and oxyfuel combustion and modification of the bigger 500 kWt BFBC pilot boiler to be able to operate under oxyfuel regime.*

At first it was necessary to design and develop suitable experimental facilities – experimental bubbling fluidized bed boilers. The smaller facility, MiniFluid, has power output about 30 kW and is optimal for easy combustion control and optimization of the oxyfuel combustion. The main benefit of this device is that it works with real combustion and does not use any synthetic gases for simulation of some states. The second device, Golem, is a pilot plant facility having power output about 500 kW, which was reconstructed and optimized for oxyfuel combustion

3) *Experimental validation of the mathematical balance model of oxyfuel combustion.*

The validation of the mathematical balance model with the results from measurement was done and details are presented in chapter 7. The results show that the differences between calculations and oxyfuel combustion at MiniFluid ranges around ±5%, which is a very good accordance between theoretical calculations and experiments. In case of the results in Golem the differences are higher with maximal deviation about 15%, which is still very good accordance. The main reason for higher difference is given by the size of the facility and lower accuracy of fuel feeding measurement, which is an important input to the calculation balance.

10.3 CONSEQUENCES FOR SCIENCE AND PRACTICE

This dissertation deals with the relatively broad issue of oxyfuel combustion as one of the possible CCS technologies and focuses especially on the problematic of bubbling fluidized bed combustion and lowering SO_2 concentrations in flue gas. CCS technologies generally are an important topic in the field of energy and power production research located just know on the border between the field of research and first applications into the practice, in this time still as the form of pilot plant projects.

This work was gradually formed as a part of more extensive research projects, such as the Grant Agency of the Czech Technical University in Prague, grant No. SGS13/181/OHK2/3T/12 "Investigation of fluidized bed behaviour for combustion of nonconventional fuels" and the grant of the Technology Agency of the Czech Republic, grant No. TA03020312 "Research of oxyfuel combustion in a bubbling fluidized bed for CCS technologies". The current focus on this problematic can be also stated by the ongoing research of the Research Centre for Low-Carbon Energy Technologies, CZ.02.1.01/0.0/0.0/16_019/0000753. From the point of view of the contribution to science research it is possible to see synergy of the results of this work with the course of multi-annual research grants. As a part of this work, the methodology of the assessment and balancing of the oxyfuel combustion itself was done. Also the possibility of SO_2 capture using the dry additive desulphurization method was proven.

The experimental combustor MiniFluid has been created and optimized. The size of the combustor is so large that it cannot be taken just as a bench scale laboratory facility that is mostly based on the principle of simulating the processes and sometimes does not correspond to the real operating conditions. On the other hand, it provides a very flexible way of controlling the combustion processes, which enables the possibility to set and study the whole range of different operating scenarios. The key states can be further verified on a larger device – Golem, which has been appropriately modified and optimized for oxyfuel operation.

The dry additive desulphurization method is one of the major benefits of combustion in the bubbling fluidized bed. This method allows a relatively effective reduction of SO_2 concentrations using a relatively cheap and easily available additive – limestone. It has been verified that use of this method is also possible under oxyfuel combustion conditions, even with better results than in the case of combustion with air. The parameters influencing the desulphurization process have been defined. The results of the SO_2 capture ratios can be an important part for the future technical-economic balances considering the use of this technology in practice.

10.4 FUTURE WORK

The results of the thesis showed that there are many open fields for further research of oxyfuel combustion in BFB. Taking into account just the topic of desulphurization at oxyfuel conditions the following issues should be studied:

- Some other experiments should be done concerning more sorts of coals and limestones.
- The effect of wet/dry flue gas recirculation should be studied taking into consideration actual concentration of water vapour concentration and its possible reaction with CaO and following reduction of SO_2 by $Ca(OH)_2$.
- In case of dry recirculation the effect of possible flow out of SO_2 by water vapour condensate and composition of the condensate should be studied.
- Also the effect of the limestone addition on ash composition should be studied in detailed, due to the possible high amount of unreacted CaO content, which can cause problems with ash deposition.
- Study the effect of oxygen staging that is primarily used for nitrogen oxides reduction, but creates the reduction conditions in the fluidized bed, which can affect the process of SO_2 capture.
- The process of SO_2 production and SO_2 capture during combustion of biomass at oxyfuel conditions should be studied, due to the fact that Bio-CCS/U is a modern topic in the research field.

11 CONCLUSION

This thesis summarizes the knowledge about oxyfuel combustion in bubbling fluidized bed boilers and specially focuses on the issue of lowering concentration of SO_2 in flue gas. The thesis contains theoretical analysis of oxyfuel process and balance model describing the oxyfuel combustion process. This model is further verified experimentally. Two experimental facilities were developed in order to experimentally study the behaviour of dry additive method of desulphurization under oxyfuel conditions.

The experiments were focused mainly on study the stoichiometry of used additives (Ca/S ratio), influence of operating parameters such as fluidized bed temperature and oxygen concentration, everything for two different sorts of limestone. One of the benefits of the thesis is scale up of the experiments on pilot size combustor – Golem. Altogether more than 180 experiments were carried out, each of them lasting approximately about one hour at stabilized combustion conditions.

In conclusion, the desulphurization under oxyfuel conditions is more efficient than in the case of air combustion at equal process conditions. By this method of desulphurization it is possible to continuously maintain a concentration of SO_2 below 100 ppm using both technologically and economically acceptable conditions (Ca/S not exceeding 4).

The goals of the thesis set above were met in all aspects and their detail analysis and discussion of the results are outlined in the previous chapters. The results of the work have been continuously published at scientific conferences and in scientific journals (see the list of own publications) and were the part of several research projects.

12 BIBLIOGRAPHY

12.1 BIBLIOGRAPHY (EXCLUDING AUTHORS OWN PUBLICATIONS)

[1] INTERNATIONAL ENERGY AGENCY. *Statistics*. [accessed. 2018-09-20]. Available at: http://www.iea.org/statistics

[2] ERIKSSON, T., NUORTIMO, K., HOTTA, A., MYÖHÄNEN, K., HYPPÄNEN, T., & PIKKARAINEN, T. Near zero CO2 emissions in coal firing with oxyfuel CFB boiler. *Proc. of the 9th International Conference on Circulating Fluidized Beds*. 2008, 13–16.

[3] BUHRE, B. J P, L. K. ELLIOTT, C. D. SHENG, R. P. GUPTA and T. F. WALL. Oxy-fuel combustion technology for coal-fired power generation. *Progress in Energy and Combustion Science*. 2005, **31** (4), 283–307. ISSN 03601285. DOI: 10.1016/j.pecs.2005.07.001

[4] OKA, S. N. *Fluidized Bed Combustion*. Marcel Dekker, Inc., 2004. ISBN 0-8247-4699-6.

[5] STANGER, Rohan and Terry WALL. Sulphur impacts during pulverised coal combustion in oxy-fuel technology for carbon capture and storage. *Progress in Energy and Combustion Science*. 2011, **37** (1), 69–88. ISSN 03601285. DOI: 10.1016/j.pecs.2010.04.001

[6] NANDY, Anirban, Chanchal LOHA, Sai GU, Pinaki SARKAR, Malay K. KARMAKAR and Pradip K. CHATTERJEE. Present status and overview of Chemical Looping Combustion technology. *Renewable and Sustainable Energy Reviews*. 2016, **59** , 597–619. ISSN 18790690. DOI: 10.1016/j.rser.2016.01.003

[7] CHAKRAVARTULA SRIVATSA, Srikanth and Sankar BHATTACHARYA. Amine-based CO2capture sorbents: A potential CO2hydrogenation catalyst. *Journal of CO2 Utilization*. 2018, **26** (March), 397–407. ISSN 22129820. DOI: 10.1016/j.jcou.2018.05.028

[8] BAI, Hsunling and An Chin YEH. Removal of CO2 Greenhouse Gas by Ammonia Scrubbing. *Industrial & Engineering Chemistry Research*. 1997, **36** (6), 2490–2493. DOI: 10.1021/ie960748j

[9] HERZOG, Howard. Advanced Post-Combustion CO 2 Capture. 2009, (April).

[10] THEO, Wai Lip, Jeng Shiun LIM, Haslenda HASHIM, Azizul Azri MUSTAFFA and Wai Shin HO. Review of pre-combustion capture and ionic liquid in carbon capture and storage. *Applied Energy*. 2016, **183** , 1633–1663. ISSN 03062619. DOI: 10.1016/j.apenergy.2016.09.103

[11] LYNGFELT, Anders and Carl LINDERHOLM. Chemical-looping combustion of solid fuels - Technology overview and recent operational results in 100 kW unit. *Energy Procedia*. 2014, **63** , 98–112. ISSN 18766102. DOI: 10.1016/j.egypro.2014.11.011

[12] KIMURA, N., K. OMATA, T. KIGA, S. TAKANO and S. SHIKISIMA. The characteristics of pulverized coal combustion in O2/CO2 mixtures for CO2 recovery. *Energy Conversion and Management*. 1995, **36** (6–9), 805–808. ISSN 01968904. DOI: 10.1016/0196-8904(95)00126-X

[13] TAN, Yewen, Mark a DOUGLAS and Kelly V THAMBIMUTHU. CO 2 capture using oxygen enhanced combustion strategies for natural gas power plants. *Fuel*. 2002, **81** (8), 1007–1016. ISSN 00162361. DOI: 10.1016/S0016-2361(02)00014-5

[14] FARZAN, H, S VECCI, MCDONALD D, K MCCAULEY, P PRANDA, R VARAGANI, F GAUTIER, J P TRANIER and N PERRIN. State of the Art of Oxy-Coal Combustion Technology for CO2 Control from Coal-Fired Boilers: Are We Ready for Commercial Installation? *32nd International Technical conference on coal utilization &*

fuel systems. 2007, 12.

[15] WALL, Terry, Yinghui LIU, Chris SPERO, Liza ELLIOTT, Sameer KHARE, Renu RATHNAM, Farida ZEENATHAL, Behdad MOGHTADERI, Bart BUHRE, Changdong SHENG, Raj GUPTA, Toshihiko YAMADA, Keiji MAKINO and Jianglong YU. An overview on oxyfuel coal combustion-State of the art research and technology development. *Chemical Engineering Research and Design*. 2009, **87** (8), 1003–1016. ISSN 02638762. DOI: 10.1016/j.cherd.2009.02.005

[16] ANHEDEN, M., U. BURCHHARDT, H. ECKE, R. FABER, O. JIDINGER, R. GIERING, H. KASS, S. LYSK, E. RAMSTRÖM and J. YAN. Overview of operational experience and results from test activities in Vattenfall's 30 MWthoxyfuel pilot plant in Schwarze Pumpe. *Energy Procedia*. 2011, **4** , 941–950. ISSN 18766102. DOI: 10.1016/j.egypro.2011.01.140

[17] UCHIDA, Terutoshi, Takahiro GOTO, Toshihiko YAMADA, Takashi KIGA and Chris SPERO. Oxyfuel combustion as CO2capture technology advancing for practical use - Callide oxyfuel project. *Energy Procedia*. 2013, **37** , 1471–1479. ISSN 18766102. DOI: 10.1016/j.egypro.2013.06.022

[18] LUPION, Monica, Iñaki ALVAREZ, Pedro OTERO, Reijo KUIVALAINEN, Jouni LANTTO, Arto HOTTA and Horst HACK. 30 MWth CIUDEN Oxy-CFB boiler - First experiences. *Energy Procedia*. 2013, **37** , 6179–6188. ISSN 18766102. DOI: 10.1016/j.egypro.2013.06.547

[19] LUO, Wei, Qiao WANG, Junjun GUO, Zhaohui LIU and Chuguang ZHENG. Exergy-based control strategy selection for flue gas recycle in oxy-fuel combustion plant. *Fuel*. 2015, **161** , 87–96. ISSN 00162361. DOI: 10.1016/j.fuel.2015.08.036

[20] ZHENG, Chuguang, Zhaohui LIU, Jun XIANG, Liqi ZHANG, Shihong ZHANG, Cong LUO and Yongchun ZHAO. Fundamental and Technical Challenges for a Compatible Design Scheme of Oxyfuel Combustion Technology. *Engineering*. 2015, **1** (1), 139–149. ISSN 20958099. DOI: 10.15302/J-ENG-2015008

[21] METCALFE, Richard, Kate THATCHER, George TOWLER, Alan PAULLEY and Jeremy ENG. Sub-surface Risk Assessment for the Endurance CO2Store of the White Rose Project, UK. *Energy Procedia*. 2017, **114** (November 2016), 4313–4320. ISSN 18766102. DOI: 10.1016/j.egypro.2017.03.1578

[22] LASEK, Janusz, Radosław LAJNERT, Krzysztof GÓD and Jarosaw ZUWAA. Analysis of the transition time from air to oxy-combustiond. *Chemical and Process Engineering - Inzynieria Chemiczna i Procesowa*. 2015, **36** (1), 113–120. ISSN 02086425. DOI: 10.1515/cpe-2015-0009

[23] HACK, Horst. Update on the Operation of the CIUDEN Oxy-CFB Boiler Demonstration Project. *PowerGen*. 2011.

[24] VARONEN, M. 4 MWth Oxy-CFB Test Runs. *63rd IEA-FBC meeting*. 2011.

[25] SURANITI, Silvestre L., Nsakala ya NSAKALA and Scott L. DARLING. Alstom oxyfuel CFB boilers: A promising option for CO2 capture. *Energy Procedia*. 2009, **1** (1), 543–548. ISSN 18766102. DOI: 10.1016/j.egypro.2009.01.072

[26] LI, Haoyu, Shiyuan LI, Qiangqiang REN, Wei LI, Mingxin XU, Jing Zhang LIU and Qinggang LU. Experimental results for oxy-fuel combustion with high oxygen concentration in a 1MWth pilot-scale circulating fluidized bed. *Energy Procedia*. 2014, **63** , 362–371. ISSN 18766102. DOI: 10.1016/j.egypro.2014.11.039

[27] TAN, Y., L. JIA, Y. WU and E. J. ANTHONY. Experiences and results on a 0.8MWth oxy-fuel operation pilot-scale circulating fluidized bed. *Applied Energy*. 2012, **92** , 343–347. ISSN 03062619. DOI: 10.1016/j.apenergy.2011.11.037

[28] JIA, L., Y. TAN, D. MCCALDEN, Y. WU, I. HE, R. SYMONDS and E. J. ANTHONY. Commissioning of a 0.8MWthCFBC for oxy-fuel combustion. *International Journal of*

Greenhouse Gas Control. 2012, **7** , 240–243. ISSN 17505836. DOI: 10.1016/j.ijggc.2011.10.009

[29] HOFBAUER, G., T. BEISHEIM, H. DIETER and G. SCHEFFKNECHT. Experiences from oxy-fuel combustion of bituminous coal in a 150 kWth circulating fluidized bed pilot facility. *Energy Procedia*. 2013, **51** , 24–30. ISSN 18766102. DOI: 10.1016/j.egypro.2014.07.003

[30] STEWART, Michael C., Robert T. SYMONDS, Vasilije MANOVIC, Arturo MACCHI and Edward J. ANTHONY. Effects of steam on the sulfation of limestone and NOx formation in an air- and oxy-fired pilot-scale circulating fluidized bed combustor. *Fuel*. 2012, **92** (1), 107–115. ISSN 00162361. DOI: 10.1016/j.fuel.2011.06.054

[31] WU, Yinghai, Chunbo WANG, Yewen TAN, Lufei JIA and Edward J. ANTHONY. Characterization of ashes from a 100kWth pilot-scale circulating fluidized bed with oxy-fuel combustion. *Applied Energy*. 2011, **88** (9), 2940–2948. ISSN 03062619. DOI: 10.1016/j.apenergy.2011.03.007

[32] CZAKIERT, T., K. SZTEKLER, S. KARSKI, D. MARKIEWICZ and W. NOWAK. Oxy-fuel circulating fluidized bed combustion in a small pilot-scale test rig. *Fuel Processing Technology*. 2010, **91** (11), 1617–1623. ISSN 03783820. DOI: 10.1016/j.fuproc.2010.06.010

[33] PRÖLL, Tobias. *Research Group Zero Emission Technologies*. 2012. Available at: http://www.portoflosangeles.org/environment/zero.asp

[34] ERIKSSON, Timo, Ossi SIPPU, Arto HOTTA, Zhen FAN, Kari MYÖHÄNEN, Timo HYPPÄNEN and Toni PIKKARAINEN. Oxyfuel CFB Boiler as a Route to Near Zero CO2 Emission Coal Firing. *PowerGen*. 2007, 1–23. Available at: http://www.parts.fwc.com/publications/tech_papers/files/TP_CCS_07_02.pdf

[35] DUAN, Lunbo, Haicheng SUN, Changsui ZHAO, Wu ZHOU and Xiaoping CHEN. Coal combustion characteristics on an oxy-fuel circulating fluidized bed combustor with warm flue gas recycle. *Fuel*. 2014, **127** , 47–51. ISSN 00162361. DOI: 10.1016/j.fuel.2013.06.016

[36] CZAKIERT, T., Z. BIS, W. MUSKALA and W. NOWAK. Fuel conversion from oxy-fuel combustion in a circulating fluidized bed. *Fuel Processing Technology*. 2006, **87** (6), 531–538. ISSN 03783820. DOI: 10.1016/j.fuproc.2005.12.003

[37] ROMEO, Luis M., Luis I. DIEZ, Isabel GUEDEA, Irene BOLEA, Carlos LUPIANEZ, Ana GONZALEZ, Javier PALLARES and Enrique TERUEL. Design and operation assessment of an oxyfuel fluidized bed combustor. *Experimental Thermal and Fluid Science*. 2011, **35** (3), 477–484. ISSN 08941777. DOI: 10.1016/j.expthermflusci.2010.11.011

[38] GUEDEA, Isabel, Luis I. DÍEZ, Javier PALLARÉS and Luis M. ROMEO. On the modeling of oxy-coal combustion in a fluidized bed. *Chemical Engineering Journal*. 2013, **228** , 179–191. ISSN 13858947. DOI: 10.1016/j.cej.2013.04.085

[39] DE LAS OBRAS-LOSCERTALES, M., A. RUFAS, L. F. DE DIEGO, F. GARCÍA-LABIANO, P. GAYÁN, A. ABAD and J. ADÁNEZ. Effects of temperature and flue gas recycle on the SO2 and NOx emissions in an oxy-fuel fluidized bed combustor. *Energy Procedia*. 2013, **37** , 1275–1282. ISSN 18766102. DOI: 10.1016/j.egypro.2013.06.002

[40] ROY, Bithi and Sankar BHATTACHARYA. Oxy-fuel fluidized bed combustion using Victorian brown coal: An experimental investigation. *Fuel Processing Technology*. 2014, **117** , 23–29. ISSN 03783820. DOI: 10.1016/j.fuproc.2013.02.019

[41] HU, Y., S. NAITO, N. KOBAYASHI and M. HASATANI. CO2, NOx and SO2 emissions from the combustion of coal with high oxygen concentration gases. *Fuel*. 2000, **79** (15), 1925–1932. ISSN 00162361. DOI: 10.1016/S0016-2361(00)00047-8

[42] WENG, Matthias, Claas GÜNTHER and Alfons KATHER. Flue Gas Concentrations and Efficiencies of a Coal-fired Oxyfuel Power Plant with Circulating Fluidised Bed Combustion. *Energy Procedia*. 2013, **37** , 1480–1489. ISSN 18766102. DOI: 10.1016/j.egypro.2013.06.023

[43] TOFTEGAARD, Maja B., Jacob BRIX, Peter A. JENSEN, Peter GLARBORG and Anker D. JENSEN. Oxy-fuel combustion of solid fuels. *Progress in Energy and Combustion Science*. 2010, **36** (5), 581–625. ISSN 03601285. DOI: 10.1016/j.pecs.2010.02.001

[44] NAKAYAMA, S., Y. NOGUCHI, T. KIGA, S. MIYAMAE, U. MAEDA, M. KAWAI, T. TANAKA, K. KOYATA and H. MAKINO. Pulverized coal combustion in O2/CO2 mixtures on a power plant for CO2 recovery. *Energy Conversion and Management*. 1992, **33** (5–8), 379–386. ISSN 01968904. DOI: 10.1016/0196-8904(92)90034-T

[45] DLOUHÝ, Tomáš, Tomáš DUPAL and Jan DLOUHÝ. A pulverized coal-fired boiler optimized for Oxyfuel combustion technology. *Acta Polytechnica*. 2012, **52** (4), 49–56. ISSN 12102709.

[46] LI, H., J. YAN, J. YAN and M. ANHEDEN. Impurity impacts on the purification process in oxy-fuel combustion based CO2 capture and storage system. *Applied Energy*. 2009, **86** (2), 202–213. ISSN 03062619. DOI: 10.1016/j.apenergy.2008.05.006

[47] MATHEKGA, H.I., B.O. OBOIRIEN and B.C. NORTH. A review of oxy-fuel combustion in fluidized bed reactors. *International Journal of Energy Research*. 2016, **40** , 878–902. ISSN 12310956. DOI: 10.1002/er

[48] CHOU, Chen Lin. Sulfur in coals: A review of geochemistry and origins. *International Journal of Coal Geology*. 2012, **100** , 1–13. ISSN 01665162. DOI: 10.1016/j.coal.2012.05.009

[49] FLEIG, Daniel, Fredrik NORMANN, Klas ANDERSSON, Filip JOHNSSON and Bo LECKNER. The fate of sulphur during oxy-fuel combustion of lignite. *Energy Procedia*. 2009, **1** (1), 383–390. ISSN 18766102. DOI: 10.1016/j.egypro.2009.01.052

[50] YAN, Jinying, Marie ANHEDEN, Richard FABER, Fredrik STARFELT, Robert PREUSCHE, Holger ECKE, Nader PADBAN, Daniel KOSEL, Norbert JENTSCH and Göran LINDGREN. Flue gas cleaning for CO2 capture from coal-fired oxyfuel combustion power generation. *Energy Procedia*. 2011, **4** , 900–907. ISSN 18766102. DOI: 10.1016/j.egypro.2011.01.135

[51] FABER, Richard, Jinying YAN, Felix STARK and Sascha PRIESNITZ. Flue gas desulphurization for hot recycle Oxyfuel combustion: Experiences from the 30MWth Oxyfuel pilot plant in Schwarze Pumpe. *International Journal of Greenhouse Gas Control*. 2011, **5** (SUPPL. 1), 2–4. ISSN 17505836. DOI: 10.1016/j.ijggc.2011.05.027

[52] CROISET, Eric, Kelly THAMBIMUTHU and Allan PALMER. Coal combustion in O2/CO2 mixtures compared with air. *The Canadian Journal of Chemical Engineering*. 2000, **78** (April 2000), 402–407. ISSN 1939-019X. DOI: 10.1002/cjce.5450780217

[53] CZAKIERT, T., K. SZTEKLER, S. KARSKI, D. MARKIEWICZ and W. NOWAK. Oxy-fuel circulating fluidized bed combustion in a small pilot-scale test rig. *Fuel Processing Technology*. 2010, **91** (11), 1617–1623. ISSN 03783820. DOI: 10.1016/j.fuproc.2010.06.010

[54] FUERTES, Antonio B., Violeta ARTOS, JoséJ PIS, Gregorio MARBÁN and JoséM PALACIOS. Sulphur retention by ash during fluidized bed combustion of bituminous coals. *Fuel*. 1992, **71** (5), 507–511. ISSN 00162361. DOI: 10.1016/0016-2361(92)90147-G

[55] MILLER, Bruce G. and David A TILLMAN, eds. *Combustion Engineering Issues for Solid Fuel Systems*. Elsevier Inc., 2008. ISBN 978-0-12-373611-6.

[56] VEJVODA, Josef, Pavel MACHAČ and Petr BURYAN. *Technologie ochrany ovzduší*

a čištění odpadních plynů. Vysoká škola chemicko-technologická v Praze, 2003. ISBN 80-7080-517-X.

[57] MARKUSZEWSKY, D R, R MROCH, G A STRASZHEIM and W E NORTON. Desulfurizatuin and Demineralization of Coal by Molten NaOH/KOH Mixures. no date.

[58] HAMERSMA, J.W., M.L. KRAFT and R.A. MEYERS. *Applicability of the Meyers Process for Chemical Desulfurization of U.S. Coal (A Survey of 15 Coals)*. 1974.

[59] CÓRDOBA, Patricia. Status of Flue Gas Desulphurisation (FGD) systems from coal-fired power plants: Overview of the physic-chemical control processes of wet limestone FGDs. *Fuel*. 2015, **144** , 274–286. ISSN 00162361. DOI: 10.1016/j.fuel.2014.12.065

[60] TOMECZEK, Jerzy. *Coal Combustion*. Malabar: Krieger Publishing Company, 1994. ISBN 0-89464-651-6.

[61] BASU, Prabir. *Combustion and Gasification in Fluidized Beds*. CRC Press, 2006. ISBN 9780849333965.

[62] ANTHONY, E.J. and D.L. GRANATSTEIN. Sulfation phenomena in fluidized bed combustion systems. *Progress in Energy and Combustion Science*. 2001, **27** (2), 215–236. ISSN 03601285. DOI: 10.1016/S0360-1285(00)00021-6

[63] MILLER, Bruce G and David TILLMAN. Combustion engineering issues for solid fuel systems. 2008.

[64] BURYAN, Petr and Siarhei SKOBLIA. Vliv přídavku biomasy na odsiřovací schopnost vápence. 2012, **4** , 1–5.

[65] HU, Guilin, Kim DAM-JOHANSEN, Stig WEDEL and Jens PETER HANSEN. Review of the direct sulfation reaction of limestone. *Progress in Energy and Combustion Science*. 2006, **32** (4), 386–407. ISSN 03601285. DOI: 10.1016/j.pecs.2006.03.001

[66] LUPIÁÑEZ, Carlos, Isabel GUEDEA, Irene BOLEA, Luis I. DÍEZ and Luis M. ROMEO. Experimental study of SO2 and NOx emissions in fluidized bed oxy-fuel combustion. *Fuel Processing Technology*. 2013, **106** (x), 587–594. ISSN 03783820. DOI: 10.1016/j.fuproc.2012.09.030

[67] DE DIEGO, Luis F., Margarita DE LAS OBRAS-LOSCERTALES, Francisco GARCÍA-LABIANO, Aránzazu RUFAS, Alberto ABAD, Pilar GAYÁN and Juan ADÁNEZ. Characterization of a limestone in a batch fluidized bed reactor for sulfur retention under oxy-fuel operating conditions. *International Journal of Greenhouse Gas Control*. 2011, **5** (5), 1190–1198. ISSN 17505836. DOI: 10.1016/j.ijggc.2011.05.032

[68] DE LAS OBRAS-LOSCERTALES, M., L. F. DE DIEGO, F. GARCÍA-LABIANO, A. RUFAS, A. ABAD, P. GAYÁN and J. ADÁNEZ. Sulfur retention in an oxy-fuel bubbling fluidized bed combustor: Effect of coal rank, type of sorbent and O2/CO2 ratio. *Fuel*. 2014, **137** , 384–392. ISSN 00162361. DOI: 10.1016/j.fuel.2014.07.097

[69] DLOUHÝ, Tomáš. *Výpočty kotlů a spalinových výměníků*. České vysoké učení technické v Praze, 2007. ISBN 978-80-01-03757-7.

[70] SPÖRL, Reinhold, Jörg MAIER, Lawrence BELO, Kalpit SHAH, Rohan STANGER, Terry WALL and Günter SCHEFFKNECHT. Mercury and SO3 emissions in oxy-fuel combustion. *Energy Procedia*. 2014, **63** (0), 386–402. ISSN 18766102. DOI: 10.1016/j.egypro.2014.11.041

[71] KUNII, Daizo and Octave LEVENSPIEL. *Fluidization Engineering*. Butterworth-Heinemann, 1991. ISBN 0409902330. DOI: 10.1016/0032-5910(69)80087-2

[72] XIUYI, Tang. Mineral Matter in Coal. In: *Encyclopedia of Life Support Systems*. UNESCO, no date.

[73] DE DIEGO, L. F., M. DE LAS OBRAS-LOSCERTALES, A. RUFAS, F. GARCÍA-LABIANO, P. GAYÁN, A. ABAD and J. ADÁNEZ. Pollutant emissions in a bubbling fluidized bed combustor working in oxy-fuel operating conditions: Effect of flue gas recirculation. *Applied Energy*. 2013, **102** (x), 860–867. ISSN 03062619. DOI:

10.1016/j.apenergy.2012.08.053

[74] FUERTES, A. B., G. VELASCO, E. FUENTE and T. ALVAREZ. Study of the direct sulfation of limestone particles at high CO2 partial pressures. *Fuel Processing Technology*. 1994, **38** (3), 181–192. ISSN 03783820. DOI: 10.1016/0378-3820(94)90047-7

[75] TAN, Y., L. JIA, Y. WU and E. J. ANTHONY. Experiences and results on a 0.8MWth oxy-fuel operation pilot-scale circulating fluidized bed. *Applied Energy*. 2012, **92** , 343–347. ISSN 03062619. DOI: 10.1016/j.apenergy.2011.11.037

12.2 AUTHORS OWN PUBLICATIONS

[I] HRDLIČKA, J., P. SKOPEC, J. OPATŘIL and T. DLOUHÝ. Oxyfuel combustion in a bubbling fluidized bed combustor. *Energy Procedia*. 2016, **86**(0), 116–123. ISSN 1876-6102. doi:10.1016/j.egypro.2016.01.012

[II] SKOPEC, P., J. HRDLIČKA, M. VODIČKA, L. PILAŘ and J. OPATŘIL. Combustion of Lignite Coal in a Bubbling Fluidized Bed Combustor under Oxyfuel Conditions. In: *Energy Procedia*. 2017. ISSN 18766102. doi:10.1016/j.egypro.2017.03.1202

[III] SKOPEC, P. and J. HRDLICKA. Specific features of the oxyfuel combustion conditions in a bubbling fluidized bed. Acta Polytechnica. 2016, 56(4). ISSN 1805-2363. doi:10.14311/AP.2016.56.0312

[IV] HRDLIČKA, J., M. VODIČKA, P. SKOPEC, F. HRDLIČKA and T. DLOUHÝ. CO2 Capture by Oxyfuel Combustion. In: F. WINTER, R. A. AGARWAL, J. HRDLIČKA and S. VARJANI, ed. CO2 Separation, Purification and Conversion to Chemicals and Fuels. Springer Nature Singapore Pte Ltd., 2018, s. 55-78. ISBN 978-981-13-3295-1. doi:10.1007/978-981-13-3296-8_5

[V] SKOPEC, P., J. HRDLIČKA and M. VODIČKA. Zkušenosti s oxyfuel spalováním ve stacionární fluidní vrstvě. In: *Energie z biomasy XVI*. 2015, pp 100–105. ISBN 978-80-214-5286-2.

[VI] SKOPEC, P., J. HRDLIČKA and M. KAVÁLEK. Specific emissions from biomass combustion. *Acta Polytechnica*. 2014, **54**(1). ISSN 12102709 18052363. doi:10.14311/AP.2014.54.0074

[VII] HRDLIČKA, J., P. SKOPEC, T. DLOUHÝ and F. HRDLIČKA. Emission factors of gaseous pollutants from small scale combustion of biofuels. *Fuel*. 2016, **165**. ISSN 00162361. doi:10.1016/j.fuel.2015.09.087

[VIII] SKOPEC, P., J. HRDLIČKA and J. OPATŘIL. Experimentální jednotka pro výzkum oxyfuel spalování v bublinkové fluidní vrstvě. In: *Seminář Středoevropského energetického institutu CENERGI II.* 2015, pp 97–101. ISBN 978-80-214-5288-6.

[IX] SKOPEC, P., J. HRDLIČKA, J. OPATŘIL and J. ŠTEFANICA. NOx emissions from bubbling fluidized bed combustion of lignite coal. *Acta Polytechnica*. 2015, **55**(4). ISSN 18052363. doi:10.14311/AP.2015.55.0275

[X] HRDLIČKA, J., P. SKOPEC and F. HRDLIČKA. Trough Air Distributor for a Bubbling Fluidized Bed Boiler with Isobaric Nozzles. In: *Proceedings of the 22nd International Conference on Fluidized Bed Conversion*. 2015, pp 109–114. ISBN 978-952-12-3222-0.

[XI] HRDLIČKA, J., P. SKOPEC, L. PILAŘ, T. DLOUHÝ and F. HRDLIČKA. Dry additive desulphurization performance of central European lignite in a BFBC. In: *Impacts of Fuel Quality on Power Production 2014*. 2014, pp 77–86.

[XII] SKOPEC, P. and J. HRDLIČKA. Vliv provozních parametrů fluidního kotle se stacionární fluidní vrstvou na tvorbu emisí SO2, NOx a CO při spalování hnědého uhlí. In: *Energie z biomasy XV*. 2014, pp 123–129. ISBN 978-80-214-5016-5.

[XIII] SKOPEC, P., J. HRDLIČKA and M. VODIČKA. Porovnání experimentálních výsledků oxyfuel spalování ve fluidní vrstvě s numerickým modelem. In: *Energie z biomasy XVII - Sborník příspěvků z konference*. 2016, pp 105–110. ISBN 978-80-214-5441-5.

[XIV] SKOPEC, P., J. HRDLIČKA and F. HRDLIČKA. Dry Additive Desulphurization in a BFBC under Oxyfuel Conditions, In: *Impact of Fuel Quality on Power Production and the Environment*. 2018, Lake Louise, Canada

13 APPENDIX

13.1 SO_2 CAPTURE UNDER AIR CONDITIONS

A. Table 1: Experiments for different temperatures under air conditions - **no limestone addition**

	Bed temp. 800°C	Bed temp. 840°C	Bed temp. 880°C	Bed temp. 920°C
O_2 concentration in FG [%]	5.0	6.1	5.6	5.3
Mean FB temperature [°C]	804	844	885	930
SO_2 measured [ppm]	784	759	798	790
SO_2 measured [mg/MJ]	824	855	870	849
SO_2 capture ratio [%]	**17.2**	**14.1**	**12.5**	**14.7**
Fuel load [kg/hod]	4.1	4.4	4.7	5.1
Superficial velocity [m/s]	1.25	1.28	1.40	1.58
CO_2 concentration in FG [%]	13.1	12.0	12.4	12.7
CO in FG [ppm]	594	339	313	130
CO in FG [mg/MJ]	273	167	150	61

A. Table 2: Experiments for different Ca/S molar ratios – **L1**

	No limestone	Ca/S = 1.5	Ca/S = 3	Ca/S = 5
O_2 concentration in FG [%]	6.1	6.1	6.4	6.2
Mean FB temperature [°C]	844	851	842	837
SO_2 measured [mg/MJ]	775	489	292	107
SO_2 capture ratio [%]	**14.1**	**45.8**	**67.8**	**88.1**
Fuel load [kg/hod]	4.4	4.4	4.4	4.3
Superficial velocity [m/s]	1.49	1.54	1.54	1.55
CO_2 concentration in FG [%]	12.0	11.9	11.9	13.7
CO in FG [mg/MJ]	152	135	85	42

A. Table 3: Experiments for different Ca/S molar ratios – **L2**

	No limestone	Ca/S = 1.5	Ca/S = 3	Ca/S = 5
O_2 concentration in FG [%]	6.1	5.4	5.8	6.6
Mean FB temperature [°C]	844	840.8	840.2	846.3
SO_2 measured [mg/MJ]	775	358.5	187.9	31.3
SO_2 capture ratio [%]	**14.1**	**60.5**	**80.5**	**96.6**
Fuel load [kg/hod]	4.4	3.8	3.8	4.5
Superficial velocity [m/s]	1.49	1.6	1.4	1.6
CO_2 concentration in FG [%]	12.0	13.9	13.4	12.8
CO in FG [mg/MJ]	152	101.2	73.6	77.1

A. Table 4: Experiments for different temperatures under air conditions – **L1 Ca/S=1.5**

	Bed temp. 800°C	Bed temp. 840°C	Bed temp. 880°C	Bed temp. 920°C
O_2 concentration in FG [%]	6.3	6.1	5.7	6.2
Mean FB temperature [°C]	802	849	878	929
SO_2 measured [ppm]	400	477	558	813
SO_2 measured [mg/MJ]	416	489	556	836
SO_2 capture ratio [%]	**53.9**	**45.8**	**38.4**	**7.3**
Fuel load [kg/hod]	4.1	4.4	4.7	5.3
Superficial velocity [m/s]	1.5	1.5	1.6	1.8
CO_2 concentration in FG [%]	11.7	11.9	12.3	12.0
CO in FG [ppm]	159	301	266	638
CO in FG [mg/MJ]	72.2	135.0	116.0	287.0

A. Table 5: Experiments for different temperatures under air conditions – **L1 Ca/S=3**

	Bed temp. 800°C	Bed temp. 840°C	Bed temp. 880°C	Bed temp. 920°C
O_2 concentration in FG [%]	5.6	6.4	6.1	5.8
Mean FB temperature [°C]	801	842	884	920
SO_2 measured [ppm]	344	281	394	593
SO_2 measured [mg/MJ]	340	292	403	597
SO_2 capture ratio [%]	**62.3**	**67.6**	**55.3**	**33.8**
Fuel load [kg/hod]	4.1	4.4	4.7	5.2
Superficial velocity [m/s]	1.3	1.5	1.6	1.8
CO_2 concentration in FG [%]	12.7	11.9	12.1	12.4
CO in FG [ppm]	318	186	215	251
CO in FG [mg/MJ]	137.9	84.5	96.4	110.5

A. Table 6: Experiments for different temperatures under air conditions – **L1 Ca/S=5**

	Bed temp. 800°C	Bed temp. 840°C	Bed temp. 880°C	Bed temp. 920°C
O_2 concentration in FG [%]	5.9	6.2	5.6	6.7
Mean FB temperature [°C]	803	837	880	924
SO_2 measured [ppm]	105	104	208	327
SO_2 measured [mg/MJ]	107	107	206	349
SO_2 capture ratio [%]	**88.2**	**88.1**	**77.1**	**61.3**
Fuel load [kg/hod]	4.1	4.3	4.6	5.1
Superficial velocity [m/s]	1.5	1.5	1.5	1.6
CO_2 concentration in FG [%]	13.9	13.7	14.4	13.3
CO in FG [ppm]	175	93	218	70
CO in FG [mg/MJ]	77.2	41.6	94.6	32.5

A. Table 7: Experiments for different temperatures under air conditions – **L2 Ca/S=1.5**

	Bed temp. 800°C	Bed temp. 840°C	Bed temp. 880°C	Bed temp. 920°C
O_2 concentration in FG [%]	7.0	5.4	5.6	5.5
Mean FB temperature [°C]	794.0	840.8	877.9	922.0
SO_2 measured [ppm]	300	364	381	440
SO_2 measured [mg/MJ]	328.5	358.5	381.2	436.9
SO_2 capture ratio [%]	**63.8**	**60.5**	**58.0**	**51.9**
Fuel load [kg/hod]	3.6	3.8	4.5	5.1
Superficial velocity [m/s]	1.7	1.6	1.8	1.9
CO_2 concentration in FG [%]	12.4	13.9	13.6	13.7
CO in FG [ppm]	164	234	160	117
CO in FG [mg/MJ]	78.8	101.2	69.9	50.9

A. Table 8: Experiments for different temperatures under air conditions – **L2 Ca/S=3**

	Bed temp. 800°C	Bed temp. 840°C	Bed temp. 880°C	Bed temp. 920°C
O_2 concentration in FG [%]	5.7	5.8	6.5	6.1
Mean FB temperature [°C]	806.8	840.2	886.4	921.1
SO_2 measured [ppm]	280	175	218	296
SO_2 measured [mg/MJ]	248.5	187.9	230.3	304.5
SO_2 capture ratio [%]	**74.3**	**80.5**	**74.6**	**66.5**
Fuel load [kg/hod]	4.1	3.8	4.5	4.7
Superficial velocity [m/s]	1.6	1.4	1.7	1.7
CO_2 concentration in FG [%]	13.8	13.4	13.0	13.2
CO in FG [ppm]	262	157	92	97
CO in FG [mg/MJ]	122.1	73.6	42.7	43.6

A. Table 9: Experiments for different temperatures under air conditions – **L2 Ca/S=5**

	Bed temp. 800°C	Bed temp. 840°C	Bed temp. 880°C	Bed temp. 920°C
O_2 concentration in FG [%]	5.6	6.6	6.0	6.2
Mean FB temperature [°C]	794.1	846.3	881.7	927.4
SO_2 measured [ppm]	37	29	55	174
SO_2 measured [mg/MJ]	36.7	31.3	56.2	180.4
SO_2 capture ratio [%]	**96.0**	**96.6**	**93.8**	**80.1**
Fuel load [kg/hod]	4.1	4.5	4.4	4.7
Superficial velocity [m/s]	1.5	1.6	1.5	1.6
CO_2 concentration in FG [%]	13.7	12.8	13.4	13.3
CO in FG [ppm]	205	166	91	77
CO in FG [mg/MJ]	89.4	77.1	40.8	34.8

A. Table 10: Experiments for different O_2 concentrations in flue gas under air conditions – **L1**

	No limestone			Ca/S=1.5			Ca/S=3		
	3% O_2 in FG	6% O_2 in FG	9% O_2 in FG	3% O_2 in FG	6% O_2 in FG	9% O_2 in FG	3% O_2 in FG	6% O_2 in FG	9% O_2 in FG
O_2 concentration in FG [%]	3.3	6.1	9.2	2.8	6.1	8.3	3.2	6.7	8.4
Mean FB temperature [°C]	847	839	844	837	847	848	849	838	850
SO_2 measured [ppm]	807	759	598	616	477	439	272	221	291
SO_2 measured [mg/MJ]	694	775	773	516	489	526	234	235	352
SO_2 capture ratio [%]	**23.1**	**14.1**	**14.3**	**42.8**	**45.8**	**41.6**	**74.1**	**73.9**	**61.0**
Fuel load [kg/hod]	4.4	4.4	4.4	4.7	4.4	4.5	4.0	4.2	4.6
Superficial velocity [m/s]	1.7	1.5	1.67	1.5	1.5	1.59	1.4	1.5	1.6
CO_2 concentration in FG [%]	14.6	12.0	9.2	15.3	11.9	10.3	16.4	13.1	11.3
CO in FG [ppm]	412	339	180	1009	301	202	113	96	110
CO in FG [mg/MJ]	154.9	151.6	102	369.1	135.0	106	42.5	44.7	58.2

A. Table 11: Experiments for different O_2 concentrations in flue gas under air conditions – **L2**

	Ca/S=1.5			Ca/S=3		
	3% O_2 in FG	6% O_2 in FG	9% O_2 in FG	3% O_2 in FG	6% O_2 in FG	9% O_2 in FG
O_2 concentration in FG [%]	3.5	5.4	8.9	2.8	5.8	8.5
Mean FB temperature [°C]	843.5	840.8	841.0	833.4	840.2	838.9
SO_2 measured [ppm]	522	363	305	147	175	182
SO_2 measured [mg/MJ]	457.9	358.5	389.5	123.6	187.9	223.9
SO_2 capture ratio [%]	**49.6**	**60.5**	**57.1**	**86.4**	**80.5**	**75.4**
Fuel load [kg/hod]	3.8	3.8	3.8	3.8	3.8	3.9
Superficial velocity [m/s]	1.4	1.6	1.5	1.3	1.4	1.6
CO_2 concentration in FG [%]	15.4	13.9	10.4	16.2	13.4	10.8
CO in FG [ppm]	799	234	118	402	157	129
CO in FG [mg/MJ]	306.9	101.2	66.2	148.2	73.6	69.5

13.2 SO_2 CAPTURE IN OXYFUEL REGIME - MINIFLUID

A. Table 12: Experiments for different temperatures under oxyfuel conditions - **no limestone**

	Bed temp. 800°C	Bed temp. 840°C	Bed temp. 880°C	Bed temp. 920°C	Bed temp. 960°C
O_2 concentr. in FG [%]	5.3	6.8	5.3	5.6	5.8
Mean FB temperature [°C]	821	854	891	926	944
SO_2 measured [ppm]	3216	3175	3345	3380	3561
SO_2 measured [mg/MJ]	479	480	497	502	530
SO_2 capture ratio [%]	**46.9**	**46.8**	**44.9**	**44.3**	**41.2**
Fuel load [kg/hod]	4.4	4.6	4.5	4.6	4.8
Superficial velocity [m/s]	1.16	1.35	1.28	1.26	1.23
CO_2 concentr. in FG [%]	89.4	88.0	89.6	89.5	89.4
CO in FG [ppm]	1032	712	1344	1159	2404
CO in FG [mg/MJ]	67	47	87	75	157

A. Table 13: Experiments for different Ca/S molar ratios – **L1**

	No limestone	Ca/S = 1.5	Ca/S = 3	Ca/S = 5
O_2 concentration in FG [%]	5.3	6.6	5.8	5.9
Mean FB temperature [°C]	891	879.2	875.8	881.1
SO_2 measured [mg/MJ]	497	142.9	59.4	20.2
SO_2 capture ratio [%]	**44.9**	**83.2**	**93.0**	**97.6**
Fuel load [kg/hod]	4.5	4.3	4.1	4.1
Superficial velocity [m/s]	1.28	1.1	1.0	1.1
CO_2 concentration in FG [%]	89.6	90.8	88.6	88.7
CO in FG [mg/MJ]	87	30.4	10.1	18.7

A. Table 14: Experiments for different Ca/S molar ratios – **L2**

	No limestone	Ca/S = 1.5	Ca/S = 3	Ca/S = 5
O_2 concentration in FG [%]	5.3	5.6	6.1	5.3
Mean FB temperature [°C]	891	882.7	882.3	879.6
SO_2 measured [mg/MJ]	497	106.7	35.9	15.0
SO_2 capture ratio [%]	**44.9**	**87.4**	**95.8**	**98.2**
Fuel load [kg/hod]	4.5	4.1	4.4	4.7
Superficial velocity [m/s]	1.28	1.0	0.9	1.05
CO_2 concentration in FG [%]	89.6	90.8	89.9	91.1
CO in FG [mg/MJ]	87	22.1	37.1	56.7

A. Table 15: Experiments for different temperatures under oxyfuel conditions – **L1 Ca/S=1.5**

	Bed temp. 840°C	Bed temp. 880°C	Bed temp. 920°C	Bed temp. 960°C
O_2 concentration in FG [%]	6.2	6.6	6.4	6.1
Mean FB temperature [°C]	846	879	920	956
SO_2 measured [ppm]	1607	1037	1998	3169
SO_2 measured [mg/MJ]	221	143	275	475
SO_2 capture ratio [%]	**73.9**	**83.2**	**67.6**	**47.4**
Fuel load [kg/hod]	3.9	4.3	4.7	4.8
Superficial velocity [m/s]	1.13	1.12	1.20	1.48
CO_2 concentration in FG [%]	90.9	90.8	90.9	88.8
CO in FG [ppm]	504	505	541	1307
CO in FG [mg/MJ]	30	30	33	86

A. Table 16: Experiments for different temperatures under oxyfuel conditions – **L1 Ca/S=3**

	Bed temp. 840°C	Bed temp. 880°C	Bed temp. 920°C	Bed temp. 960°C
O_2 concentration in FG [%]	5.7	5.8	5.9	5.9
Mean FB temperature [°C]	841	876	921	955
SO_2 measured [ppm]	1194	420	820	1350
SO_2 measured [mg/MJ]	170	59	116	191
SO_2 capture ratio [%]	**80.0**	**93.0**	**86.3**	**77.5**
Fuel load [kg/hod]	3.8	4.1	4.7	5.0
Superficial velocity [m/s]	0.87	1.00	1.25	1.20
CO_2 concentration in FG [%]	87.9	88.6	88.4	88.6
CO in FG [ppm]	369	163	392	446
CO in FG [mg/MJ]	23	10	24	28

A. Table 17: Experiments for different temperatures under oxyfuel conditions – **L1 Ca/S=5**

	Bed temp. 840°C	Bed temp. 880°C	Bed temp. 920°C	Bed temp. 960°C
O_2 concentration in FG [%]	5.7	5.9	6.1	5.6
Mean FB temperature [°C]	843	881	920	960
SO_2 measured [ppm]	419	143	321	1010
SO_2 measured [mg/MJ]	59	20	46	146
SO_2 capture ratio [%]	**93.0**	**97.6**	**94.6**	**82.8**
Fuel load [kg/hod]	4.4	4.1	4.8	4.9
Superficial velocity [m/s]	1.03	1.06	1.19	1.14
CO_2 concentration in FG [%]	88.9	88.7	88.3	86.4
CO in FG [ppm]	326	302	309	1137
CO in FG [mg/MJ]	20	19	19	72

A. Table 18: Experiments for different temperatures under oxyfuel conditions – **L2 Ca/S=1.5**

	Bed temp. 840°C	Bed temp. 880°C	Bed temp. 920°C	Bed temp. 960°C
O_2 concentration in FG [%]	6.2	5.6	5.9	6.1
Mean FB temperature [°C]	841	883	917	959
SO_2 measured [ppm]	1061	774	1072	2532
SO_2 measured [mg/MJ]	147	107	148	353
SO_2 capture ratio [%]	**82.7**	**87.4**	**82.5**	**58.5**
Fuel load [kg/hod]	3.8	4.1	4.4	4.7
Superficial velocity [m/s]	1.03	1.03	0.99	1.03
CO_2 concentration in FG [%]	90.3	90.8	90.4	89.9
CO in FG [ppm]	402	367	481	828
CO in FG [mg/MJ]	24	22	29	50

A. Table 19: Experiments for different temperatures under oxyfuel conditions – **L2 Ca/S=3**

	Bed temp. 840°C	Bed temp. 880°C	Bed temp. 920°C	Bed temp. 960°C
O_2 concentration in FG [%]	6.8	6.1	6.1	5.9
Mean FB temperature [°C]	837	882	919	957
SO_2 measured [ppm]	293	258	678	1934
SO_2 measured [mg/MJ]	41	36	95	270
SO_2 capture ratio [%]	**95.1**	**95.8**	**88.8**	**68.1**
Fuel load [kg/hod]	3.8	4.4	4.5	4.5
Superficial velocity [m/s]	0.85	0.91	0.99	0.93
CO_2 concentration in FG [%]	88.9	89.9	89.2	89.5
CO in FG [ppm]	521	610	1121	1050
CO in FG [mg/MJ]	32	37	69	64

A. Table 20: Experiments for different temperatures under oxyfuel conditions – **L2 Ca/S=5**

	Bed temp. 840°C	Bed temp. 880°C	Bed temp. 920°C	Bed temp. 960°C
O_2 concentration in FG [%]	6.0	5.3	5.3	5.9
Mean FB temperature [°C]	840	880	927	968
SO_2 measured [ppm]	56	109	336	1590
SO_2 measured [mg/MJ]	8	15	46	219
SO_2 capture ratio [%]	**99.1**	**98.2**	**94.6**	**74.2**
Fuel load [kg/hod]	3.9	4.7	4.7	5.0
Superficial velocity [m/s]	0.83	1.05	0.94	0.90
CO_2 concentration in FG [%]	89.1	91.1	91.3	90.9
CO in FG [ppm]	738	943	860	390
CO in FG [mg/MJ]	45	57	52	24

A. Table 21: Experiments for different oxygen in flue gas under oxyfuel conditions – **No limestone**

	3% O_2 in FG	5% O_2 in FG	6% O_2 in FG	9% O_2 in FG
O_2 concentration in FG [%]	3.5	5.3	6.1	8.9
Mean FB temperature [°C]	883	889	878	879
SO_2 measured [ppm]	4027	3345	3185	3225
SO_2 measured [mg/MJ]	572	497	463	482
SO_2 capture ratio [%]	**36.5**	**44.9**	**48.7**	**46.5**
Fuel load [kg/hod]	4.1	4.5	4.1	4.1
Superficial velocity [m/s]	1.15	1.28	1.18	1.17
CO_2 concentration in FG [%]	93.6	89.6	91.6	88.9
CO in FG [ppm]	2384	1344	628	302
CO in FG [mg/MJ]	148	87	40	20

A. Table 22: Experiments for different oxygen in flue gas under oxyfuel conditions – **L1 Ca/S=1.5 and 3**

	Ca/S = 1.5			Ca/S = 3		
	3% O_2 in FG	6% O_2 in FG	9% O_2 in FG	3% O_2 in FG	6% O_2 in FG	9% O_2 in FG
O_2 concentration in FG [%]	3.6	5.9	9.0	2.9	5.8	8.5
Mean FB temperature [°C]	882	883	877	873	868	869
SO_2 measured [ppm]	2042	1997	2080	763	420	218
SO_2 measured [mg/MJ]	291	292	314	104	59	32
SO_2 capture ratio [%]	**67.7**	**67.6**	**65.1**	**87.8**	**93.0**	**96.3**
Fuel load [kg/hod]	4.4	4.3	4.4	5.1	4.1	4.4
Superficial velocity [m/s]	1.12	1.19	1.25	1.23	1.00	1.07
CO_2 concentration in FG [%]	93.3	90.9	88.0	92.1	88.6	86.6
CO in FG [ppm]	3282	1945	404	603	163	121
CO in FG [mg/MJ]	205	125	27	36	10	8

A. Table 23: Experiments for different oxygen in flue gas under oxyfuel conditions – **L2 Ca/S=3**

	Ca/S = 3		
	3% O_2 in FG	6% O_2 in FG	9% O_2 in FG
O_2 concentration in FG [%]	2.9	6.1	8.5
Mean FB temperature [°C]	870	884	882
SO_2 measured [ppm]	354	258	218
SO_2 measured [mg/MJ]	48	36	31
SO_2 capture ratio [%]	**94.4**	**95.8**	**96.3**
Fuel load [kg/hod]	4.4	4.4	4.2
Superficial velocity [m/s]	0.94	0.91	0.94
CO_2 concentration in FG [%]	92.5	89.9	87.0
CO in FG [ppm]	3036	610	516
CO in FG [mg/MJ]	180	37	32

13.3 SO_2 CAPTURE IN OXYFUEL REGIME - GOLEM

A. Table 24: Experiments for different temperatures under oxyfuel conditions - **no limestone, Golem**

	Bed temp. 840°C	Bed temp. 880°C	Bed temp. 920°C	Bed temp. 960°C
O_2 concentr. in FG [%]	2.1	3.9	3.2	2.3
Mean FB temperature [°C]	843	876	918	968
SO_2 measured [ppm]	2870	2657	2915	3169
SO_2 measured [mg/MJ]	432	400	439	480
SO_2 capture ratio [%]	**53.1**	**56.5**	**52.3**	**47.8**
Fuel load [kg/hod]	45.9	43.7	42.1	42.5
Superficial velocity [m/s]	1.25	1.13	1.03	0.99
CO_2 concentr. in FG [%]	90.2	90.0	90.2	89.6
CO in FG [ppm]	4359	3525	4756	5996
CO in FG [mg/MJ]	287	232	313	397

A. Table 25: Experiments for different Ca/S molar ratios – **L1, Golem**

	No limestone	Ca/S = 1.5	Ca/S = 3	Ca/S = 5
O_2 concentration in FG [%]	2.1	4.7	6.7	6.1
Mean FB temperature [°C]	843	842	838	842
SO_2 measured [mg/MJ]	432	151	105	41
SO_2 capture ratio [%]	**53.1**	**83.6**	**88.6**	**95.5**
Fuel load [kg/hod]	45.9	32.9	44.7	51.6
Superficial velocity [m/s]	1.2	1.0	1.2	1.4
CO_2 concentration in FG [%]	90.2	86.2	84.3	80.2
CO in FG [mg/MJ]	286.8	208.7	194.3	178.2

A. Table 26: Experiments for different Ca/S molar ratios – **L2, Golem**

	No limestone	Ca/S = 1.5	Ca/S = 3	Ca/S = 5
O_2 concentration in FG [%]	2.1	6.1	6.4	6.6
Mean FB temperature [°C]	843	836	839	841
SO_2 measured [mg/MJ]	432	80	49	22
SO_2 capture ratio [%]	**53.1**	**91.3**	**94.7**	**97.7**
Fuel load [kg/hod]	45.9	46.1	48.7	42.4
Superficial velocity [m/s]	1.2	1.4	1.5	1.3
CO_2 concentration in FG [%]	90.2	80.1	78.8	76.5
CO in FG [mg/MJ]	286.8	81.7	130.6	60.3

A. Table 27: Experiments for different temperatures under oxyfuel conditions – **L1 Ca/S=1.5, Golem**

	Bed temp. 840°C	Bed temp. 880°C	Bed temp. 920°C	Bed temp. 960°C
O_2 concentration in FG [%]	4.7	4.2	3.2	5.4
Mean FB temperature [°C]	842	881	924	957
SO_2 measured [ppm]	957	1630	2801	2281
SO_2 measured [mg/MJ]	150	278	424	382
SO_2 capture ratio [%]	**83.6**	**69.7**	**53.9**	**58.4**
Fuel load [kg/hod]	32.9	38.6	39.6	46.1
Superficial velocity [m/s]	1.01	1.07	1.03	1.21
CO_2 concentration in FG [%]	86.2	79.5	89.7	80.9
CO in FG [ppm]	3032	3503	5606	1668
CO in FG [mg/MJ]	209	262	371	122

A. Table 28: Experiments for different temperatures under oxyfuel conditions – **L1 Ca/S=3, Golem**

	Bed temp. 840°C	Bed temp. 880°C	Bed temp. 920°C	Bed temp. 960°C
O_2 concentration in FG [%]	6.7	6.9	6.2	5.2
Mean FB temperature [°C]	838	878	924	964
SO_2 measured [ppm]	651	802	1741	2340
SO_2 measured [mg/MJ]	105	130	277	373
SO_2 capture ratio [%]	**88.6**	**85.9**	**69.9**	**59.5**
Fuel load [kg/hod]	44.7	44.7	46.7	49.8
Superficial velocity [m/s]	1.24	1.25	1.20	1.16
CO_2 concentration in FG [%]	84.3	84.0	85.2	85.1
CO in FG [ppm]	2759	2794	3741	4547
CO in FG [mg/MJ]	194	193	261	317

A. Table 29: Experiments for different temperatures under oxyfuel conditions – **L1 Ca/S=5, Golem**

	Bed temp. 800°C	Bed temp. 840°C	Bed temp. 880°C	Bed temp. 920°C	Bed temp. 960°C
O_2 conc. in FG [%]	5.2	6.1	5.9	6.4	8.1
Mean FB temp. [C]	809	842	882	920	959
SO_2 measured [ppm]	696	243	675	1237	1597
SO_2 measured [mg/MJ]	120	41	115	214	279
SO_2 capture ratio [%]	**87.0**	**95.5**	**87.5**	**76.8**	**69.7**
Fuel load [kg/hod]	54.8	51.6	46.0	47.1	48.0
Superficial velocity [m/s]	1.60	1.42	1.24	1.26	1.30
CO_2 conc. in FG [%]	78.9	80.2	79.6	78.5	77.6
CO in FG [ppm]	2858	2406	2792	2102	143
CO in FG [mg/MJ]	215	178	208	159	110

A. Table 30: Experiments for different temperatures under oxyfuel conditions – **L2 Ca/S=1.5, Golem**

	Bed temp. 840°C	Bed temp. 880°C	Bed temp. 920°C	Bed temp. 960°C
O_2 concentration in FG [%]	6.1	7.0	5.5	5.7
Mean FB temperature [°C]	836	883	915	961
SO_2 measured [ppm]	472	1375	1941	2522
SO_2 measured [mg/MJ]	80	233	324	432
SO_2 capture ratio [%]	**91.3**	**74.7**	**64.8**	**53.1**
Fuel load [kg/hod]	46.1	52.0	47.3	56.9
Superficial velocity [m/s]	1.37	1.44	1.38	1.57
CO_2 concentration in FG [%]	80.1	80.0	81.3	79.2
CO in FG [ppm]	1103	1451	1393	2277
CO in FG [mg/MJ]	82	108	102	171

A. Table 31: Experiments for different temperatures under oxyfuel conditions – **L2 Ca/S=3, Golem**

	Bed temp. 840°C	Bed temp. 880°C	Bed temp. 920°C	Bed temp. 960°C
O_2 concentration in FG [%]	6.4	5.2	5.4	6.2
Mean FB temperature [°C]	839	885	925	964
SO_2 measured [ppm]	285	735	1667	1918
SO_2 measured [mg/MJ]	49	123	275	328
SO_2 capture ratio [%]	**94.7**	**86.7**	**70.1**	**64.3**
Fuel load [kg/hod]	48.7	50.3	57.7	57.7
Superficial velocity [m/s]	1.45	1.48	1.67	1.56
CO_2 concentration in FG [%]	78.8	81.3	82.1	79.3
CO in FG [ppm]	1733	2207	2113	2214
CO in FG [mg/MJ]	131	161	153	166

A. Table 32: Experiments for different temperatures under oxyfuel conditions – **L2 Ca/S=5, Golem**

	Bed temp. 840°C	Bed temp. 880°C	Bed temp. 920°C	Bed temp. 960°C
O_2 concentration in FG [%]	6.6	6.3	6.2	7.9
Mean FB temperature [°C]	841	879	921	963
SO_2 measured [ppm]	122	387	809	2261
SO_2 measured [mg/MJ]	22	66	149	414
SO_2 capture ratio [%]	**97.7**	**92.8**	**83.8**	**55.0**
Fuel load [kg/hod]	42.4	41.4	38.2	44.6
Superficial velocity [m/s]	1.30	1.18	1.18	1.36
CO_2 concentration in FG [%]	76.5	79.6	73.5	74.1
CO in FG [ppm]	776	1687	714	1112
CO in FG [mg/MJ]	60	126	58	89

A. Table 33: Experiments for different oxygen in flue gas under oxyfuel conditions – **L1 Ca/S=1.5, Golem**

	Ca/S = 1.5		
	3% O_2 in FG	6% O_2 in FG	9% O_2 in FG
O_2 concentration in FG [%]	4.2	5.8	7.5
Mean FB temperature [°C]	881	875	881
SO_2 measured [ppm]	2657	1176	971
SO_2 measured [mg/MJ]	278	206	174
SO_2 capture ratio [%]	**69.7**	**77.6**	**81.1**
Fuel load [kg/hod]	38.6	46.7	48.4
Superficial velocity [m/s]	1.07	1.29	1.44
CO_2 concentration in FG [%]	79.5	77.4	75.6
CO in FG [ppm]	3525	920	585
CO in FG [mg/MJ]	262	70	46

A. Table 34: Experiments for different oxygen in flue gas under oxyfuel conditions – **L2 Ca/S=3, Golem**

	Ca/S = 3		
	3% O_2 in FG	6% O_2 in FG	9% O_2 in FG
O_2 concentration in FG [%]	3.7	5.2	10.2
Mean FB temperature [°C]	878	885	878
SO_2 measured [ppm]	717	801	412
SO_2 measured [mg/MJ]	120	123	74
SO_2 capture ratio [%]	**86.9**	**86.7**	**91.9**
Fuel load [kg/hod]	49.2	50.3	42.8
Superficial velocity [m/s]	1.42	1.48	1.31
CO_2 concentration in FG [%]	81.0	81.3	75.5
CO in FG [ppm]	3147	2734	513
CO in FG [mg/MJ]	231	161	40

13.4 COMPARISON OF THE RESULTS FROM MINIFLUID AND GOLEM

A. Table 35: Comparison of the result from MiniFluid and Golem for Ca/S=3

		Limestone L1		Limestone L2	
		MiniFluid	Golem	MiniFluid	Golem
840°C	O_2 concentration in FG [%]	5.7	6.7	6.8	6.4
	Mean FB temperature [°C]	841	838	837	839
	SO_2 measured [ppm]	1194	651	293	285
	SO_2 measured [mg/MJ]	170	105	41	49
	SO_2 capture ratio [%]	**80.0**	**88.6**	**95.1**	**94.7**
	Fuel load [kg/hod]	3.8	44.7	3.8	48.7
	Superficial velocity [m/s]	0.87	1.24	0.85	1.45
	CO_2 concentration in FG [%]	87.9	84.3	88.9	78.8
	CO in FG [ppm]	369	2759	521	1733
	CO in FG [mg/MJ]	23	194	32	131
880°C	O_2 concentration in FG [%]	5.8	6.9	6.1	5.2
	Mean FB temperature [°C]	876	878	882	885
	SO_2 measured [ppm]	420	802	258	735
	SO_2 measured [mg/MJ]	59	130	36	123
	SO_2 capture ratio [%]	**93.0**	**85.9**	**95.8**	**86.7**
	Fuel load [kg/hod]	4.1	44.7	4.4	50.3
	Superficial velocity [m/s]	1.00	1.25	0.91	1.48
	CO_2 concentration in FG [%]	88.6	84.0	89.9	81.3
	CO in FG [ppm]	163	2794	610	2207
	CO in FG [mg/MJ]	10	193	37	161
920°C	O_2 concentration in FG [%]	5.9	6.2	6.1	5.4
	Mean FB temperature [°C]	921	924	919	925
	SO_2 measured [ppm]	820	1741	678	1667
	SO_2 measured [mg/MJ]	116	277	95	275
	SO_2 capture ratio [%]	**86.3**	**69.9**	**88.8**	**70.1**
	Fuel load [kg/hod]	4.7	46.7	4.5	57.7
	Superficial velocity [m/s]	1.25	1.20	0.99	1.67
	CO_2 concentration in FG [%]	88.4	85.2	89.2	82.1
	CO in FG [ppm]	392	3741	1121	2113
	CO in FG [mg/MJ]	24	261	69	153
960°C	O_2 concentration in FG [%]	5.9	5.2	5.9	6.2
	Mean FB temperature [°C]	955	964	957	964
	SO_2 measured [ppm]	1350	2340	1934	1918
	SO_2 measured [mg/MJ]	191	373	270	328
	SO_2 capture ratio [%]	**77.5**	**59.5**	**68.1**	**64.3**
	Fuel load [kg/hod]	5.0	49.8	4.5	57.7
	Superficial velocity [m/s]	1.20	1.16	0.93	1.56
	CO_2 concentration in FG [%]	88.6	85.1	89.5	79.3
	CO in FG [ppm]	446	4547	1050	2214
	CO in FG [mg/MJ]	28	317	64	166

13.5 DIFFERENT VIEWS ON DESULPHURIZATION EFFICIENCY

A. Table 36: Summary of the desulphurization efficiency and limestone utilization – measurements in MiniFluid under air conditions

	Ca/S ratio	State	EF_{SO2} [g/kg_{fuel}]	$\eta_{capture}$ [%]	$\eta_{desulp.}$ [%]	$\eta_{lime.total}$ [%]
	No limestone	T800°C	15.98	17.2	-	23.5
		T840°C	16.57	14.1	-	19.3
		T880°C	16.87	12.5	-	17.2
		T920°C	16.45	14.7	-	20.2
Limestone L1	Ca/S=1.5	T800°C	8.89	53.9	44.3	25.5
		T840°C	10.45	45.8	36.9	21.7
		T880°C	11.89	38.4	29.5	18.1
		T920°C	17.88	7.3	0.0	3.5
	Ca/S=3	T800°C	7.28	62.3	54.5	18.4
		T840°C	6.25	67.6	62.3	20.0
		T880°C	8.62	55.3	48.9	16.3
		T920°C	12.76	33.8	22.4	10.0
	Ca/S=5	T800°C	2.28	88.2	85.7	17.9
		T840°C	2.29	88.1	86.2	17.9
		T880°C	4.41	77.1	73.9	15.7
		T920°C	7.46	61.3	54.6	12.5
Limestone L2	Ca/S=1.5	T800°C	6.56	63.8	56.0	28.4
		T840°C	7.16	60.5	53.7	26.9
		T880°C	7.62	58.0	51.7	25.8
		T920°C	8.73	51.9	43.2	23.1
	Ca/S=3	T800°C	4.96	74.3	66.7	22.2
		T840°C	3.76	80.5	75.8	24.9
		T880°C	4.60	74.6	70.8	20.9
		T920°C	6.08	66.5	60.4	18.7
	Ca/S=5	T800°C	0.73	96.0	95.1	18.8
		T840°C	0.63	96.6	96.0	18.9
		T880°C	1.12	93.8	92.9	18.3
		T920°C	3.60	80.1	76.5	15.7

A. Table 37 Summarization of the results and different view on the desulphurization efficiency and limestone utilization – measurements at MiniFluid under oxyfuel conditions

	Ca/S ratio	State	EF_{SO2} [g/kg_{fuel}]	$\eta_{capture}$ [%]	$\eta_{desulp.}$ [%]	$\eta_{lime.total}$ [%]
	No limestone	T840°C	10.23	46.9	-	64.1
		T880°C	10.26	46.8	-	61.5
		T920°C	10.62	44.9	-	60.7
		T960°C	10.74	44.3	-	56.5
Limestone L1	Ca/S=1.5	T840°C	4.73	73.9	53.9	32.9
		T880°C	3.06	83.2	71.2	37.0
		T920°C	5.89	67.6	45.2	30.1
		T960°C	10.15	47.4	10.5	19.8
	Ca/S=3	T840°C	3.64	80.0	64.5	22.2
		T880°C	1.27	93.0	88.0	25.9
		T920°C	2.48	86.3	76.9	24.0
		T960°C	4.08	77.5	64.0	21.6
	Ca/S=5	T840°C	1.26	93.0	87.7	17.8
		T880°C	0.43	97.6	95.9	18.7
		T920°C	0.97	94.6	90.9	18.1
		T960°C	3.13	82.8	72.4	15.8
Limestone L2	Ca/S=1.5	T840°C	3.15	82.7	69.3	36.8
		T880°C	2.28	87.4	78.5	38.9
		T920°C	3.18	82.5	70.4	36.7
		T960°C	7.54	58.5	33.5	26.0
	Ca/S=3	T840°C	0.88	95.1	91.4	26.7
		T880°C	0.77	95.8	92.8	26.9
		T920°C	2.03	88.8	81.1	24.9
		T960°C	5.78	68.1	49.0	19.1
	Ca/S=5	T840°C	0.17	99.1	98.4	19.4
		T880°C	0.32	98.2	97.0	18.5
		T920°C	0.99	94.6	90.8	19.2
		T960°C	4.68	74.2	58.7	14.5

A. Table 38: Summarization of the results and different view on the desulphurization efficiency and limestone utilization – measurements at Golem under oxyfuel conditions

	Ca/S ratio	State	EF_{SO2} [g/kg_{fuel}]	$\eta_{capture}$ [%]	$\eta_{desulphurization}$ [%]	$\eta_{limestone}$ [%]
	No limestone	T840°C	7.98	53.1	-	61.4
		T880°C	7.41	56.5	-	65.3
		T920°C	8.11	52.3	-	60.5
		T960°C	8.88	47.8	-	55.3
Limestone L1	Ca/S=1.5	T840°C	2.78	83.6	65.1	34.4
		T880°C	5.15	69.7	30.5	31.9
		T920°C	7.84	53.9	0.0	22.2
		T960°C	7.07	58.4	20.3	24.0
	Ca/S=3	T840°C	1.94	88.6	75.7	22.9
		T880°C	2.40	85.9	67.7	22.2
		T920°C	5.13	69.9	39.6	18.1
		T960°C	6.90	59.5	22.3	15.4
	Ca/S=5	T840°C	0.76	95.5	90.5	17.0
		T880°C	2.13	87.5	71.3	15.6
		T920°C	3.95	76.8	51.3	13.7
		T960°C	5.16	69.7	41.9	12.4
Limestone L2	Ca/S=1.5	T840°C	1.48	91.3	81.5	37.5
		T880°C	4.31	74.7	41.8	30.7
		T920°C	5.99	64.8	26.1	26.6
		T960°C	7.99	53.1	10.0	21.8
	Ca/S=3	T840°C	0.91	94.7	88.6	24.7
		T880°C	2.27	86.7	69.3	22.6
		T920°C	5.10	70.1	47.3	18.3
		T960°C	6.07	64.3	31.7	16.8
	Ca/S=5	T840°C	0.40	97.7	95.0	17.8
		T880°C	1.22	92.8	83.5	16.9
		T920°C	2.76	83.8	66.0	15.3
		T960°C	7.66	55.0	13.8	10.0